NASA CONTRACTOR REPORT

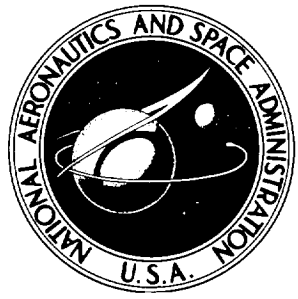

NASA CR-2228
PART I

NASA CR-2228
PART I

AN IMPROVED METHOD FOR THE AERODYNAMIC ANALYSIS OF WING-BODY-TAIL CONFIGURATIONS IN SUBSONIC AND SUPERSONIC FLOW

Part I - Theory and Application

by F. A. Woodward

Prepared by
AEROPHYSICS RESEARCH CORPORATION
Bellevue, Wash. 98009
for Langley Research Center

NATIONAL AERONAUTICS AND SPACE ADMINISTRATION • WASHINGTON, D. C. • MAY 1973

AN IMPROVED METHOD FOR THE AERODYNAMIC ANALYSIS OF WING-BODY-TAIL CONFIGURATIONS IN SUBSONIC AND SUPERSONIC FLOW

PART I - THEORY AND APPLICATION

By F. A. Woodward
Analytical Methods, Incorporated

SUMMARY

A new method has been developed for calculating the pressure distribution and aerodynamic characteristics of wing-body-tail combinations in subsonic and supersonic potential flow. A computer program has been developed to perform the numerical calculations.

The configuration surface is subdivided into a large number of panels, each of which contains an aerodynamic singularity distribution. A constant source distribution is used on the body panels, and a vortex distribution having a linear variation in the streamwise direction is used on the wing and tail panels. The normal components of velocity induced at specified control points by each singularity distribution are calculated and make up the coefficients of a system of linear equations relating the strengths of the singularities to the magnitude of the normal velocities.

The singularity strengths which satisfy the boundary condition of tangential flow at the control points for a given Mach number and angle of attack are determined by solving this system of equations using an iterative procedure. Once the singularity strengths are known, the pressure coefficients are calculated, and the forces and moments acting on the configuration determined by numerical integration.

Several examples of pressure distributions calculated by this program are presented, and compared with experimental data. Good correlation between theory and experiment has been achieved.

TABLE OF CONTENTS

1. Report No.	2. Government Accession No.	3. Recipient's Catalog No.
NASA CR-2228, Pt. I		

4. Title and Subtitle	5. Report Date
AN IMPROVED METHOD FOR THE AERODYNAMIC ANALYSIS OF WING-BODY-TAIL CONFIGURATIONS IN SUBSONIC AND SUPERSONIC FLOW PART I - THEORY AND APPLICATION	May 1973
	6. Performing Organization Code
7. Author(s) F. A. Woodward	8. Performing Organization Report No.
	10. Work Unit No. 501-06-01-06
9. Performing Organization Name and Address Aerophysics Research Corporation Box 187 Bellevue, Washington 98009 *Under Subcontract by: Analytical Methods, Inc. 9320 S. E. Shoreland Drive Bellevue, Washington 98004	11. Contract or Grant No. NAS1-10408
	13. Type of Report and Period Covered Contractor Report
12. Sponsoring Agency Name and Address National Aeronautics and Space Administration Washington, D. C. 20546	14. Sponsoring Agency Code
15. Supplementary Notes	

16. Abstract

A new method has been developed for calculating the pressure distribution and aerodynamic characteristics of wing-body-tail combinations in subsonic and supersonic potential flow. A computer program has been developed to perform the numerical calculations.

The configuration surface is subdivided into a large number of panels, each of which contains an aerodynamic singularity distribution. A constant source distribution is used on the body panels, and a vortex distribution having a linear variation in the streamwise direction is used on the wing and tail panels. The normal components of velocity induced at specified control points by each singularity distribution are calculated and make up the coefficients of a system of linear equations relating the strengths of the singularities to the magnitude of the normal velocities.

The singularity strengths which satisfy the boundary condition of tangential flow at the control points for a given Mach number and angle of attack are determined by solving this system of equations using an interative procedure. Once the singularity strengths are known, the pressure coefficients are calculated, and the forces and moments acting on the configuration determined by numerical integration.

Several examples of pressure distributions calculated by this program are presented, and compared with experimental data. Good correlation between theory and experiment has been achieved.

17. Key Words (Suggested by Author(s))	18. Distribution Statement
Potential Flow Pressure Distribution Lifting Surface Theory Vortex Representation Solution of Linear Equations	Unclassified

19. Security Classif. (of this report)	20. Security Classif. (of this page)	21. No. of Pages	22. Price*
Unclassified	Unclassified	128	$3.00

*For sale by the National Technical Information Service, Springfield, Virginia 22151

INTRODUCTION

A unified approach to the aerodynamic analysis of wing-body-tail configurations in subsonic and supersonic flow was originally presented in references 1 and 2. This method has been extended by the introduction of several new aerodynamic singularity distributions which substantially improve its capability to represent arbitrary shapes. For example, the new method permits the analysis of non-circular bodies, provides a more accurate representation of rounded wing leading edges, and allows the determination of wing interference effects in the presence of body closure.

A computer program has been developed to perform the numerical calculations. The program accepts the standard geometry input format currently in use at the Langley Research Center, and described in reference 3. The graphics capability of the program of reference 3 may be used to obtain a visual display of the configuration input geometry. In addition, the new program has two boundary condition options available for determining the pressure distribution on lifting surfaces. In the first option, the aerodynamic singularities are located on the mean plane of the surface, and approximate planar boundary conditions applied to determine the singularity strengths. In the second option, the aerodynamic singularities are located on the upper and lower surfaces of the lifting component, and exact surface boundary conditions applied. This results in a more accurate pressure distribution, but requires considerably more computer time. Surface boundary conditions are always applied in the determination of the body pressure distribution.

Part I of this report outlines the aerodynamic theory, describes the input requirements of the computer program, and compares the program output with experimental data for several isolated wings, bodies, and wing-body combinations. Part II contains a detailed description of the computer program, including a complete program listing and sample case.

The author wishes to acknowledge the contributions made by Mr. E. W. Geller to the aerodynamic theory, and the assistance given by Dr. T. S. Chow in the formulation of the matrix solution techniques, and by Mr. D. N. Bergman in the development of the computer program.

LIST OF SYMBOLS

A consistent set of units is assumed throughout this report.

a	Aerodynamic influence coefficient, tangent of body panel inclination angle δ, or wing panel edge slope parameter $(\lambda_2 - \lambda_1)$
A	Matrix of aerodynamic influence coefficients, or cross-sectional area
b	Wing thickness influence coefficient, or wing panel span, or major axis of ellipse
c	Panel chord length, or reference chord length
C	Aerodynamic coefficient
d	Distance of control point from singularity origin, or body diameter
D	Diagonal block matrix
e	Distance of control point from wing panel tip intersection
E	Off-diagonal block matrix
F, G, H	Velocity distribution functions
I	Integral expression
k	Supersonic scaling factor, or iteration number
K	Kernel function
ℓ	Length of line source or vortex, or body length
m	Body panel edge slope dy/dx
M	Mach number, or pitching moment
n	Direction cosine of panel normal vector, or velocity component normal to panel
N	Normal force, or number of aerodynamic singularities

NW	Number of wing and tail singularities
NB	Number of body singularities
q	Magnitude of velocity at control point
r	Radial distance
R	Reynolds number
s	Auxiliary variable
S	Wing reference area
t	Auxiliary velocity distribution function, or wing thickness
T	Tangential force
u, v, w	Components of induced velocity
V	Induced velocity at control point
x, y, z	Cartesian coordinates of points

Greek

α	Angle of attack
β	Mach number parameter, $(1 - M^2)^{\frac{1}{2}}$
γ	Ratio of specific heats for air, or aerodynamic singularity strengths
δ	Inclination angle of panel with x axis
Δ	Incremental value
ε	Minor axis of ellipse
θ	Inclination angle of panel with x,y plane
λ	Tangent of panel sweepback angle dx/dy, or direction cosine of coordinate transformation

Λ	Sweepback angle
μ, ν	Direction cosines of coordinate transformation
ξ, η	Integration variables along x and y axes
π	Ratio of circumference to diameter of circle
ρ	Radial distance of control point from streamwise line through wing panel tip intersection
ϕ	Velocity potential, or angle between velocity vector and x axis
χ	Integration variable
ω	Velocity component normal to panel

Subscripts

B	Body
base	Body base
c	Wing camber
D	Drag
i	Index of panel control point
j	Index of influencing panel
k	Index of panel corner point
L	Lift
M	Pitching moment
max	Maximum
N	Normal force
p	Pressure
t	Wing thickness

T	Tangential force
W	Wing
x, y, z	Refer to x, y, z axes

AERODYNAMIC THEORY

Description of Method

The configuration surface is divided into a large number of panels, each of which contains an aerodynamic singularity distribution. A constant source distribution is used on the body panels, and a vortex distribution having a linear variation in the streamwise direction is used on the wing and tail panels. A typical configuration panel subdivision is shown on Figure 1.

Analytical expressions are derived for the perturbation velocity field induced by each panel singularity distribution. These expressions are used to calculate the coefficients of a system of linear equations relating the magnitude of the normal velocities at the panel control points to the unknown singularity strengths. The singularity strengths which satisfy the boundary condition of tangential flow at the control points for a given Mach number and angle of attack are determined by solving this system of equations by an iterative procedure. The pressure coefficients at panel control points are then calculated in terms of the perturbation velocity components, and the forces and moments acting on the configuration obtained by numerical integration.

The following paragraphs describe the derivation of the perturbation velocity components induced by the aerodynamic singularities, the formation and solution of the boundary condition equations, and the procedure used to calculate the pressure coefficients, forces, and moments on the configuration. Two non-standard integrals appearing repeatedly in these derivations are given in Appendix I.

Derivation of the Incompressible Velocity Components

Formulas for the perturbation velocity components u, v, and w induced by the aerodynamic singularity distributions in incompressible flow are derived by superposition of elementary line sources or vortices located in the plane of the panel. The resulting expressions are subsequently transformed by Gothert's rule to obtain the compressible velocity component formulas for subsonic and supersonic flow.

Elementary line source.- The velocity at a point P(x, y, z) induced by a point source of unit strength located on the x axis a distance ξ from the origin is given by:

$$V = \frac{1}{4\pi\left[(x - \xi)^2 + y^2 + z^2\right]} \qquad (1)$$

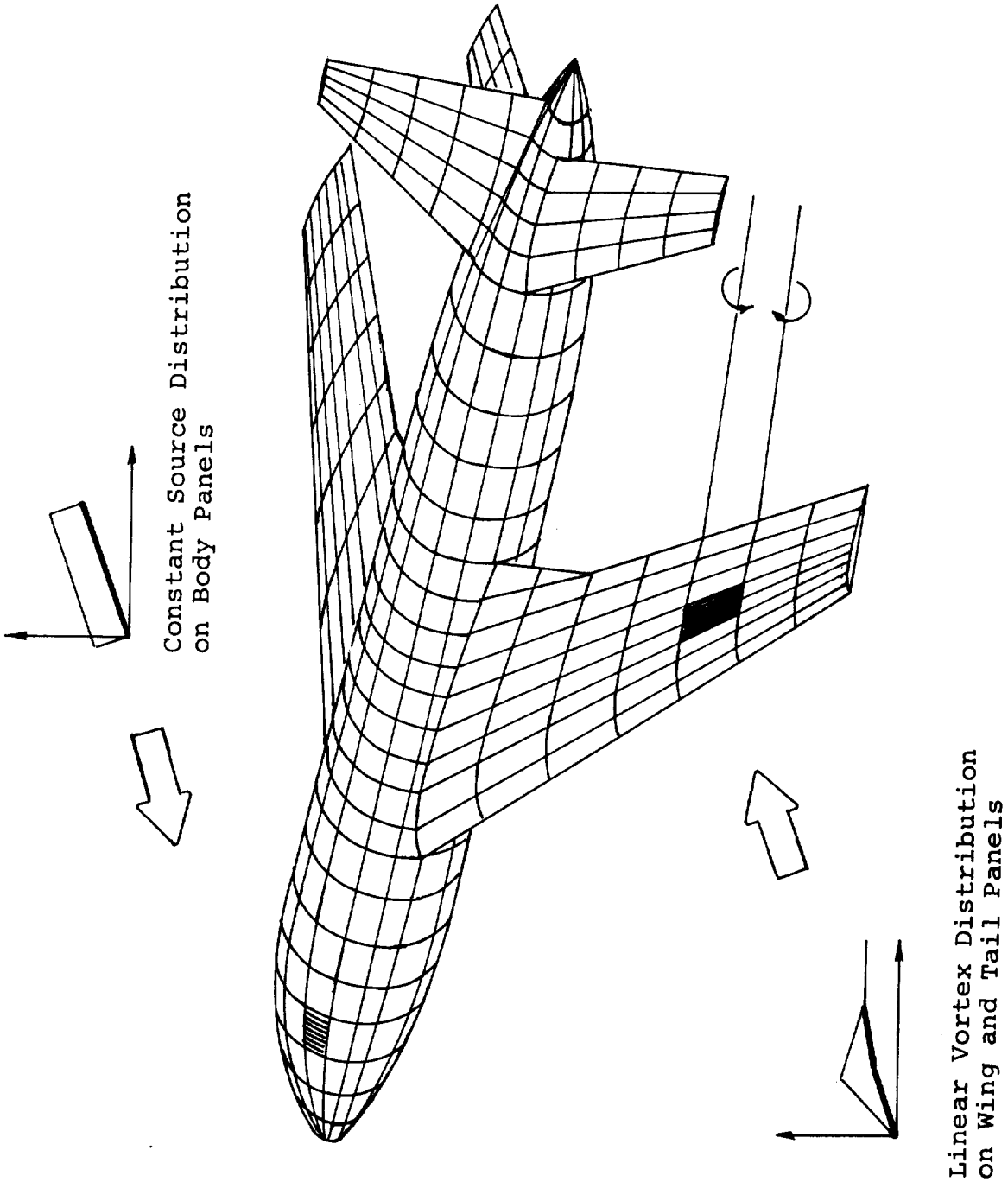

Figure 1 - Aerodynamic Representation

The velocity is directed along the line joining the point source and the field point P.

The u, v, and w components of velocity at the point P induced by a unit strength line source coincident with the x axis and having a length ℓ is obtained by resolving V into its x, y, and z components and integrating with respect to ξ. The geometry is illustrated on the following sketch:

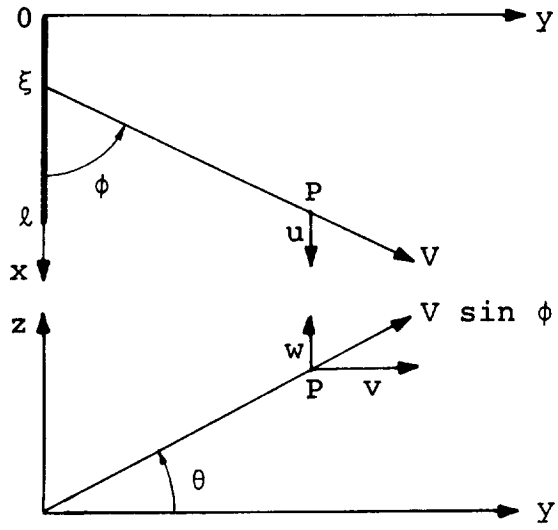

$$u = \int_0^{\ell} V \cos\phi \, d\xi$$

$$= \frac{1}{4\pi} \int_0^{\ell} \frac{(x - \xi)\, d\xi}{\left[(x - \xi)^2 + y^2 + z^2\right]^{3/2}} = \frac{1}{4\pi}\left[\frac{1}{d_2} - \frac{1}{d_1}\right] \qquad (2)$$

$$v = \int_0^{\ell} V \sin\phi \cos\theta \, d\xi$$

$$= \frac{y}{4\pi} \int_0^{\ell} \frac{d\xi}{\left[(x - \xi)^2 + y^2 + z^2\right]^{3/2}} = -\frac{y}{4\pi r^2}\left[\frac{x_2}{d_2} - \frac{x_1}{d_1}\right] \qquad (3)$$

$$w = \int_0^{\ell} V \sin\phi \sin\theta \, d\xi$$

$$= \frac{z}{4\pi} \int_0^{\ell} \frac{d\xi}{\left[(x - \xi)^2 + y^2 + z^2\right]^{3/2}} = -\frac{z}{4\pi r^2}\left[\frac{x_2}{d_2} - \frac{x_1}{d_1}\right] \qquad (4)$$

where $r = \sqrt{y^2 + z^2}$

$x_1 = x$ $\qquad$ $x_2 = x - \ell$

$d_1 = \sqrt{x^2 + r^2}$ $\qquad$ $d_2 = \sqrt{(x - \ell)^2 + r^2}$

$\phi = \tan^{-1} \frac{r}{x - \xi}$ $\qquad$ $\theta = \tan^{-1} \frac{z}{y}$

The three components of velocity satisfy Laplace's equation, since

$$\frac{\partial u}{\partial x} + \frac{\partial v}{\partial y} + \frac{\partial w}{\partial z} = 0$$

and $u = \frac{\partial \phi}{\partial x}$, $v = \frac{\partial \phi}{\partial y}$, $w = \frac{\partial \phi}{\partial z}$, where ϕ is the velocity potential of the line source.

The elementary line source is used as the basis of the more complex source distributions derived in this report.

Elementary line vortex.- The velocity at the point P induced by a unit strength line vortex coincident with the x axis and having a length ℓ is obtained by applying Biot-Savart's law to each element of the vortex and integrating.

$$V = \frac{1}{4\pi} \int_0^{\ell} \frac{\sin \phi \, d\xi}{(x - \xi)^2 + y^2 + z^2}$$

The velocity vector is normal to the plane containing the x axis and the point P.

Noting that $\sin \phi = \frac{r}{\left[(x - \xi)^2 + y^2 + z^2\right]^{1/2}}$ and integrating with respect to ξ,

$$V = - \frac{1}{4\pi r} \left[\frac{x_2}{d_2} - \frac{x_1}{d_1} \right] \tag{5}$$

There is no axial component of velocity induced by the line vortex. The v and w components are obtained by resolving V into its y and z components. Thus,

$$u = 0 \tag{6}$$

$$v = -V \sin\theta = \frac{z}{4\pi r^2}\left[\frac{x_2}{d_2} - \frac{x_1}{d_1}\right] \tag{7}$$

$$w = V \cos\theta = \frac{-y}{4\pi r^2}\left[\frac{x_2}{d_2} - \frac{x_1}{d_1}\right] \tag{8}$$

The notation is defined following equation (4). The three components of velocity can also be shown to satisfy Laplace's equation.

The elementary line vortex solution is used as the basis of the more complex vortex distributions derived in this report. Care must be taken during these derivations to ensure that all vortex lines form closed rings and thus satisfy Helmholtz's vortex theorem.

Rotation of coordinates.- In the following applications, the line source or vortex coordinate system is in general rotated with respect to the reference coordinate system of the panel. Using primed coordinates to refer to the rotated line source or vortex, and defining $\lambda = \tan\Lambda$ to be the tangent of the sweep angle of the rotated system, the following coordinate transformations apply:

$$x' = \frac{\lambda x + y}{(1 + \lambda^2)^{1/2}} \tag{9}$$

$$y' = \frac{\lambda y - x}{(1 + \lambda^2)^{1/2}} \tag{10}$$

$$z' = z \tag{11}$$

The geometry of the rotated coordinate system is illustrated in the following sketch:

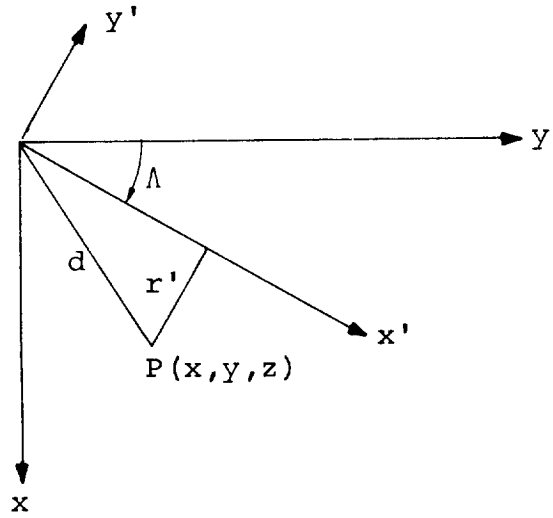

The distance d from the field point to the origin is unchanged in this transformation, but the perpendicular distance of the point from the line source or vortex is given by

$$r' = \sqrt{\frac{(x - \lambda y)^2}{1 + \lambda^2} + z^2}$$

The velocity components are transformed into the reference coordinate system as follows:

$$u = \frac{\lambda u' - v'}{(1 + \lambda^2)^{1/2}} \tag{12}$$

$$v = \frac{\lambda v' + u'}{(1 + \lambda^2)^{1/2}} \tag{13}$$

$$w = w' \tag{14}$$

Constant source distribution on unswept panel with streamwise taper.- The velocity components induced at a point P by a constant source distribution in the plane of the panel are derived by summing the influences of a series of elementary line sources extending across the panel parallel to the leading edge. The geometry of the elementary line source located a distance ξ from the leading edge and having a strength $d\xi$ is illustrated in the following sketch:

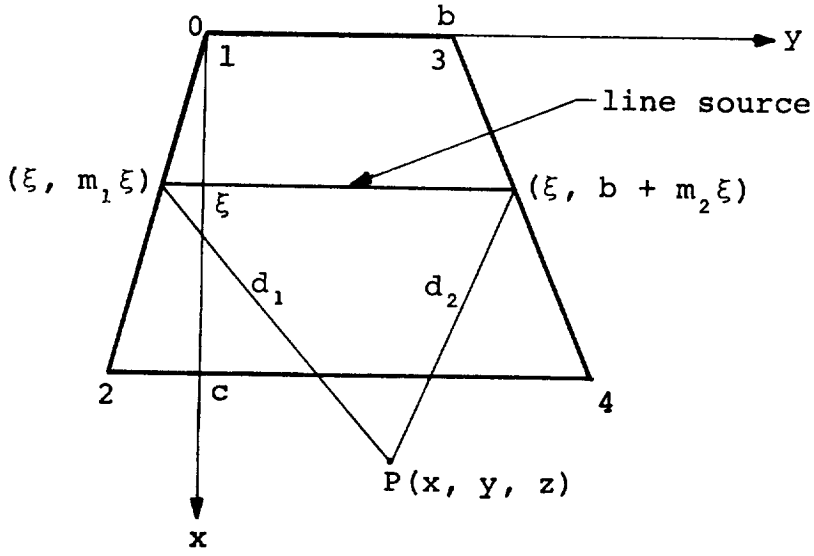

In the following derivation, it is assumed that the panel lies in the x, y plane. The distance of the point P from the left end of the line source is $d_1 = \left[(y - m_1\xi)^2 + (x - \xi)^2 + z^2\right]^{1/2}$

and the distance from the right end of the line source is $d_2 = [(y - b - m_2\xi)^2 + (x - \xi)^2 + z^2]^{\frac{1}{2}}$. The panel edge slopes $m = dy/dx$ may be arbitrary. The velocity components are obtained by applying a 90 degree coordinate rotation to the line source velocity formulas given by equations (2) - (4), and integrating across the panel chord as follows:

$$u = -v' = \frac{-1}{4\pi}\int_0^c \frac{(x - \xi)\, d\xi}{(x - \xi)^2 + z^2}\left[\frac{y - m_1\xi}{d_1} - \frac{y - b - m_2\xi}{d_2}\right] \tag{15}$$

$$v = u' = \frac{1}{4\pi}\int_0^c \left[\frac{1}{d_1} - \frac{1}{d_2}\right] d\xi \tag{16}$$

$$w = w' = \frac{-z}{4\pi}\int_0^c \frac{d\xi}{(x - \xi)^2 + z^2}\left[\frac{y - m_1\xi}{d_1} - \frac{y - b - m_2\xi}{d_2}\right] \tag{17}$$

Only the first integral in each formula need be evaluated, as the second integral may be obtained by a simple coordinate translation. For the same reason the integrals are evaluated only at the lower limit. The resulting velocity components correspond to the influence of the inboard corner of the panel leading edge. Denoting these results by the subscript one,

$$u_1 = \frac{1}{4\pi}\left[\frac{m_1}{(1 + m_1^2)^{\frac{1}{2}}}\sinh^{-1}\frac{x + m_1 y}{[(y - m_1 x)^2 + (1 + m_1^2)z^2]^{\frac{1}{2}}} - \sinh^{-1}\frac{y}{(x^2 + z^2)^{\frac{1}{2}}}\right] \tag{18}$$

$$v_1 = \frac{-1}{4\pi(1 + m_1^2)^{\frac{1}{2}}}\sinh^{-1}\frac{x + m_1 y}{[(y - m_1 x)^2 + (1 + m_1^2)z^2]^{\frac{1}{2}}} \tag{19}$$

$$w_1 = \frac{1}{4\pi}\tan^{-1}\frac{z(x^2 + y^2 + z^2)^{\frac{1}{2}}}{-x(y - m_1 x) + m_1 z^2} \tag{20}$$

The velocity components induced by the remaining three corners are obtained by applying the above formulas with the origin shifted to the corner under consideration, and using the appropriate edge slope.

The influence of the complete panel is obtained by summing the influences of the four corners, where the subscripts refer to the corner numbers shown on the sketch.

$$u = u_1 - u_2 - u_3 + u_4 \tag{21}$$

$$v = v_1 - v_2 - v_3 + v_4 \tag{22}$$

$$w = w_1 - w_2 - w_3 + w_4 \tag{23}$$

The velocity components given by equations (18) - (20) are expressed in terms of a coordinate system lying in the plane of the panel. One additional rotation of coordinates about the y axis is required to obtain the formulas used in the computer program. Referring to the following sketch, the panel coordinate system now denoted by primes, is rotated through an angle δ with respect to the unprimed reference coordinate system. The reference system also has its origin at the inboard corner of the panel leading edge, but the x axis is parallel to the body reference axis.

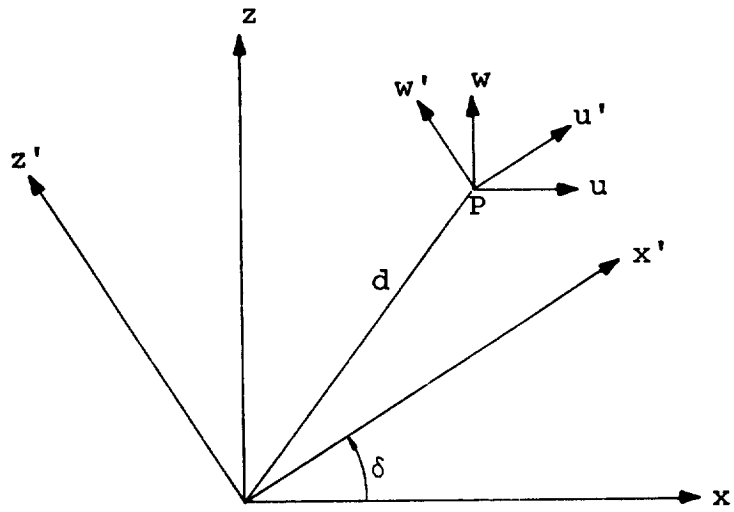

Defining $a = \tan\delta$, the coordinate transformations are

$$x' = \frac{x + az}{(1 + a^2)^{1/2}} \tag{24}$$

$$y' = y \tag{25}$$

$$z' = \frac{z - ax}{(1 + a^2)^{1/2}} \tag{26}$$

$$m' = \frac{m}{(1 + a^2)^{\frac{1}{2}}} \tag{27}$$

Similarly, the velocity components become:

$$u = \frac{u' - aw'}{(1 + a^2)^{\frac{1}{2}}}$$

$$= \frac{1}{4\pi(1 + a^2)^{\frac{1}{2}}} \left[mG - H - aF \right] \tag{28}$$

$$v = v' = \frac{-G(1 + a^2)^{\frac{1}{2}}}{4\pi} \tag{29}$$

$$w = \frac{w' + au'}{(1 + a^2)^{\frac{1}{2}}}$$

$$= \frac{1}{4\pi(1 + a^2)^{\frac{1}{2}}} \left[F + a(mG - H) \right] \tag{30}$$

where:

$$F = \tan^{-1} \frac{(z - ax)(x^2 + y^2 + z^2)^{\frac{1}{2}}}{-x(y - mx) - z(ay - mz)}$$

$$G = \frac{1}{(1 + a^2 + m^2)^{\frac{1}{2}}} \sinh^{-1} \frac{x + my + az}{\left[(y - mx)^2 + (ay - mz)^2 + (z - ax)^2 \right]^{\frac{1}{2}}}$$

$$H = \sinh^{-1} \frac{y}{(x^2 + z^2)^{\frac{1}{2}}}$$

Constant source distribution on swept panel with spanwise taper.- The velocity components induced at a point P by a constant source distribution in the plane of a swept panel are derived in a similar manner by summing the influences of a series of elementary line sources extending across the panel parallel to the leading edge. In this case, the line sources

are swept back by the angle Λ. The geometry of an elementary line source located a distance ξ from the leading edge, and having strength $d\xi$, is illustrated on the following sketch:

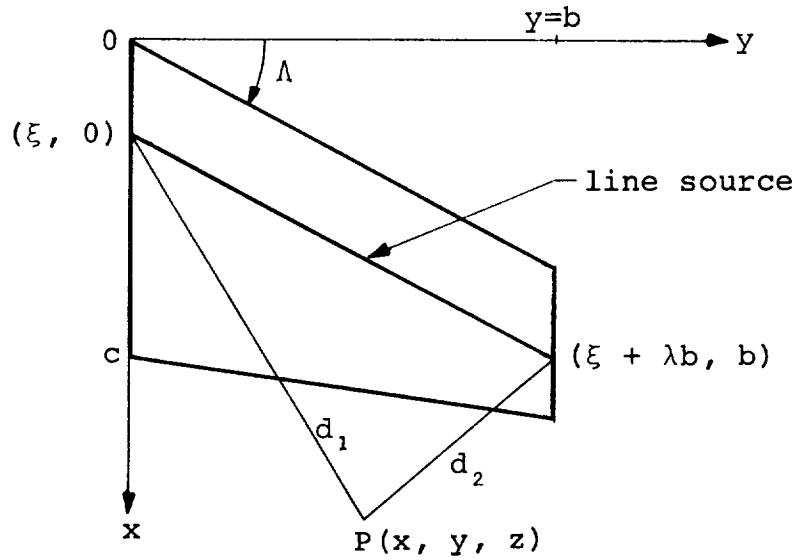

The panel is assumed to lie in the x, y plane. The distance of the point P from the left end of the line source is $d_1 = \left[(x - \xi)^2 + y^2 + z^2\right]^{\frac{1}{2}}$ and the distance from the right end of the line source is $d_2 = \left[(x - \xi - \lambda b)^2 + (y - b)^2 + z^2\right]^{\frac{1}{2}}$, where λ is the tangent of the leading edge sweepback angle Λ. The velocity components are obtained by rotating the coordinates of the line source velocity formulas through the angle Λ, and integrating across the panel chord as follows:

$$u = \frac{\lambda u' - v'}{(1 + \lambda^2)^{\frac{1}{2}}}$$

$$= \frac{1}{4\pi(1 + \lambda^2)^{\frac{1}{2}}} \int_0^c \left\{ \lambda \left[\frac{1}{d_2} - \frac{1}{d_1} \right] \right.$$

$$\left. + \frac{x - \xi - \lambda y}{r^2} \left[\frac{\lambda(x - \xi) + y}{d_1} - \frac{\lambda(x - \xi - \lambda b) + y - b}{d_2} \right] \right\} d\xi \qquad (31)$$

$$v = \frac{\lambda v' + u'}{(1 + \lambda^2)^{\frac{1}{2}}}$$

$$= \frac{1}{4\pi(1 + \lambda^2)^{\frac{1}{2}}} \int_0^c \left\{ \frac{1}{d_2} - \frac{1}{d_1} - \frac{\lambda(x - \xi - \lambda y)}{r^2} \left[\frac{\lambda(x - \xi) + y}{d_1} \right.\right.$$

$$\left.\left. - \frac{\lambda(x - \xi - \lambda b) + y - b}{d_2} \right] \right\} d\xi \qquad (32)$$

$$w = w'$$

$$= \frac{z(1 + \lambda^2)^{\frac{1}{2}}}{4\pi} \int_0^c \frac{d\xi}{r^2} \left[\frac{\lambda(x - \xi) + y}{d_1} - \frac{\lambda(x - \xi - \lambda b) + y - b}{d_2} \right] \qquad (33)$$

where $r^2 = (x - \xi - \lambda y)^2 + (1 + \lambda^2)\, z^2$

In order to obtain the results in standard form the integrals are divided by $(1 + \lambda^2)^{\frac{1}{2}}$ prior to their evaluation. As before, only those integrals associated with the inboard edge of the panel require evaluation, and then only at their lower limit. The resulting velocity components correspond to the influence of the inboard corner of the panel leading edge. Denoting these results by the subscript one,

$$u_1 = \frac{-1}{4\pi(1 + \lambda^2)^{\frac{1}{2}}} \sinh^{-1} \frac{\lambda x + y}{\left[(x - \lambda y)^2 + (1 + \lambda^2) z^2\right]^{\frac{1}{2}}} \qquad (34)$$

$$v_1 = \frac{1}{4\pi} \left[\frac{\lambda}{(1 + \lambda^2)^{\frac{1}{2}}} \sinh^{-1} \frac{\lambda x + y}{\left[(x - \lambda y)^2 + (1 + \lambda^2) z^2\right]^{\frac{1}{2}}} \right.$$

$$\left. - \sinh^{-1} \frac{x}{(y^2 + z^2)^{\frac{1}{2}}} \right] \qquad (35)$$

$$w_1 = \frac{1}{4\pi}\left[\tan^{-1}\frac{z\left[x^2 + y^2 + z^2\right]^{\frac{1}{2}}}{-xy + \lambda(y^2 + z^2)} - \tan^{-1}\frac{z}{y}\right] \tag{36}$$

The velocity components induced by the remaining three corners are obtained by applying the above formulas with the origin shifted, and using the value of λ corresponding to the leading or trailing edge. The influence of the complete panel is obtained by summing the influences of the four corners as indicated by equations (21) - (23).

Linearly varying source distribution on swept panel with spanwise taper.- The velocity components induced by a source distribution having a linear variation in the chordwise direction are derived in the same manner as described in the preceding section for the constant source distribution. In this case, however, the expressions under the integral signs in equations (31) - (33) are multiplied by ξ prior to integration. The velocity components induced by the inboard corner of the panel leading edge are given below:

$$u_1 = \frac{-1}{4\pi}\left\{\frac{x - \lambda y}{(1 + \lambda^2)^{\frac{1}{2}}}\sinh^{-1}\frac{\lambda x + y}{\left[(x - \lambda y)^2 + (1 + \lambda^2)z^2\right]^{\frac{1}{2}}}\right.$$

$$+ y\sinh^{-1}\frac{x}{(y^2 + z^2)^{\frac{1}{2}}}$$

$$\left. - z\left[\tan^{-1}\frac{z(x^2 + y^2 + z^2)^{\frac{1}{2}}}{-xy + \lambda(y^2 + z^2)} - \tan^{-1}\frac{z}{y}\right]\right\} \tag{37}$$

$$v_1 = \frac{1}{4\pi}\left\{(x - \lambda y)\left[\frac{\lambda}{(1 + \lambda^2)^{\frac{1}{2}}}\sinh^{-1}\frac{\lambda x + y}{\left[(x - \lambda y)^2 + (1 + \lambda^2)z^2\right]^{\frac{1}{2}}}\right.\right.$$

$$\left. - \sinh^{-1}\frac{x}{(y^2 + z^2)^{\frac{1}{2}}}\right] + x + \left[x^2 + y^2 + z^2\right]^{\frac{1}{2}}$$

$$\left. - \lambda z\left[\tan^{-1}\frac{z(x^2 + y^2 + z^2)^{\frac{1}{2}}}{-xy + \lambda(y^2 + z^2)} - \tan^{-1}\frac{z}{y}\right]\right\} \tag{38}$$

$$w_1 = \frac{1}{4\pi}\left\{(x - \lambda y)\left[\tan^{-1}\frac{z(x^2 + y^2 + z^2)^{\frac{1}{2}}}{-xy + \lambda(y^2 + z^2)} - \tan^{-1}\frac{z}{y}\right]\right.$$

$$+ z\left[(1 + \lambda^2)^{\frac{1}{2}}\sinh^{-1}\frac{\lambda x + y}{\left[(x - \lambda y)^2 + (1 + \lambda^2)z^2\right]^{\frac{1}{2}}}\right.$$

$$\left.\left. - \lambda \sinh^{-1}\frac{x}{(y^2 + z^2)^{\frac{1}{2}}}\right]\right\} \qquad (39)$$

The velocity components induced by the remaining three corners are obtained by applying the above formulas with the origin shifted, and using the appropriate value of λ. The influence of the complete panel is obtained by summing the influences of the four corners as indicated by equations (21) - (23).

Constant vortex distribution on swept panel with spanwise taper.- The velocity components induced at a point P by a constant vortex distribution in the plane of a swept panel are derived by summing the influences of elementary line vortices extending across the panel parallel to the leading edge, and concentrated edge vortices extending back to infinity from the panel side edges. The geometry of an elementary line vortex located a distance ξ from the leading edge, and having strength $d\xi$, is illustrated on the following sketch:

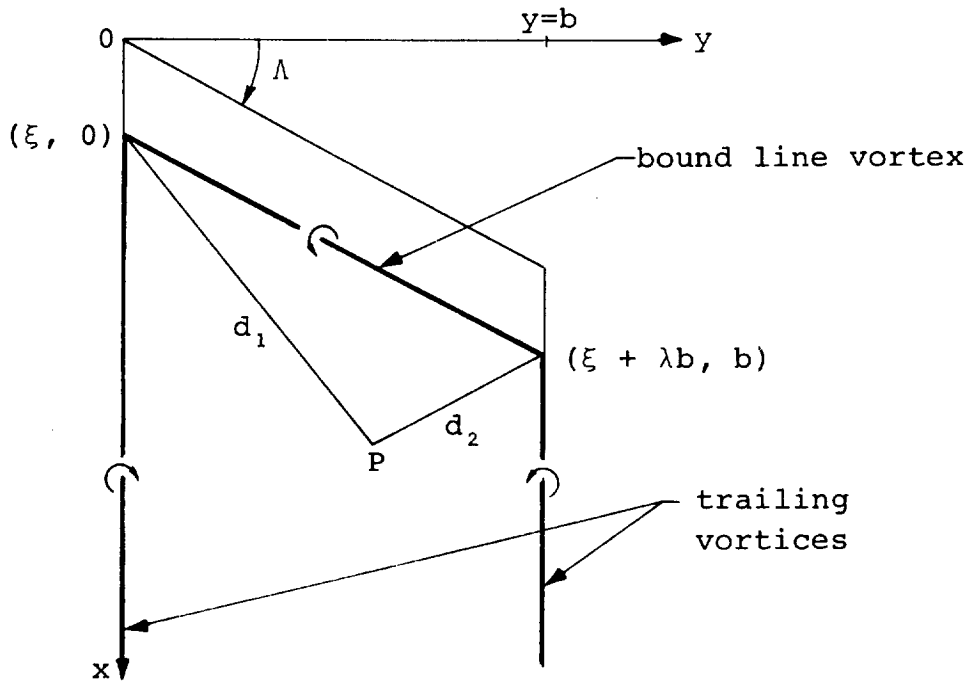

The influence of the bound vortices are considered first. The distance of the point P from the left end of the vortex is $d_1 = [(x - \xi) + y^2 + z^2]^{\frac{1}{2}}$, and the distance from the right end of the vortex is $d_2 = [(x - \xi - \lambda b)^2 + (y - b)^2 + z^2]^{\frac{1}{2}}$, where λ is the tangent of the leading edge sweepback angle as before. The velocity components are obtained by rotating the coordinates of the line vortex velocity formulas through the angle Λ, and integrating from the leading edge to infinity as follows:

$$u = \int_0^\infty \frac{\lambda u' - v'}{(1 + \lambda^2)^{\frac{1}{2}}} \, d\xi$$

$$= \frac{z}{4\pi} \int_0^\infty K \, d\xi \tag{40}$$

$$v = - \lambda u \tag{41}$$

$$w = \frac{-1}{4\pi} \int_0^\infty (x - \xi - \lambda y) K \, d\xi \tag{42}$$

where $K = \frac{1}{r^2} \left[\frac{\lambda(x - \xi) + y}{d_1} - \frac{\lambda(x - \xi - \lambda b) + y - b}{d_2} \right]$

and $r^2 = (x - \xi - \lambda y)^2 + (1 + \lambda^2) z^2$

Only those integrals corresponding to the inboard edge of the panel require evaluation, since the outboard edge can be obtained by a coordinate translation. In this case, however, both upper and lower limits of the integrals must be evaluated to obtain the correct results. The resulting velocity components give the influence of a semi-infinite region bounded by the leading edge and the x axis, with origin at the inboard leading edge corner of the panel. They are identified by the subscript one.

$$u_1 = \frac{1}{4\pi} \left[\tan^{-1} \frac{z(x^2 + y^2 + z^2)^{\frac{1}{2}}}{-xy + \lambda(y^2 + z^2)} - \tan^{-1} \frac{z}{y} \right] \tag{43}$$

$$v_1 = -\lambda u_1 \tag{44}$$

$$w_1 = \frac{1}{4\pi}\left[(1+\lambda^2)^{\frac{1}{2}} \sinh^{-1}\frac{\lambda x + y}{\left[(x-\lambda y)^2 + (1+\lambda^2)z^2\right]^{\frac{1}{2}}}\right.$$

$$\left. - \lambda \sinh^{-1}\frac{x}{(y^2+z^2)^{\frac{1}{2}}} - \lambda \log (y^2+z^2)^{\frac{1}{2}}\right] \tag{45}$$

It should be noted that the last term of equation (45) is obtained by considering the influence of both inboard and outboard edges of the panel simultaneously as the upper limit of the integral approaches infinity.

The edge vortex contributes only to the v and w components of velocity. The velocity components are obtained by integrating equations (7) and (8) for a line vortex of infinite length with respect to ξ, as follows:

$$\Delta v_1 = \frac{z}{4\pi}\int_0^\infty \frac{d\xi}{y^2+z^2}\left[1 + \frac{x-\xi}{\left[(x-\xi)^2 + y^2 + z^2\right]^{\frac{1}{2}}}\right]$$

$$= \frac{z}{4\pi}\left[\frac{x + (x^2+y^2+z^2)^{\frac{1}{2}}}{y^2+z^2}\right] \tag{46}$$

$$\Delta w_1 = \frac{-y}{4\pi}\left[\frac{x + (x^2+y^2+z^2)^{\frac{1}{2}}}{y^2+z^2}\right] \tag{47}$$

Therefore, the velocity components induced by the inboard leading edge corner of the panel are given by equation (43), the sum of equations (44) and (46), and the sum of equations (45) and (47). The velocity components induced by the remaining three corners are obtained by applying these equations with the origin shifted, and using the appropriate value of λ. The influence of the complete panel is obtained by summing the influences of the four corners as indicated by equations (21) - (23).

Linearly varying vortex distribution on swept panel with spanwise taper.- A vortex distribution is considered which has a linear variation in the chordwise direction, and lies within the triangular region bounded by the panel leading and trailing edges extended to intersection, and the panel inboard edge. The velocity components induced at a point P by this vortex distribution are derived in three steps. In the first step, the velocities induced by a horseshoe vortex of strength $\xi\, d\xi$ having its bound segment located along a radial line from the intersection of the leading and trailing edges are evaluated and integrated across the panel chord. The geometry of the bound and trailing segments of the horseshoe vortex are shown on the following sketch.

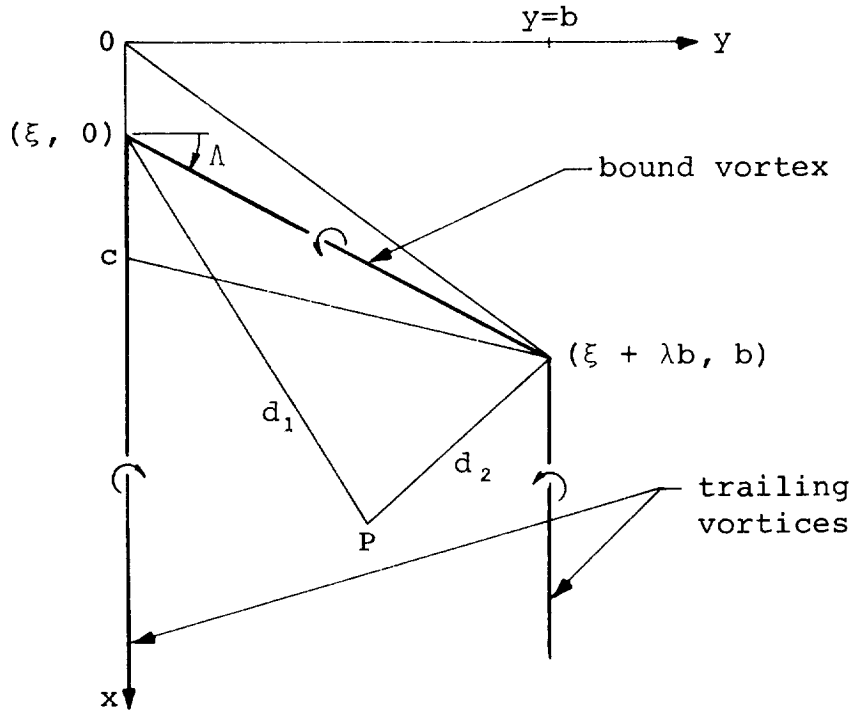

The bound vortex is located a distance ξ from the panel origin. The point P is located a distance $d_1 = [(x - \xi)^2 + y^2 + z^2]^{1/2}$ from the inboard end of the vortex, and a distance $d_2 = [(x - \xi - \lambda b)^2 + (y - b)^2 + z^2]^{1/2}$ from the outboard end. In this derivation, the slope of the vortex is a linear function of ξ, $\lambda = \lambda_1 + a\xi/c$, where $a = \lambda_2 - \lambda_1$, $b = c/a$, and λ_1 and λ_2 are the slopes of the leading and trailing edges of the panel, respectively. The line vortex formulas are rotated through the angle Λ, as before, to obtain expressions for the velocity components of the bound vortex prior to integration.

The velocity components are given below in integral form:

$$u = \frac{z}{4\pi c}\int_0^c \frac{K\xi}{r^2}\, d\xi \tag{48}$$

$$v = -\lambda u \tag{49}$$

$$w = -\frac{1}{4\pi c}\int_0^c \frac{(x - \xi - \lambda y)K\xi}{r^2}\, d\xi \tag{50}$$

where $\lambda = \lambda_1 + a\xi/c$

$$K = \frac{\lambda(x - \xi) + y}{d_1} - \frac{\lambda(x - \xi - \lambda b) + y - b}{d_2}$$

$$r^2 = (x - \xi - \lambda y)^2 + (1 + \lambda^2)z^2$$

These integrals are evaluated by making use of the following substitution in terms of the integration variable χ.

$$\xi = \frac{c\left[(x - \lambda_1 y)(c - ay) - a\lambda_1 z^2\right]}{(c - ay)^2 + a^2 z^2} - \chi \tag{51}$$

After a lengthy integration procedure, the velocity components induced by the inboard edge of the panel are obtained. In the following formulas, the parameter λ is redefined as the panel leading edge slope.

$$u = \frac{c}{4\pi\rho^2}\left\{ z\left[\frac{ad}{c} + \left(\lambda - \frac{2as}{\rho^2}\right)G_2\right] + \frac{z}{\rho^2}\left[(c\lambda - ax)as - (c - ay)e^2\right] G_1 - \frac{1}{\rho^2}\left[(c\lambda - ax)az^2 + (c - ay)s\right] F_1 \right\}_0^c \tag{52}$$

$$v = -(c\lambda - ax)(c - ay)u/\rho^2 - azt \tag{53}$$

$$w = -(c - ay)t + (c\lambda - ax)azu/\rho^2 \tag{54}$$

where
$$t = \frac{-1}{4\pi\rho^2}\left\{ d\left[\frac{a(x+\xi)}{2c} - \frac{(c\lambda - ax)(c - ay)}{\rho^2}\right]\right.$$

$$+\left[\frac{c}{\rho^4}\left[(c - ay)(c\lambda - ax)s + ae^2z^2\right] - y + \frac{ar^2}{2c}\right]G_2$$

$$-\frac{e^2}{\rho^4}\left[(c - ay)s + (c\lambda - ax)az^2\right]G_1$$

$$\left.+\frac{zc}{\rho^4}\left[(c - ay)e^2 - (c\lambda - ax)as\right]F_1\right\}_0^c \tag{55}$$

and
$$d = \left[(x - \xi)^2 + r^2\right]^{\frac{1}{2}}$$

$$r^2 = y^2 + z^2$$

$$\rho^2 = (c - ay)^2 + a^2z^2$$

$$e^2 = (c\lambda - ax)^2 + \rho^2$$

$$s = (c - ay)(x - \lambda y) + a\lambda z^2$$

$$F_1 = \tan^{-1}\frac{zd}{(\lambda - a\xi/c)r^2 - y(x - \xi)} \tag{56}$$

$$G_1 = \frac{1}{e}\sinh^{-1}\frac{(c\lambda - ax)(x - \xi) + y(c - ay) - az^2}{c\left[\left[x - \lambda y + (c - ay)\xi/c\right]^2 + z^2\left[1 + (\lambda - a\xi/c^2)\right]\right]^{\frac{1}{2}}} \tag{57}$$

$$G_2 = \sinh^{-1} \frac{x - \xi}{r} \tag{58}$$

It should be noted that the functions F_1, G_1 and G_2 differ from those defined following equation (30).

The distribution of vorticity corresponding to these functions can be determined by examining the behaviour of the axial velocity u for z = 0. From equation (51),

$$u = \frac{-c(x - \lambda y)}{4(c - ay)^2}$$

Along the panel leading edge, $x = \lambda y$ and therefore $u = 0$. Along the trailing edge $x = c + \lambda_2 y$, therefore

$$u = \frac{-c}{4(c - ay)} \tag{59}$$

Thus, the vorticity distribution is seen to vary linearly chordwise, and inversely as the local chord spanwise.

The contribution of the trailing vortex originating along the inboard edge of the panel is considered next. This vortex contributes only v and w components of velocity, which are obtained by multiplying equations (7) and (8) for a line vortex of infinite length by ξ, and integrating. The results are as follows:

$$\Delta v = \frac{z}{4\pi c} \int \frac{\xi \, d\xi}{y^2 + z^2} \left[1 + \frac{x - \xi}{\left[(x - \xi)^2 + y^2 + z^2\right]^{\frac{1}{2}}}\right]$$

$$= \frac{-z}{8\pi c} \left\{ \frac{x - \xi}{r^2} \left[x - \xi + \left[(x - \xi)^2 + r^2\right]^{\frac{1}{2}}\right] + G_2 \right\}_0^c$$

$$- \frac{z}{4\pi r^2} \left[x - c + \left[(x - c)^2 + r^2\right]^{\frac{1}{2}}\right] \tag{60}$$

Similarly,

$$\Delta w = \frac{-y}{8\pi c} \left\{ \frac{x - \xi}{r^2} \left[x - \xi + \left[(x - \xi)^2 + r^2\right]^{\frac{1}{2}}\right] + G_2 \right\}_0^c$$

$$+ \frac{y}{4\pi r^2} \left[x - c + \left[(x - c)^2 + r^2\right]^{\frac{1}{2}}\right] \tag{61}$$

The first term in the braces gives the velocities induced by a pair of line vortices of quadratic strength along the x axis, and the last term gives the velocities induced by a linearly varying vortex from the panel trailing edge. The combination gives the contribution of a line vortex of quadratic strength to the trailing edge, followed by a constant vortex of strength c/2 extending downstream in the wake. A constant vortex of equal but opposite strength trails downstream from the outboard tip of the triangular panel.

In the second step, the velocities induced by a vortex distribution having a linear variation in both chordwise and spanwise directions is derived and subtracted from those given above to obtain the velocity components corresponding to a vortex distribution having a linear variation chordwise, but remaining constant spanwise. In this step, the bound vortex located along the radial line from the intersection of the panel leading and trailing edges is given a linear variation in the spanwise direction prior to performing the chordwise integration. The linearly varying bound vortex is made up by superimposing a series of horseshoe vortices of strength $\xi d\xi d\eta$ with inboard edge located at η, and outboard edge located at b. The geometry is illustrated below:

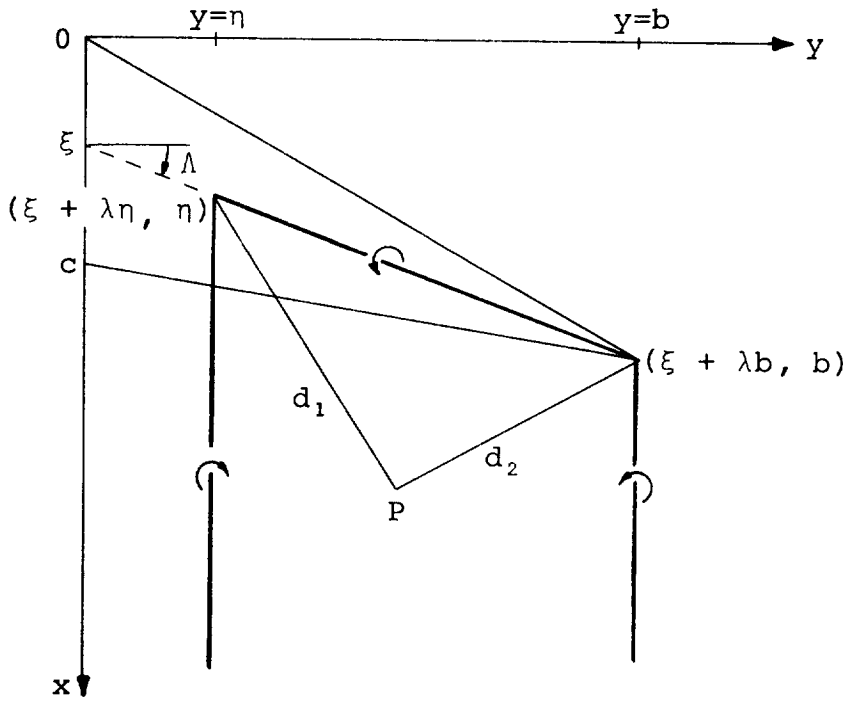

The contribution of the bound segment of this elementary horseshoe vortex is obtained from the line vortex formulas, with the origin shifted to the point $(\xi + \lambda\eta, \eta)$, and the coordinates rotated through the angle Λ. The point P is located a distance $d_1 = [(x - \xi - \lambda\eta)^2 + (y - \eta)^2 + z^2]^{1/2}$ from the inboard end of the bound vortex, and $d_2 = [(x - \xi - \lambda b)^2 + (y - b)^2 + z^2]^{1/2}$ from the outboard end. The velocity components are given below in integral form:

$$u = \frac{z}{4\pi c} \int_0^c \frac{\xi \, d\xi}{r^2} \int_0^b K \, d\eta \tag{62}$$

$$v = - \lambda u \tag{63}$$

$$w = \frac{-1}{4\pi c} \int_0^c \frac{\xi(x - \xi - \lambda y) \, d\xi}{r^2} \int_0^b K \, d\eta \tag{64}$$

where $\lambda = \lambda_1 + a\xi/c$

$$a = \lambda_2 - \lambda_1$$

$$K = \frac{\lambda(x - \xi - \lambda\eta) + y - \eta}{d_1} - \frac{\lambda(x - \xi - \lambda b) + y - b}{d_2}$$

$$r^2 = (x - \xi - \lambda y)^2 + (1 + \lambda^2) z^2$$

Only the first term in the K integral requires evaluation, as the second term cancels in the superposition process. Integrating this with respect to η,

$$I = \int_0^b \frac{\lambda(x - \xi) + y - (1 + \lambda^2)\eta}{d_1} \, d\eta$$

$$= d - d_2 \tag{65}$$

where $d = [(x - \xi)^2 + y^2 + z^2]^{1/2}$

and d_2 is the same as previously defined.

The integrals (60) - (62) may now be written

$$u = \frac{z}{4\pi c}\int_0^c \frac{(d - d_2)\xi\, d\xi}{r^2} \tag{66}$$

$$v = -\lambda u \tag{67}$$

$$w = \frac{-1}{4\pi c}\int_0^c \frac{(d - d_2)(x - \xi - \lambda y)\xi}{r^2}\, d\xi \tag{68}$$

These integrals are evaluated, using the substitution given by equation (51). The velocity components induced by the inboard edge of the panel are given below, where λ is redefined as the panel leading edge slope.

$$u = \frac{-c}{4\pi\rho^2}\left\{ z\left[x - \frac{2(c\lambda - ax)(y(c - ay) - az^2)}{\rho^2}\right] G_2 - zd \right.$$

$$- \frac{z}{\rho^2}\left[(c\lambda - ax)cs - e^2(y(c - ay) - az^2)\right] G_1$$

$$\left. + \frac{1}{\rho^2}\left[(c\lambda - ax)cz^2 + s(y(c - ay) - az^2)\right] F_1 \right\}_0^c \tag{69}$$

$$v = -(c\lambda - ax)(c - ay)u/\rho^2 - azt \tag{70}$$

$$w = -(c - ay)t + (c\lambda - ax)azu/\rho^2 \tag{71}$$

where $t = \frac{c}{4\pi\rho^2}\left\{ \frac{d}{c}\left[\frac{(c\lambda - ax)(y(c - ay) - az^2)}{\rho^2} - \frac{x + \xi}{2}\right]\right.$

$$\left. + \left[\frac{-1}{\rho^4}\left[(c\lambda - ax)(y(c - ay) - az^2)s + ce^2z^2\right] + \frac{r^2}{2c}\right] G_2 \right.$$

$$+ \frac{e^2}{\rho^2}\left[(y(c - ay) - az^2)s + c(c\lambda - ax)z^2\right]G_1$$

$$+ \frac{z}{\rho^2}\left[(c\lambda - ax)cs - e^2(y(c - ay) - az^2)\right]F_1 \Bigg\}_0^c \qquad (72)$$

and the remaining functions and variables are defined following equation (55).

The distribution of vorticity corresponding to these new velocity functions is given by the value of u for z = 0. From equation (68)

$$u = \frac{-cy(x - \lambda y)}{4(c - ay)^2}$$

The axial velocity is zero along the leading edge, and along the trailing edge, where $x = c + \lambda_2 y$,

$$u = \frac{-cy}{4(c - ay)} \qquad (73)$$

If the new axial velocity function is multiplied by a/c and subtracted from the original, the value of u along the trailing edge will be constant. This can be seen by multiplying equation (73) by a/c and subtracting from equation (59). The result is:

$$u = \frac{-c}{4(c - ay)} + \frac{ay}{4(c - ay)} = -\frac{1}{4}$$

Thus, the combined functions give the desired vortex distribution on the panel, which is zero along the leading edge, constant along the trailing edge, and varies linearly in the chordwise direction. The velocity components corresponding to this vortex distribution are given below:

$$u = \frac{-1}{4\pi\rho^2}\left\{sF_1 + z\left[e^2G_1 - (c\lambda - ax)G_2\right]\right\}_0^c \qquad (74)$$

$$v = -(c\lambda - ax)(c - ay)u/\rho^2 - azt \qquad (75)$$

$$w = -(c - ay)t + (c\lambda - ax)azu/\rho^2 \qquad (76)$$

where: $$t = \frac{c}{4\pi\rho^2}\left\{\frac{s}{\rho^2}\left[e^2G_1 - (c\lambda - ax)G_2\right] - \frac{ze^2}{\rho^2}F_1\right.$$

$$\left. + \left(y - \frac{ar^2}{c}\right)G_2 + \frac{c\lambda - ax}{c}d\right\}_0^c \qquad (77)$$

and the remaining functions and variables are defined following equation (55). It should be noted that the final velocity functions given by equations (74) - (77) are considerably simpler than either of the preceding sets.

The derivation of the velocity component formulas for this vortex distribution is completed by adding the contribution of the wake. Returning to the sketch on page 26, it can be seen that the elementary horseshoe vortices generate a trailing vortex sheet of constant strength. This vortex sheet contributes only to the v and w components of velocity. The v component of velocity will be derived first by integrating equation (7) for a line vortex of infinite length, as follows:

$$\Delta v = \frac{-az}{4\pi c^2}\int_0^c \xi\, d\xi \int_0^b \frac{d\eta}{(y-\eta)^2 + z^2}\left[1 + \frac{x - \xi - \lambda\eta}{d_1}\right] \qquad (78)$$

where $d_1 = \left[(x - \xi - \lambda\eta)^2 + (y - \eta)^2 + z^2\right]^{\frac{1}{2}}$

and $\lambda = \lambda_1 + a\xi/c$

The inner integral is evaluated first, giving

$$\Delta v = \frac{-a}{4\pi c^2}\int_0^c \left[\tan^{-1}\frac{z\left[(x-\xi)^2 + r^2\right]^{\frac{1}{2}}}{-y(x-\xi) + \lambda r^2} - \tan^{-1}\frac{z}{y}\right]\xi\, d\xi$$

$$= \frac{-a}{8\pi}\left\{\left[\tan^{-1}\frac{z\,(x-\xi)^2 + r^2\,^{\frac{1}{2}}}{-y(x-\xi) + \lambda r^2} - \tan^{-1}\frac{z}{y}\right]\right.$$

$$\left. - \frac{zt}{c} + \frac{(x - \lambda y)(c - ay) + a\lambda z^2}{(c - ay)^2 + a^2z^2}u\right\}_0^c \qquad (79)$$

where u and t are given by equations (74) and (77) respectively, $r = (y^2 + z^2)^{\frac{1}{2}}$, and λ is redefined as the leading edge slope λ_1.

The w component of velocity is derived in a similar manner, by integrating equation (8) for a line vortex of infinite length. Here,

$$\Delta w = \frac{a}{4\pi c^2}\int_0^c \xi\, d\xi \int_0^b \frac{(y-\eta)d\eta}{(y-\eta)^2 + z^2}\left[1 + \frac{x - \xi - \lambda\eta}{d_1}\right] \tag{80}$$

where d_1 is defined above, and $\lambda = \lambda_1 + a\xi/c$.

The inner integral is evaluated first, giving

$$\Delta w = \frac{a}{4\pi c^2}\int_0^c \left[\frac{\lambda}{(1+\lambda^2)^{1/2}} \sinh^{-1}\frac{y + \lambda(x-\xi)}{\left[(x - \xi - \lambda y)^2 + (1+\lambda^2)z^2\right]^{1/2}}\right.$$

$$\left. - \sinh^{-1}\frac{x-\xi}{r} + \log r\right] \xi\, d\xi \tag{81}$$

Only the last two integrals can be evaluated in closed form. Thus

$$\Delta w = \frac{a}{4\pi c^2}\left[I_1 - I_2 + I_3\right] \tag{82}$$

where

$$I_1 = \int_0^c \frac{\lambda\xi}{(1+\lambda^2)^{1/2}} \sinh^{-1}\frac{y + \lambda(x-\xi)}{\left[(x - \xi - \lambda y)^2 + (1+\lambda^2)z^2\right]^{1/2}} d\xi \tag{83}$$

$$I_2 = \frac{1}{4}\left\{ (3x + \xi)\left[d - (x-\xi)G_2\right] + d^2 G_2 \right\}_0^c \tag{84}$$

$$I_3 = \frac{c^2}{2}\log r \tag{85}$$

where $\lambda = \lambda_1 + a\xi/c$, and d, r, and G_2 are defined following equation (55). Equation (83) is integrated numerically in the computer program.

It should be noted that Δv and Δw as derived above have been multiplied by -a/c prior to integration in order to correctly account for the contribution of the wake.

The velocity components induced by a vortex distribution which has a linear variation in the chordwise direction, and remains constant in the spanwise direction have now been derived for a triangular region bounded by the panel leading and trailing edges, and the inboard side edge. In the third step of this analysis, these velocity component formulas are combined to give the influence of a swept, tapered panel of arbitrary span. This is accomplished by superimposing two of these triangular regions having common outboard intersections and equal values of the leading and trailing edge slopes. The superposition process is illustrated by the following sketch:

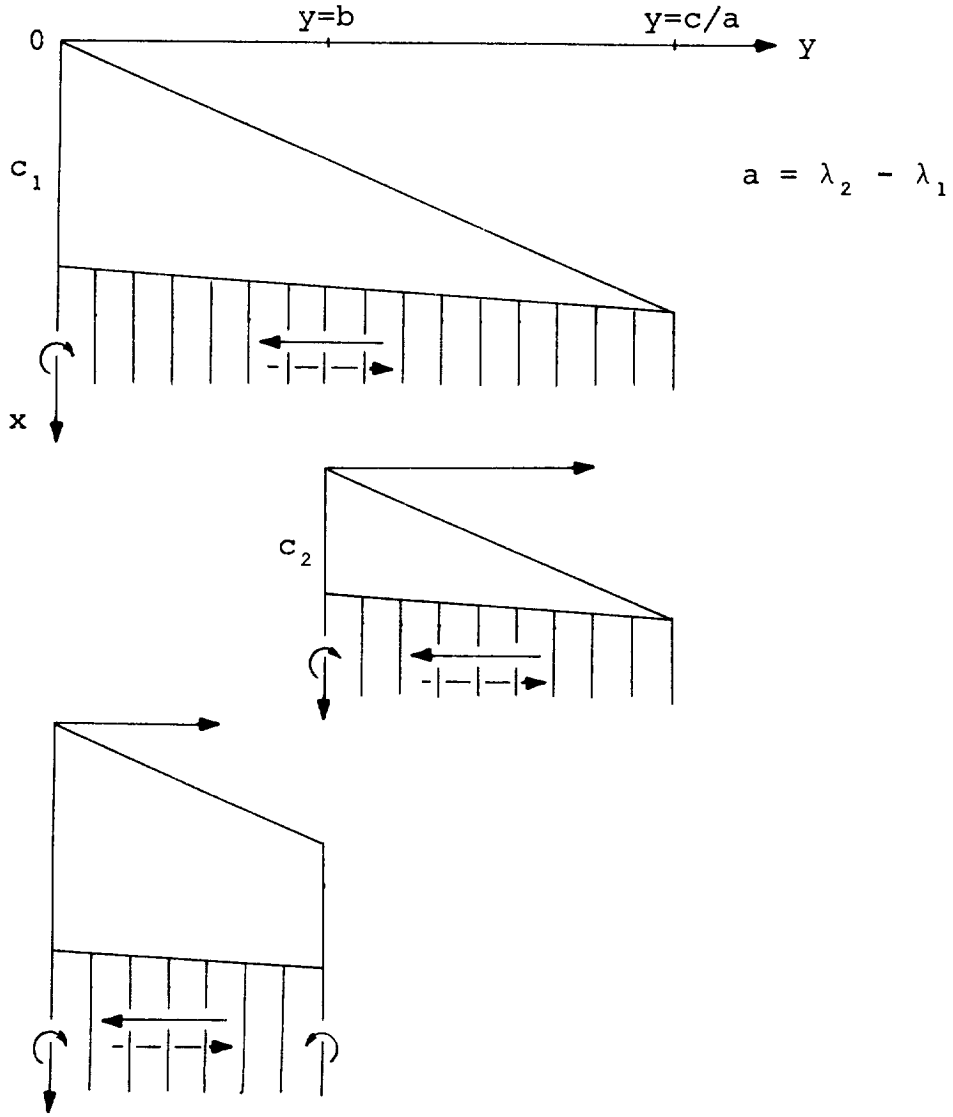

The upper triangular panel has a concentrated vortex of strength c_1 trailing from the inboard edge, and a vortex sheet of strength a behind the trailing edge. There is no concentrated vortex shed from the outboard tip, since the circulation around the trailing vortex sheet is equal and opposite to that of the concentrated edge vortex. A similar vortex pattern is shed by the second triangular panel, except that the concentrated vortex has a strength c_2.

The influence of a swept, tapered panel of finite span b can be obtained by superimposing the two triangular panels as indicated. It should be noted that the concentrated vortices trailing from the edges of this panel are of unequal strength if the panel is tapered, the difference being made up by the vortex sheet in the wake. The vortex distribution on the panel is zero along the leading edge, and varies linearly in the chordwise direction to a constant value along the trailing edge. The axial component of velocity u is given by equation (74), the v component of velocity is given by the sum of equations (60), (75) and (81), and the w component of velocity is given by the sum of equations (61), (76), and (82).

If the influence of a triangular panel is required, special care must be taken in the evaluation of equations (74) and (77). In this case, the chord of the outboard panel subtracted in the superposition process is zero, and two terms in the equations become indeterminate. The limiting values of these terms are given below.

First, the function G_1 becomes:

$$\lim_{c\to 0} \left[G_1 \right]_0^c = \frac{1}{2} \log \frac{(x - \lambda_1 y)^2 + (1 + \lambda_1^2) z^2}{(x - \lambda_2 y)^2 + (1 + \lambda_2)^2 z^2} \tag{86}$$

where λ_1 and λ_2 are the slopes of the panel leading and trailing edges.

Second, the last two terms in the expression for t become:

$$\lim_{c\to 0} \left[\frac{1}{c} (r^2 G_2 + xd) \right]_0^c = (x^2 + r^2)^{\frac{1}{2}} \tag{87}$$

The remaining terms in the equations are unchanged.

Derivation of the Compressible Velocity Components

The compressible velocity components induced by the source and vortex distributions are obtained by applying Gothert's rule to the incompressible velocity components derived in the previous section. The original derivation of Gothert's rule presented in reference 4 considered only compressible subsonic flows; here the rule is extended to include supersonic flows as well. The extended rule states that the velocity components u, v, and w at a point $P(x, y, z)$ in a compressible flow are equal to the real parts of u_i, βv_i and βw_i, where u_i, v_i and w_i are the incompressible velocity components evaluated at a point $P(x, \beta y, \beta z)$, and $\beta = (1 - M^2)^{\frac{1}{2}}$. In subsonic flow, this rule agrees exactly with that given by Gothert if each of the compressible velocity components are divided by the constant β^2. In supersonic flow, the compressible velocity components become complex functions, and care must be taken to extract the real parts of these functions in order to obtain the correct results. However, this procedure is generally much simpler than formally evaluating the velocity components by integration, and provides a straightforward method for obtaining the supersonic velocity fields corresponding to any existing incompressible flow solution.

A simple example of the extended rule is obtained by transforming the velocity components induced by a line source located along the x axis. The velocity component formulas given by equations (2) - (4) are unchanged by this transformation, except that $d_1 = (x^2 + \beta^2 r^2)^{\frac{1}{2}}$ and $d_2 = ((x - \ell)^2 + \beta^2 r^2)^{\frac{1}{2}}$. Both these terms are real in subsonic flow; but in supersonic flow, both are imaginary ahead of the Mach cone from the origin, d_1 is real but d_2 is imaginary between the Mach cone from the origin and the rear Mach cone, and both are real behind the rear Mach cone. Thus the velocity components are zero ahead of the Mach cone from the origin, and the finite length of the source has no influence on the velocity field except within the rear Mach cone. Considerable advantage is taken of this ability to correctly define the regions of influence of each term in the velocity component formulas in the following applications.

The compressible velocity components for each of the five basic singularity distributions used in this method are presented in the following sections.

Constant source distribution on unswept panel with streamwise taper.- The incompressible velocity components for this source distribution are given by equations (28) - (30). The corresponding compressible velocity components are:

$$u = \frac{-k}{4\pi(1 + \beta^2 a^2)^{\frac{1}{2}}} \left[aF - (\beta^2 mG - H)/\beta^2 \right] \tag{88}$$

$$v = \frac{-k(1 + \beta^2 a^2)^{\frac{1}{2}}}{4\pi} G \tag{89}$$

$$w = \frac{k}{4\pi(1 + \beta^2 a^2)^{\frac{1}{2}}} \left[F + a(\beta^2 mG - H) \right] \tag{90}$$

where $$F = \tan^{-1} \frac{(z - ax)\, d}{-x(y - mx) - \beta^2 z(ay - mz)} \tag{91}$$

$$G = \frac{1}{e} \sinh^{-1} \frac{x'}{\beta r'} \tag{92}$$

$$H = \beta \sinh^{-1} \frac{\beta y}{(x^2 + \beta^2 z^2)^{\frac{1}{2}}} \tag{93}$$

and $$\beta^2 = 1 - M^2$$

$$k = \begin{cases} 1 \text{ for } M \leqslant 1 \\ \\ 2 \text{ for } M > 1 \end{cases}$$

$$d = (x^2 + \beta^2 r^2)^{\frac{1}{2}}$$

$$e = \left[1 + \beta^2 (a^2 + m^2) \right]^{\frac{1}{2}}$$

$$d' = de$$

$$r' = \left[(y - mx)^2 + (z - ax)^2 + \beta^2 (ay - mz)^2 \right]^{\frac{1}{2}}$$

$$x' = x + \beta^2 (my + az)$$

The constant k gives the correct scaling factor for the supersonic velocity components.

In supersonic flow, the real parts of the functions F, G, and H must be determined. The function F is zero everywhere ahead of the Mach cone from the origin, except for panels having supersonic side edges, when $F = \pm \pi$ within the "two-dimensional" region bounded by the Mach waves from the side edge and the Mach cone from the origin. The boundaries of the two-dimensional region are given in the following sketch, which shows the traces of the Mach waves and Mach cone from the origin on a plane perpendicular to the x axis.

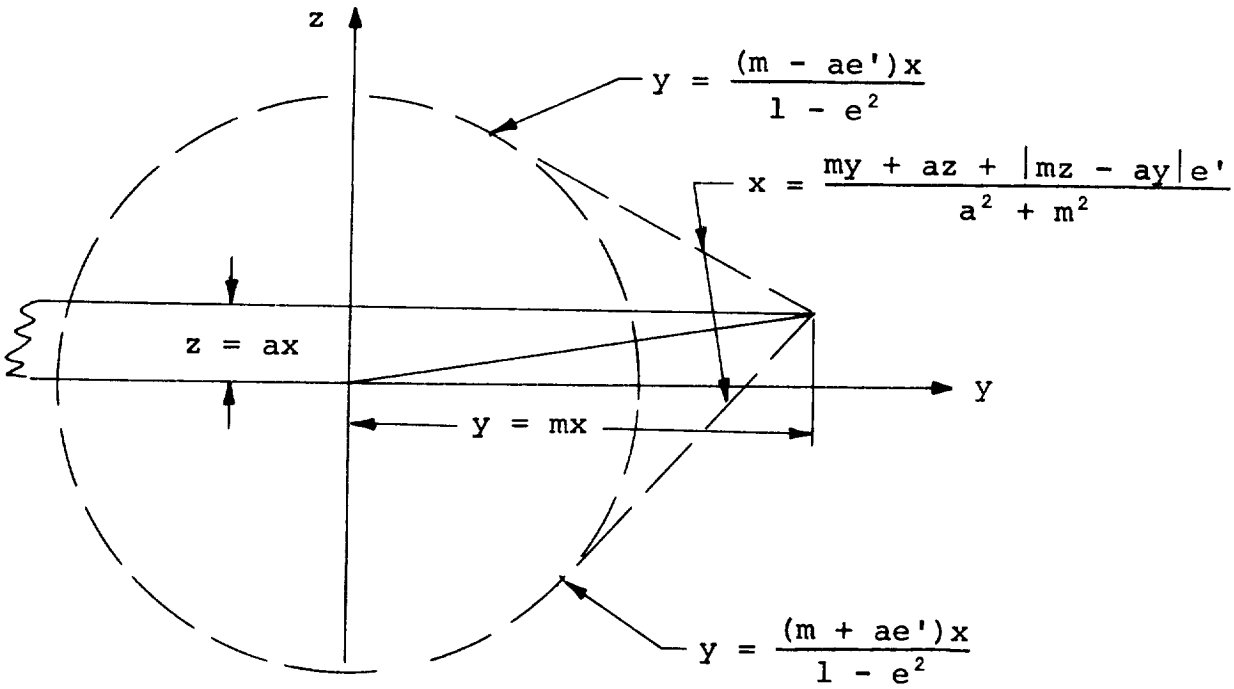

The function G takes several different forms depending on the relative sweepback on the side edges. Expressing the function in logarithmic form,

$$G = \frac{1}{e} \log \frac{x' + d'}{\beta' r'} \qquad \text{for } e^2 > 0$$

or $$G = \frac{d}{x'} \qquad \text{for } e^2 = 0$$

or $$G = \frac{1}{e'} \cos^{-1} \frac{x'}{\beta' r'} \qquad \text{for } e^2 < 0 \text{ and } -\beta' r' < x' < \beta' r'$$

or $\quad G = \pm \frac{\pi}{e'} \quad$ for $e^2 < 0$, $x' \leqslant -\beta' r'$ and $x > \frac{my + az + |ay - mz|e'}{a^2 + m^2}$

or $\quad G = 0 \quad$ elsewhere (94)

where $\quad \beta' = (M^2 - 1)^{\frac{1}{2}}$

$$e' = \left[-1 - \beta^2(a^2 + m^2)\right]^{\frac{1}{2}}$$

Finally, in supersonic flow, the function H becomes:

$$H = \beta' \tan^{-1}\frac{d}{\beta' y} \quad \text{for } x > \beta r$$

or $\quad H = 0 \quad$ elsewhere (95)

Constant source distribution on swept panel with spanwise taper.- The incompressible velocity components for this source distribution are given by equations (34) - (36). The corresponding compressible velocity components are:

$$u = \frac{-kG_1}{4\pi} \tag{96}$$

$$v = \frac{k}{4\pi}\left[\lambda G_1 - G_2\right] \tag{97}$$

$$w = \frac{k}{4\pi}\left[F_1 - F_2\right] \tag{98}$$

where $\quad F_1 = \tan^{-1}\frac{z\, d}{-xy + \lambda r^2} \tag{99}$

$$F_2 = \tan^{-1}\frac{z}{y} \tag{100}$$

$$G_1 = \frac{1}{e}\sinh^{-1}\frac{\lambda x + \beta^2 y}{\beta\left[(x - \lambda y)^2 + (\beta^2 + \lambda^2)z^2\right]^{\frac{1}{2}}} \tag{101}$$

$$G_2 = \sinh^{-1}\frac{x}{\beta r} \tag{102}$$

and

$$k = \begin{cases} 1 \text{ for } M \leqslant 1 \\ 2 \text{ for } M > 1 \end{cases}$$

$$d = (x^2 + \beta^2 r^2)^{\frac{1}{2}}$$

$$e^2 = \beta^2 + \lambda^2$$

$$r^2 = y^2 + z^2$$

In supersonic flow, the real parts of the functions F_1, F_2, G_1 and G_2 must be determined. The function F_2 is always real, and can be dropped from equation (98) without affecting the results since the contributions from the four corners of the panel always cancel. The function F_1 is zero everywhere ahead of the Mach cone from the origin, except for panels having supersonic leading edges, when $F_1 = \pm \pi$ within the "two-dimensional" region bounded by the Mach waves from the leading edge and the Mach cone from the origin. The boundaries of the two-dimensional region for this case are shown on the following sketch:

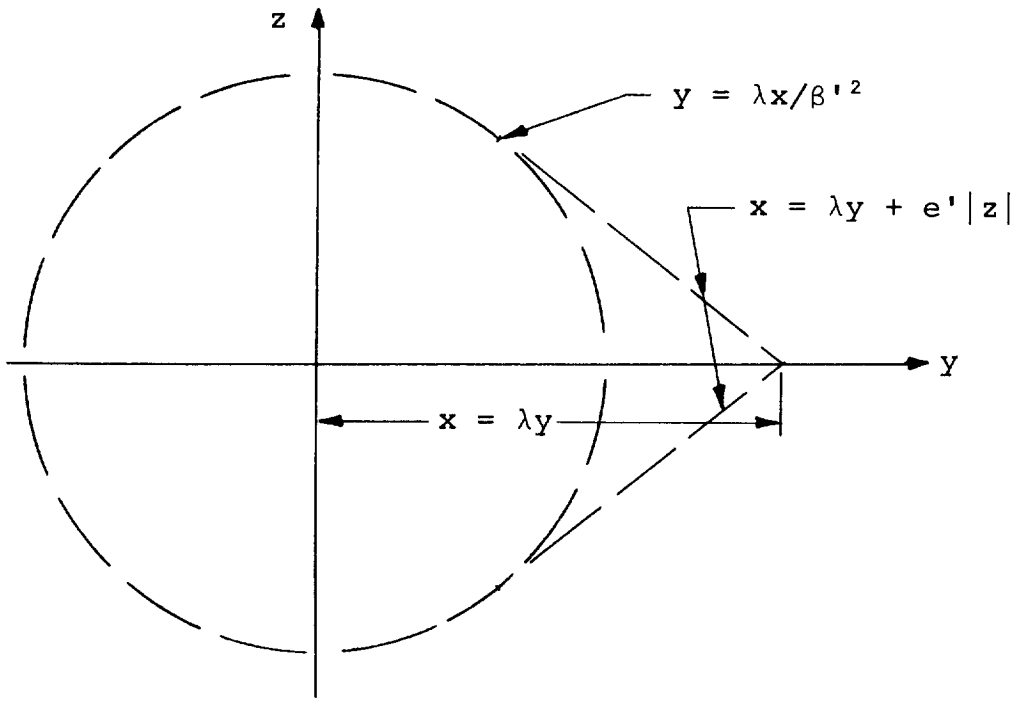

The function G_1 takes several different forms depending on the relative sweepback of the panel leading edge. Expressing the function in logarithmic form,

$$G_1 = \frac{1}{e} \log \frac{x' + d'}{\beta' r'} \qquad \text{for } e^2 > 0$$

$$\text{or} \qquad G_1 = \frac{d}{x'} \qquad \text{for } e^2 = 0$$

$$\text{or} \qquad G_1 = \frac{1}{e'} \cos \frac{x'}{\beta' r'} \qquad \text{for } e^2 < 0 \text{ and } -\beta' r' < x' < \beta' r'$$

$$\text{or} \qquad G_1 = \pm \frac{\pi}{e'} \qquad \text{for } e^2 < 0,\ x' < -\beta' r' \text{ and } x > \lambda y + e'|z|$$

$$\text{or} \qquad G_1 = 0 \qquad \text{elsewhere} \qquad (103)$$

where $\beta' = (M^2 - 1)^{\frac{1}{2}}$ $\qquad x' = \lambda x + \beta^2 y$

$e' = (-\beta^2 - \lambda^2)^{\frac{1}{2}}$ $\qquad r' = \left[(x - \lambda y)^2 + e^2 z^2\right]^{\frac{1}{2}}$

$d' = ed$

The function G_2 becomes:

$$G_2 = \log \frac{x + d}{\beta' r} \qquad \text{for } x > \beta r$$

$$\text{or} \qquad G_2 = 0 \qquad \text{elsewhere} \qquad (104)$$

Linearly varying source distribution on swept panel with spanwise taper.- The incompressible velocity components for this source distribution are given by equations (37) - (39). The corresponding compressible velocity components are:

$$u = \frac{-k}{4\pi} \left[(x - \lambda y) G_1 + y G_2 - z(F_1 - F_2)\right] \qquad (105)$$

$$v = \frac{k}{4\pi} \left[(x - \lambda y)(\lambda G_1 - G_2) + x + d - \lambda z(F_1 - F_2)\right] \qquad (106)$$

$$w = \frac{k}{4\pi}\left[(x - \lambda y)(F_1 - F_2) + z\left[e^2 G_1 - \lambda G_2\right]\right] \tag{107}$$

where the functions F_1, F_2, G_1, G_2, d, e, k, and r are defined by equations (99) - (102). In supersonic flow, the behaviour of functions F_1 and F_2 is described following equation (102) and the real parts of G_1 and G_2 are given by equations (103) and (104). The sum (x + d) appearing in equation (106) is replaced by d in supersonic flow, and is real only within the Mach cone from the origin.

Constant vortex distribution on swept panel with spanwise taper.- The incompressible velocity components for the bound vortex distribution are given by equations (43) - (45). The corresponding compressible velocity components are:

$$u = \frac{k}{4\pi}\left[F_1 - F_2\right] \tag{108}$$

$$v = -\lambda u \tag{109}$$

$$w = \frac{k}{4\pi}\left[e^2 G_1 - \lambda G_2\right] \tag{110}$$

where the functions F_1, F_2, G_1, G_2, d, e, k, and r are defined by equations (99) - (102). In supersonic flow, the behaviour of the functions F_1 and F_2 is described following equation (102), and the real parts of G_1 and G_2 are given by equations (103) and (104).

The contribution of the edge vortices in compressible flow is given by

$$\Delta u = 0 \tag{111}$$

$$\Delta v = \frac{kz}{4\pi}\,\frac{x + d}{r^2} \tag{112}$$

$$\Delta w = -\frac{ky}{4\pi}\,\frac{x + d}{r^2} \tag{113}$$

In supersonic flow, the sum (x + d) appearing in the above equations is replaced by d, and is real only within the Mach cone from the origin.

Linearly varying vortex distribution on swept panel with spanwise taper.- The incompressible velocity components for the bound vortex distribution are given by equations (74) - (77). The corresponding compressible velocity components are:

$$u = \frac{-k}{4\pi\rho^2}\left\{ sF_1 + z\left[e^2G_1 - (c\lambda - ax)G_2\right]\right\}_0^c \tag{114}$$

$$v = -(c\lambda - ax)(c - ay)u/\rho^2 - azt \tag{115}$$

$$w = -(c - ay)t + (c\lambda - ax)azu/\rho^2 \tag{116}$$

where

$$t = \frac{ck}{4\pi\rho^2}\left\{ \frac{s}{\rho^2}\left[e^2G_1 - (c\lambda - ax)G_2\right] - \frac{ze^2}{\rho^2}F_1 + \beta^2\left(y - \frac{ar^2}{c}\right)G_2 + (c\lambda - ax)\,d\right\}_0^c \tag{117}$$

where

$$k = \begin{cases} 1 \text{ for } M \leqslant 1 \\ 2 \text{ for } M > 1 \end{cases}$$

$$a = \lambda - \lambda_2$$

$$d = \left[(x - \xi)^2 + \beta^2 r^2\right]^{\frac{1}{2}}$$

$$r^2 = y^2 + z^2$$

$$\rho^2 = (c - ay)^2 + a^2z^2$$

$$e^2 = (c\lambda - ax)^2 + \beta^2\rho^2$$

$$s = (c - ay)(x - \lambda y) + a\lambda z^2$$

and

$$F_1 = \tan^{-1} \frac{zd}{-y(x - \xi) + (\lambda - a\xi/c)r^2} \tag{118}$$

$$G_1 = \frac{1}{e} \sinh^{-1} \frac{(c\lambda - ax)(x - \xi) + \beta^2[y(c - ay) - az^2]}{\beta c[[x - \lambda y + (c - ay)\xi/c]^2 + z^2[\beta^2 + (\lambda + a\xi/c)^2]]^{\frac{1}{2}}} \tag{119}$$

$$G_2 = \sinh^{-1} \frac{x - \xi}{\beta r} \tag{120}$$

In supersonic flow, the behaviour of function F_1 is described following equation (102), and the real parts of G_1 and G_2 are given by equations (103) and (104), where

$$x' = (c\lambda - ax)(x - \xi) + \beta^2[y(c - ay) - az^2]$$

$$r' = c[[x - \lambda y + (c - ay)\xi/c]^2 + z^2[\beta^2 + (\lambda + a\xi/c)^2]]^{\frac{1}{2}}$$

$$d' = e\, d$$

$$e' = [-(c\lambda - ax)^2 - \beta^2\rho^2]^{\frac{1}{2}}$$

Finally, the contribution of the vortex sheet in the wake in compressible flow is given by

$$\Delta u = 0 \tag{121}$$

$$\Delta v = \frac{-a}{8\pi} \left\{ k(F_1 - F_2) - \frac{zt}{c} + \frac{(x - \lambda y)(c - ay) + a\lambda z^2}{(c - ay)^2 + a^2 z^2} u \right\}_0^c \tag{122}$$

where u and t are given by equations (114) and (117) respectively.

$$\Delta w = \frac{ka}{4\pi c^2} \left[I_1 - I_2 + I_3 \right] \tag{123}$$

where I_1, I_2 and I_3 are given by equations (83) - (85), with the Gothert transformation applied.

Aerodynamic Representation

The source and vortex distributions derived in the preceding sections provide the basis for the aerodynamic representation of the configuration. The strengths of these singularities are determined by satisfying the boundary condition of tangential flow at panel control points for given Mach number and angle of attack. In general, the control points are located at the panel centroids, except where noted below. The body is represented by constant source distributions on surface panels, but two optional methods are available to represent the wing and tail surfaces.(Here, tail surface implies any horizontal or vertical tail or canard surface.)

Planar boundary condition option.- In this option, the panels are located in the mean plane of the wing or tail surfaces. Linearly varying source distributions are used to simulate the airfoil thickness, and linearly varying vortex distributions are used to simulate the effects of camber, twist, and incidence.

The slope of the airfoil thickness distribution is approximated by linear segments between the panel leading and trailing edges. This linear distribution is constructed by superimposing a series of triangular source distributions extending over two adjacent panels. The strength of the triangular source distribution is determined by the slope of the thickness distribution at the intermediate panel edge, as illustrated below:

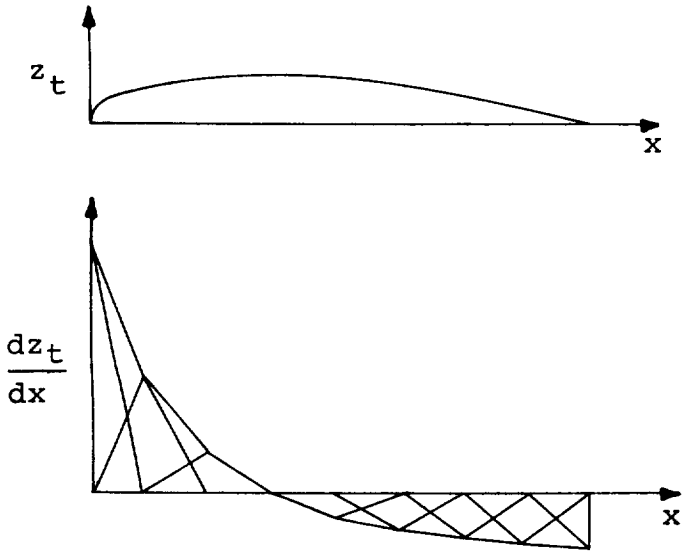

Chordwise thickness and slope distributions

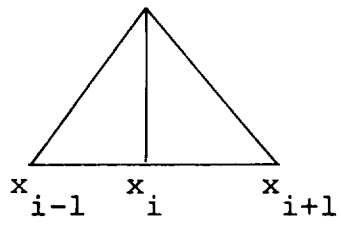

Triangular source distribution

The same method is used to approximate the chordwise vortex distribution on the wing. In this case, the strengths of the vortex distributions are determined by satisfying the boundary condition that the resultant normal velocity is zero at panel control points. A typical chordwise vortex distribution is shown below:

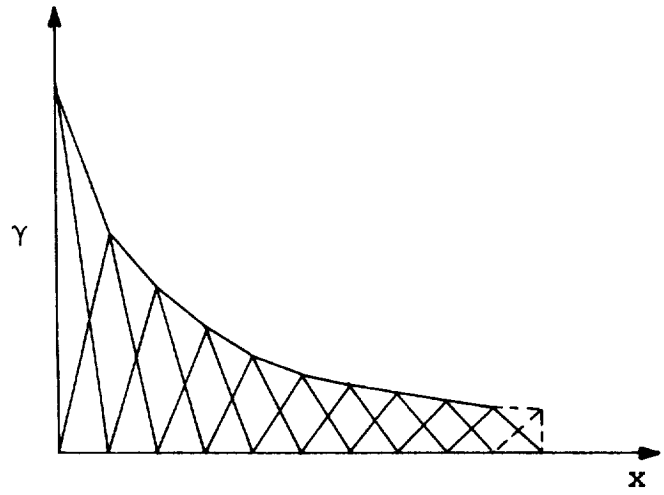

Chordwise vortex distribution

In subsonic flow, or if the trailing edge is swept behind the Mach line in supersonic flow, the Kutta condition implies that the vorticity goes to zero along the trailing edge. In this case, the control points are located at the panel centroids. If the trailing edge lies ahead of the Mach line in supersonic flow, an additional vortex singularity is added at the trailing edge, as indicated by the dashed line in the above sketch. In this case, an additional control point is added on the trailing edge of the wing, and the intermediate control points adjusted linearly between the leading edge control point and the trailing edge. If the leading edge of the wing lies on or is swept behind the Mach line, the leading edge control point is located at the centroid as before, otherwise the leading edge control point is located on the wing leading edge.

In the non-planar boundary condition option, the panels are located on the upper and lower surfaces of the wing and tail, and linear vortex distributions alone are used to simulate both lift and thickness effects. The upper and lower surface vortex distributions are similar to those described above, and the two vortex sheets are joined together at the

leading edge by equating the vortex strengths of the leading edge panels. The resulting continuous distribution of vorticity around the chord is illustrated below.

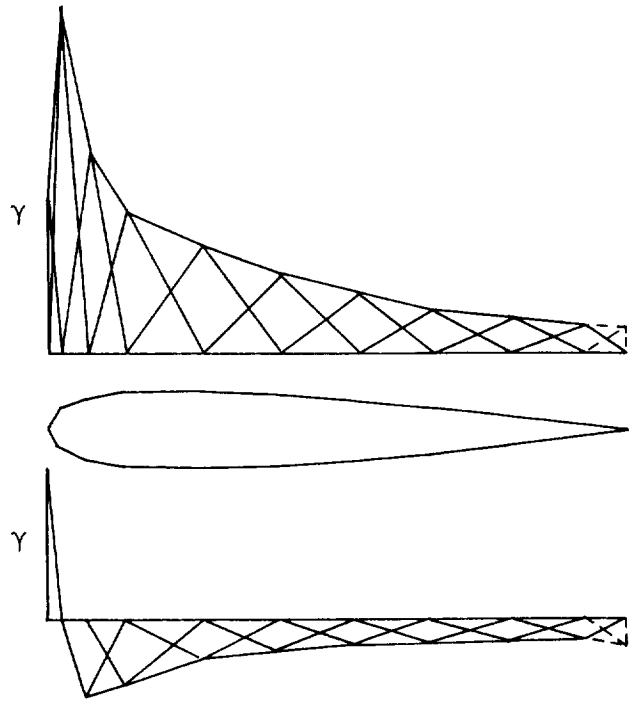

In subsonic flow, the non-planar boundary condition option presents the problem that one more control point exists than the number of vortex distributions if the Kutta condition is enforced at the trailing edge. An additional source or vortex distribution must be included to make the resulting system of equations determinate. One way to resolve this problem is to introduce an additional pair of trailing edge vortices having equal and opposite strength, as indicated by the dashed line on the above sketch. Another method is to add an internal line source at some point in the interior of the airfoil. In either method, the strength of the additional line source or vortex approaches zero and has small effect on the final solution. The second method is recommended, however, since the first tends to generate an ill-conditioned system of equations for airfoils with small trailing edge angles.

In supersonic flow, a similar problem exists if the trailing edge lies on or is swept behind the Mach line. If the trailing edge lies ahead of the Mach line, additional trailing edge vortex singularities must be added on the upper and lower

surfaces, and the strengths of these determined by satisfying the boundary conditions at additional control points on the trailing edge. The remaining vortex strengths are determined as described above. If the leading edge lies ahead of the Mach line, the vortex distributions on the upper and lower surfaces of the airfoil are determined independently using control points located on the panel leading and trailing edges.

The influence of the trailing vortices in the wake is included in the velocity component formulas derived for the constant and linearly varying vortex distributions. Since the wake is assumed to lie in the plane of the panel in these derivations, the wake vortices must be rotated at the leading edge of each downstream panel to follow the contour of the upper or lower surface of the wing to the trailing edge. The paths of the trailing edge vortices are illustrated on the following sketch.

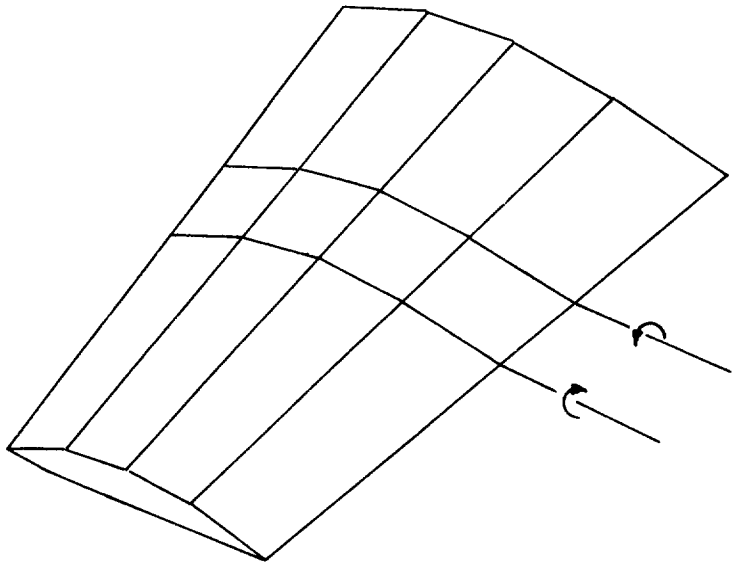

The Boundary Condition Equations

A system of linear equations is established which relates the magnitude of the velocity normal to the surface at each panel control point to the aerodynamic singularity strengths. The geometrical relationship between each influencing panel and control point is required to evaluate the coefficients of this system of equations.

Wing and body panel geometry.- A typical panel subdivision of a configuration which includes a wing, body, and tail is illustrated on figure 1 (page 8). A reference coordinate system is established with origin at or near the nose of the body, having its x axis on the center line and parallel to the body axis, and a vertical z axis. Since symmetry about the xz plane is assumed throughout this analysis, panels are located only on the positive y (right hand) side of the configuration.

The body panel corners are defined by the intersections of a series of planes normal to the x axis, and longitudinal meridian lines. A maximum of 30 rings of panels may be used, each containing up to 20 rows of panels around the circumference. The body panels are numbered in sequence from the bottom to the top of each ring, starting with the forward ring.

The wing and tail surface panel corners are defined by the intersections of a series of vertical planes parallel to the x axis, and lines of constant percent chord. A maximum of 20 columns of panels may be used, including those on the wing and all other horizontal or vertical tail or canard surfaces, and each column may contain up to 30 rows of panels. The wing and tail panels are numbered in sequence from the leading edge to the trailing edge of each column, starting with the inboard column of the wing.

For each panel, the corner point coordinates, centroid coordinates, inclination angles, area, and chord length through the centroid are calculated, using the method outlined in Appendix II. It should be noted that the panel inclination angles δ and θ are related to the direction cosines of the normal as follows:

$$\begin{aligned} n_x &= -\sin\delta \\ n_y &= -\cos\delta\sin\theta \\ n_z &= \cos\delta\cos\theta \end{aligned} \qquad (124)$$

A primed system of coordinates is introduced, originating at corner point k of panel j, and inclined at the angle θ_j with respect to the xy plane. For body panels, the x' axis is parallel to the reference x axis, and the y' axis lies in the plane of the panel through the leading edge. The panel is inclined at the angle δ_j to the x'y' plane. For wing panels, the x' axis lies in the plane of the panel along the inboard side edge, and is perpendicular to the y axis. The z' axis is normal to the panel. In this case, the x' axis is inclined at the angle δ_j to the x axis. The geometry of the wing and body panels, and panel corner point numbering convention, is illustrated below:

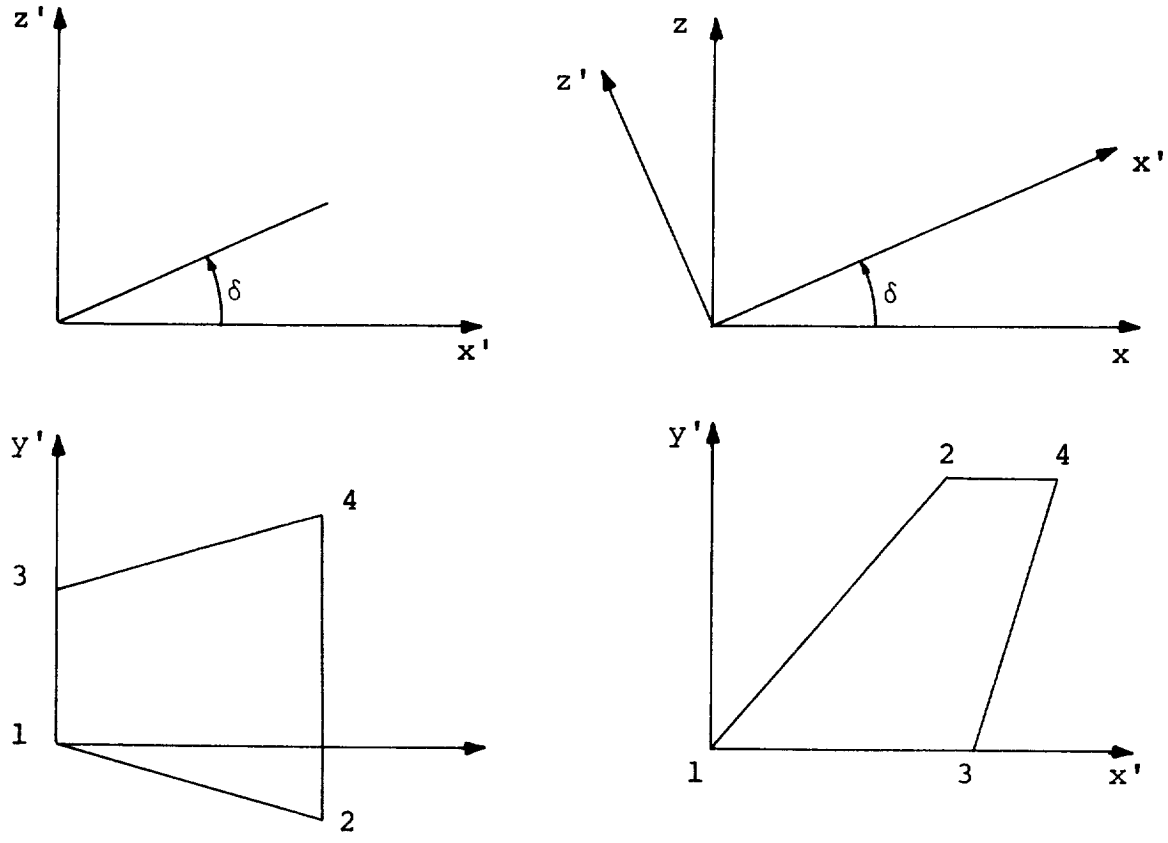

Body panel

Wing panel

The control point of a panel is defined as that point on the panel where the boundary conditions are satisfied, and each panel has a unique control point associated with it. The control point of panel i is normally located at the panel centroid. Exceptions to this rule exist for wing or tail surfaces using

planar boundary conditions, as described in the previous section. The coordinates of the control point are given in terms of the primed system originating at corner k of panel j as follows:

For body panels, and wing panels using the planar boundary condition option,

$$x_i' = \Delta x$$

$$y_i' = \Delta y \cos \theta_j + \Delta z \sin \theta_j$$

$$z_i' = \Delta z \cos \theta_j - \Delta y \sin \theta_j \qquad (125)$$

where $\Delta x = x_i - x_k$

$\Delta y = y_i - y_k$

$\Delta z = z_i - z_k$

For wing panels using the non-planar boundary condition option,

$$x_i' = \lambda_1 \Delta x + \lambda_2 \Delta y + \lambda_3 \Delta z$$

$$y_i' = \mu_1 \Delta x + \mu_2 \Delta y + \mu_3 \Delta z$$

$$z_i' = \nu_1 \Delta x + \nu_2 \Delta y + \nu_3 \Delta z \qquad (126)$$

where Δx, Δy and Δz are defined above, and

$$\lambda_1 = \frac{n_z}{(n_x^2 + n_z^2)^{\frac{1}{2}}} \qquad \lambda_2 = 0 \qquad \lambda_3 = \frac{-n_x}{(n_x^2 + n_z^2)^{\frac{1}{2}}}$$

$$\nu_1 = n_x \qquad \nu_2 = n_y \qquad \nu_3 = n_z$$

$$\mu_1 = \frac{-n_x n_y}{(n_x^2 + n_z^2)^{\frac{1}{2}}} \qquad \mu_2 = (n_x^2 + n_z^2)^{\frac{1}{2}} \qquad \mu_3 = \frac{-n_y n_z}{(n_x^2 + n_z^2)^{\frac{1}{2}}} \qquad (127)$$

The direction cosines n_x, n_y and n_z are given by equation (124) with subscript j applied to the angles θ and δ. It should be noted that equations (126) reduce to (125) for $\delta_j = 0$.

The coordinates of the image of control point i on the opposite side of the xz plane are given by equations (125) or (126) with $\Delta y = - y_i - y_k$. The image control point is used to calculate panel symmetry effects.

Calculation of the normal velocity at the control points.- The resultant velocity normal to panel i at the control point is the sum of the normal component of the free stream velocity vector and the normal velocities induced by the panel singularity distributions. In the following analysis, the free stream velocity vector is assumed to have unit magnitude, and lie in the xy plane at an angle α to the x axis. The component of the velocity vector normal to panel i is

$$\omega_i = \sin \alpha \cos \theta_i \cos \delta_i - \cos \alpha \sin \delta_i \tag{128}$$

The three components of velocity parallel to the reference axes at control point i are given by the following equations:

$$\Delta u_i = \sum_{j=1}^{N} \left[\left(\lambda_1 u'_{ij} + \mu_1 v'_{ij} + \nu_1 w'_{ij} \right) + \left(\lambda_1 \bar{u}'_{ij} + \mu_1 \bar{v}'_{ij} + \nu_1 \bar{w}'_{ij} \right) \right] \gamma_j \tag{129}$$

$$\Delta v_i = \sum_{j=1}^{N} \left[\left(\lambda_2 u'_{ij} + \mu_2 v'_{ij} + \nu_2 w'_{ij} \right) - \left(\lambda_2 \bar{u}'_{ij} + \mu_2 \bar{v}'_{ij} + \nu_2 \bar{w}'_{ij} \right) \right] \gamma_j \tag{130}$$

$$\Delta w_i = \sum_{j=1}^{N} \left[\left(\lambda_3 u'_{ij} + \mu_3 v'_{ij} + \nu_3 w'_{ij} \right) + \left(\lambda_3 \bar{u}'_{ij} + \mu_3 \bar{v}'_{ij} + \nu_3 \bar{w}'_{ij} \right) \right] \gamma_j \tag{131}$$

where N is the total number of singularities

γ_j is the strength of the j^{th} singularity

u'_{ij}, v'_{ij}, w'_{ij} are the three components of velocity induced at control point i by panel j, given in the primed coordinate system of panel j

$\bar{u}'_{ij}$, $\bar{v}'_{ij}$, $\bar{w}'_{ij}$ are the three components of velocity induced at image point i by panel j given in the primed coordinate system of panel j

and the coefficients of the transformation λ, μ, ν, are given by equations (127), where the direction cosines are associated with panel j.

The normal component of velocity at panel i induced by the panel singularity distributions is given in terms of the above velocity components as follows:

$$\Delta\omega_i = \nu_1 \Delta u_i + \nu_2 \Delta v_i + \nu_3 \Delta w_i \tag{132}$$

The coefficients ν_1, ν_2, and ν_3 are also given by equation (127), except that the direction cosines are associated with panel i.

Combining equations (128) and (132), the resultant normal velocity at control point i is

$$n_i = \omega_i + \Delta\omega_i$$

$$= \omega_i + \sum_{j=1}^{N} a_{ij}\gamma_j \tag{133}$$

where the aerodynamic influence coefficient a_{ij} can be obtained from equations (129) - (132).

For body panels, and wing panels using the planar boundary condition option, the x' axis is parallel to the reference x axis, and $\delta_j = 0$. In this case, the normal and tangential

velocity at control point i can be written

$$w_i'' = \sum_{j=1}^{N} \left[w'_{ij} \cos (\theta_j - \theta_i) + v'_{ij} \sin (\theta_j - \theta_i) + \bar{w}'_{ij} \cos (\theta_j + \theta_i) + \bar{v}'_{ij} \sin (\theta_j + \theta_i) \right] \gamma_j \qquad (134)$$

$$v_i'' = \sum_{j=1}^{N} \left[v'_{ij} \cos (\theta_j - \theta_i) - w'_{ij} \sin (\theta_j - \theta_i) - \bar{v}'_{ij} \cos (\theta_j + \theta_i) + \bar{w}'_{ij} \sin (\theta_j + \theta_i) \right] \gamma_j \qquad (135)$$

and the three components of velocity parallel to the reference axes at control point i are:

$$\Delta u_i = \sum_{j=1}^{N} (u'_{ij} + \bar{u}'_{ij}) \gamma_j$$

$$\Delta v_i = v_i'' \cos \theta_i - w_i'' \sin \theta_i$$

$$\Delta w_i = w_i'' \cos \theta_i + v_i'' \sin \theta_i \qquad (136)$$

Then, from equation (132)

$$\Delta \omega_i = w_i'' \cos \delta_i - \Delta u_i \sin \delta_i \qquad (137)$$

Formation of the boundary condition equations.- The boundary condition equations are obtained by setting $n_i = 0$ in equation (133). The complete set of equations may be written:

$$\sum_{i=1}^{N} \sum_{j=1}^{N} a_{ij} \gamma_j = - \sum_{i=1}^{N} \omega_i \qquad (138)$$

Alternatively, in matrix notation,

$$[A_{ij}] \{\gamma_j\} = - \{\omega_i\} \qquad (139)$$

where A_{ij} is the matrix of aerodynamic influence coefficients, and ω_i is given by equation (128). In general, the matrix is subdivided into four partitions in order to simplify the calculation procedures. The first partition, ABB, gives the influence of the body panels on the body control points, the second, ABW, gives the influence of the wing panels on the body control points, the third, AWB, gives the influence of the body panels on the wing control points, and the fourth, AWW, gives the influence of the wing panels on the wing control points. Equation (139) is rewritten in terms of these four partitions below.

$$\begin{bmatrix} ABB & ABW \\ AWB & AWW \end{bmatrix} \begin{Bmatrix} \gamma_B \\ \gamma_W \end{Bmatrix} = - \begin{Bmatrix} \omega_B \\ \omega_W \end{Bmatrix} \tag{140}$$

The subscripts W and B refer to wing or body panels. In the present program, the maximum order of each partition is 600.

The right side of the boundary condition equations is modified if the planar boundary condition option is selected. In this case, the slope of the wing surface is given by:

$$\tan \delta_i = \left(\frac{dz_c}{dx} \pm \frac{dz_t}{dx} \right)_i \tag{141}$$

where $\frac{dz_c}{dx}$ is the slope of the wing camber surface.

$\frac{dz_t}{dx}$ is the slope of the wing thickness distribution.

The positive sign applies to the upper surface, the negative sign to the lower surface.
In addition, the normal velocity at control point i is given by

$$\Delta\omega_i = \sum_{j=1}^{N} a_{ij} \gamma_j + \cos \alpha \sum_{j=1}^{NW} b_{ij} \left(\frac{dz_t}{dx} \right)_j \tag{142}$$

where $b_{ij} = \cos \delta_i \left(w_{ij} \cos \theta_i - v_{ij} \sin \theta_i - u_{ij} \tan \delta_i \right)$

NW is the number of wing panels,

and u_{ij}, v_{ij}, w_{ij} are the velocity components induced at control point i by the source distribution on wing panel j

The second term in equation (142) is multiplied by cos α, the projection of the free stream velocity vector in the plane of the wing.

Combining equations (128) and (142)

$$n_i = \cos \delta_i [\sin \alpha \cos \theta_i - \cos \alpha \tan \delta_i] + \sum_{j=1}^{N} a_{ij} \gamma_j + \cos \alpha \sum_{j=1}^{NW} b_{ij} \left(\frac{dz_t}{dx} \right)_j \quad (143)$$

Setting $n_i = 0$, the new boundary condition equations are:

$$\sum_{i=1}^{N} \sum_{j=1}^{N} a_{ij} \gamma_j = \sum_{i=1}^{N} \omega_i \quad (144)$$

where $\omega_i = \cos \delta_i [\cos \alpha \tan \delta_i - \sin \alpha \cos \theta_i] - \cos \alpha \sum_{j=1}^{NW} b_{ij} \left(\frac{dz_t}{ax} \right)_j \quad (145)$

On the wing, tan δ_i is given by equation (141). Furthermore, for panels lying in the plane of the wing,

$$\frac{dz_t}{dx} \cos \delta_i = \sum_{j=1}^{NW} b_{ij} \left(\frac{dz_t}{dx} \right)_j$$

So that

$$\omega_i = \cos \delta_i \left[\cos \alpha \left(\frac{dz_c}{dx} \right)_i - \sin \alpha \cos \theta_i \right] \quad (146)$$

For non-coplanar wing or tail segments, equation (145) must be used.

Solution of the boundary condition equations.- Several methods could be employed to solve the boundary condition equations for the unknown source and vortex strengths. For example, equation (139) could be solved by direct inversion, even though this is generally impractical for dense matrices of orders up to 1200. On the other hand, the partitioned matrix of equation (140) can be solved using the method described in reference 1, which requires the inversion of only the diagonal partitions, having a maximum order of 600, together with matrix multiplications of the off-diagonal partitions.

A rapidly convergent iteration scheme for solving large order systems of equations has been reported in reference 5. In this method, as applied in this report, the partitions are further subdivided into smaller blocks, with no block exceeding order 60. The matrix elements in each block are carefully chosen to represent some well defined feature of the original configuration. For example, a body block represents the influence of one ring of panels around the body, while a wing block represents the influence of one chordwise column of wing panels. For wings using the non-planar boundary condition option, the block size corresponds to the total number of panels on the upper and lower surface of the column.

The initial iteration calculates the source and vortex strengths corresponding to each block in isolation. For this step, only the diagonal blocks are present in the aerodynamic matrix. Once the initial approximation to the source and vortex strengths is determined, the interference effect of each block on all the others is calculated by matrix multiplication. The incremental normal velocities obtained are subtracted from the normal velocities specified by the boundary conditions. This process is repeated 15 to 20 times, or until the residual interference velocities are small enough to ensure that convergence has occured. At present the computer program repeats the iteration a fixed number of times, namely 15.

The procedure is illustrated below for an aerodynamic matrix consisting of nine blocks. The unknown singularity strengths are designated γ_j, the specified normal velocities ω_i.

To solve $$A_{ij} \quad \gamma_j = \omega_i$$

where $$A_{ij} = \begin{bmatrix} A_{11} & A_{12} & A_{13} \\ A_{21} & A_{22} & A_{23} \\ A_{31} & A_{32} & A_{33} \end{bmatrix}$$

Put $A = D + E$

$$= \begin{bmatrix} A_{11} & 0 & 0 \\ 0 & A_{22} & 0 \\ 0 & 0 & A_{33} \end{bmatrix} + \begin{bmatrix} 0 & A_{12} & A_{13} \\ A_{21} & 0 & A_{23} \\ A_{31} & A_{32} & 0 \end{bmatrix}$$

Therefore $[D + E]\{\gamma\} = \{\omega\}$

or $$\{\gamma\} = D^{-1}\{\omega - E\{\gamma\}\}$$

First approximation:

$$\{\gamma\}^1 = D^{-1}\{\omega\}$$

Calculate $$\Delta\omega^1 = E\{\gamma\}^1$$

Second approximation:

$$\{\gamma\}^2 = D^{-1}\{\omega - \Delta\omega^1\}$$

Similarly, k^{th} approximation:

$$\{\gamma\}^k = D^{-1}\{\omega - \Delta\omega^{k-1}\}$$

Note that $$D^{-1} = \begin{bmatrix} A_{11}^{-1} & 0 & 0 \\ 0 & A_{22}^{-1} & 0 \\ 0 & 0 & A_{33}^{-1} \end{bmatrix}$$

Calculation of Pressures, Forces, and Moments

Once the strengths of the aerodynamic singularities have been determined, the three components of velocity at a point i can be determined as follows:

$$u_i = \Delta u_i + \cos \alpha \tag{147}$$

$$v_i = \Delta v_i \tag{148}$$

$$w_i = \Delta w_i + \sin \alpha \tag{149}$$

where Δu_i, Δv_i and Δw_i are given by equations (129) - (131).

If the planar boundary condition option has been selected, the incremental velocity components induced by the wing thickness distribution must also be calculated and added to the above equations. The pressure coefficient is then calculated using the exact isentropic formula

$$C_{p_i} = \frac{-2}{\gamma M^2} \left\{ \left[1 + \frac{\gamma - 1}{2} M^2 (1 - q_i^2) \right]^{3.5} - 1 \right\} \tag{150}$$

where $q_i^2 = u_i^2 + v_i^2 + w_i^2$

For $M = 0$,

$$C_{p_i} = 1 - q_i^2 \tag{151}$$

The forces and moments acting on the configuration can then be calculated by numerical integration. The normal force, tangential force, and pitching moment about the origin of coordinates of panel i are given by:

$$N_i = - A_i C_{p_i} \cos \theta_i \cos \delta_i \tag{152}$$

$$T_i = A_i C_{p_i} \sin \delta_i \tag{153}$$

$$M_i = N_i x_i - T_i z_i \tag{154}$$

where A_i is the panel area

θ_i, δ_i are the panel inclination angles, defined by equation (124)

x_i, z_i are the coordinates of the panel control point

The total force and moment coefficients acting on the configuration are obtained by summing the panel forces and moments on both sides of the plane of symmetry.

$$C_N = \frac{1}{S} \sum_{i=1}^{N} 2N_i \tag{155}$$

$$C_T = \frac{1}{S} \sum_{i=1}^{N} 2T_i \tag{156}$$

$$C_M = \frac{1}{S\bar{c}} \sum_{i=1}^{N} 2M_i \tag{157}$$

Finally, the lift and drag coefficients are:

$$C_L = C_N \cos \alpha - C_T \sin \alpha \tag{158}$$

$$C_D = C_N \sin \alpha + C_T \cos \alpha \tag{159}$$

The computer program computes the forces and moment acting on the body, the wing and tail surfaces, and the complete configuration. In addition, section forces and moment may be calculated for the wing and tail surfaces as an optional output.

COMPUTER PROGRAM

Program Description

A computer program has been developed to calculate the pressure distribution and aerodynamic characteristics of wing-body-tail combinations in subsonic and supersonic flow. The program is written in CDC FORTRAN IV, version 2.3 for a SCOPE 3.0 operating system and library file. It is designed for the CDC 6000 series of computers, occupies 70,000 (octal) words, and operates in OVERLAY mode. The program requires five peripheral disc files in addition to the input and output files.

Program Structure

The overlay structure of the program is illustrated on Figure 2. The main overlay program is designated USSAERO, and calls the three primary overlay programs GEOM, VELCMP, and SOLVE. In turn, GEOM calls seven secondary overlay programs CONFIG, NEWORD, WNGPAN, NEWRAD, BODPAN, NUTORD, and TALPAN, while VELCMP calls three secondary overlay programs BODVEL, LINVEL, and WNGVEL.

The complete program consists of 14 overlay programs and 19 subroutines. Detailed descriptions of each program and subroutine are given in Part II of this report. These descriptions give the purpose of the program or subroutine, outline the method used, and list the names of the principal variables and constants.

Operating Instructions

The program deck and data deck are loaded in the following sequence: job card, system control cards, end-of-record card, program deck, end-of-record card, input data deck, and end-of-file card. The input data deck is described in the following section.

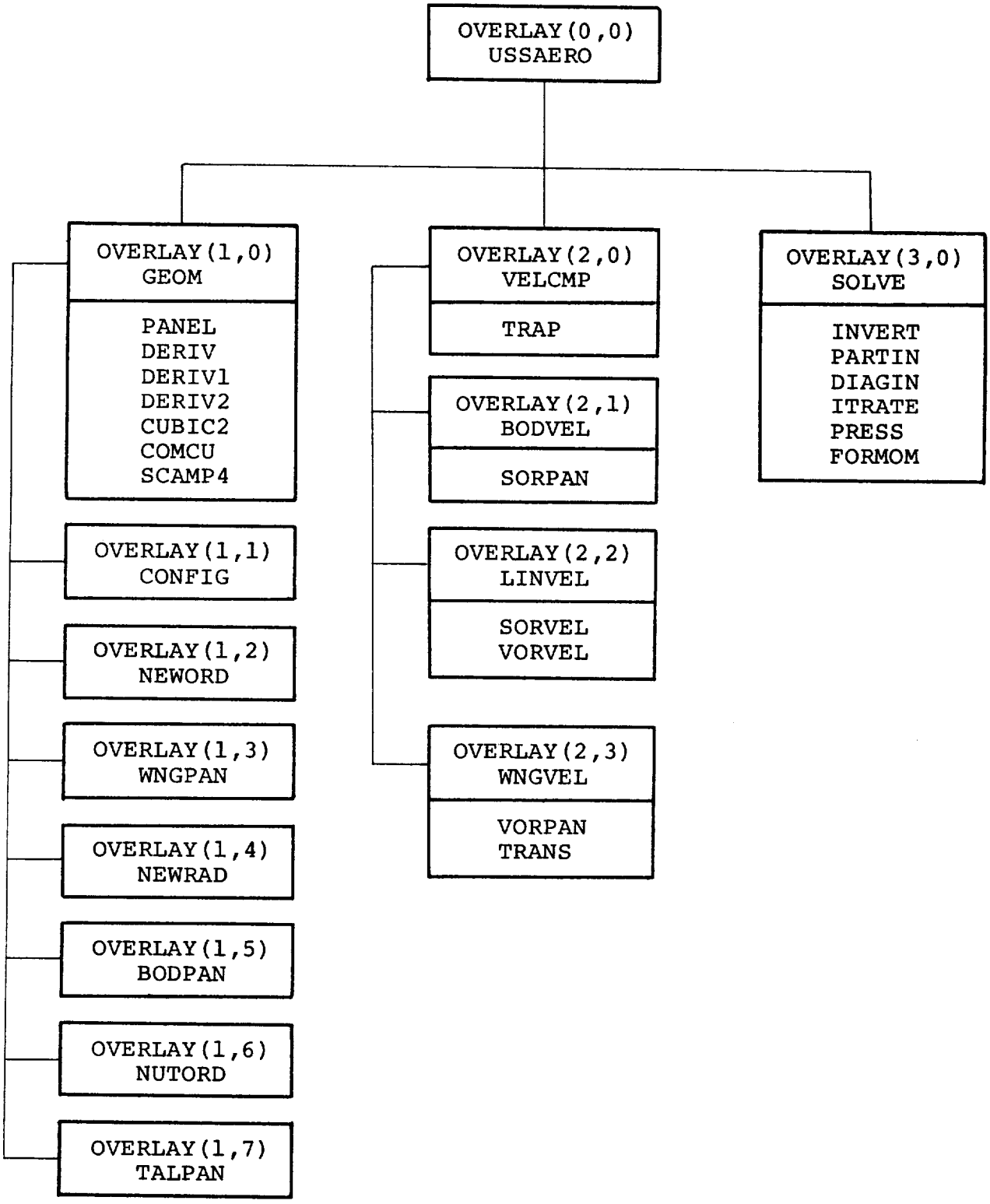

Figure 2 - Program Overlay Structure

Program Input Data

The input to this program consists of two basic parts, namely, the numerical description of the configuration geometry as described in reference 3, and an auxiliary data set specifying the singularity paneling scheme, program options, Mach number, and angle of attack. The program input is illustrated by the sample case presented in Appendix III.

Description of configuration geometry input cards.- The configuration is defined to be symmetrical about the xz plane, therefore only one side of the configuration need be described. The convention used in this program is to present that half of the configuration located on the positive y side of the xz plane. The number of input cards depends on the number of components used to describe the configuration, and the amount of detail used to describe each component.

Card 1 - Identification.- Card 1 contains any desired identifying information in columns 1-80.

Card 2 - Control integers.- Card 2 contains 24 integers, each punched right justified in a 3-column field. Columns 73-80 may be used in any desired manner. Card 2 contains the following:

Columns	Variable	Value	Description
1-3	J0	0	No reference area
		1	Reference area to be read
4-6	J1	0	No wing data
		1	Cambered wing data to be read
		-1	Uncambered wing data to be read
7-9	J2	0	No fuselage data
		1	Data for arbitrarily shaped fuselage to be read
		-1	Data for circular fuselage to be read (With J6=0, fuselage will be cambered. With J6=-1, fuselage will be symmetrical with xy-plane. With J6=1, entire configuration will be symmetrical with xy-plane)
10-12	J3	0	No pod (nacelle) data
		1	Pod (nacelle) data to be read

Columns	Variable	Value	Description
13-15	J4	0	No fin (vertical tail) data
		1	Fin (vertical tail) data to be read
16-18	J5	0	No canard (horizontal tail) data
		1	Canard (horizontal tail) data to be read
19-21	J6	0	A cambered circular or arbitrary fuselage if J2 is nonzero
		1	Complete configuration is symmetrical with respect to xy-plane, which implies an uncambered circular fuselage if there is a fuselage
		-1	Uncambered circular fuselage with J2 nonzero
22-24	NWAF	2-20	Number of airfoil sections used to describe the wing
25-27	NWAFOR	3-30	Number of ordinates used to define each wing airfoil section. If the value of NWAFOR is input with a negative sign, the program will expect to read lower surface ordinates also
28-30	NFUS	1-4	Number of fuselage segments
31-33	NRADX(1)	3-30	Number of points used to represent half-section of first fuselage segment. If fuselage is circular, the program computes the indicated number of y- and z-ordinates
34-36	NFORX(1)	2-30	Number of stations for first fuselage segment
37-39	NRADX(2)	3-30	Same as NRADX(1), but for second fuselage segment
40-42	NFORX(2)	2-30	Same as NFORX(1), but for second fuselage segment
43-45	NRADX(3)	3-30	Same as NRADX(1), but for third fuselage segment

Columns	Variable	Value	Description
46-48	NFORX(3)	2-30	Same as NFORX(1), but for third fuselage segment
49-51	NRADX(4)	3-30	Same as NRADX(1), but for fourth fuselage segment
52-54	NFORX(4)	2-30	Same as NFORX(1), but for fourth fuselage segment
55-57	NP	0-9	Number of pods described
58-60	NPODOR	4-30	Number of stations at which pod radii are to be specified
61-63	NF	0-6	Number of fins (vertical tails) to be described
64-66	NFINOR	3-10	Number of ordinates used to describe each fin (vertical tail) airfoil section
67-69	NCAN	0-2	Number of canards (horizontal tails) to be described
70-72	NCANOR	3-10	Number or ordinates used to define each canard (horizontal tail) airfoil section. If the value of NCANOR is input with a negative sign, the program will expect to read lower surface ordinates also, otherwise the airfoil is assumed to be symmetrical

Cards 3, 4, . . . - remaining input data cards.- The remaining input data cards contain a detailed description of each component of the configuration. Each card contains up to 10 values, each value punched in a 7-column field with a decimal point and may be identified in columns 73-80. The cards are arranged in the following order: reference area, wing data cards, fuselage data cards, pod data cards, fin (vertical tail) data cards, and canard (horizontal tail) data cards.

Reference area card: The reference area value is punched in columns 1-7 and may be identified as REFA in columns 73-80.

Wing data cards: The first wing data card (or cards) contains the locations in percent chord at which the ordinates of

all the wing airfoils are to be specified. There will be exactly NWAFOR locations in percent chord given. Each card may be identified in columns 73-80 by the symbol XAFJ where J denotes the last location in percent chord given on that card.

The next wing data cards (there will be NWAF cards) each contain four numbers which give the origin and chord length of each of the wing airfoils that is to be specified. The card representing the most inboard airfoil is given first, followed by the cards for successive airfoils. These cards contain the following:

Columns	Contents
1-7	x-ordinate of airfoil leading edge
8-14	y-ordinate of airfoil leading edge
15-21	z-ordinate of airfoil leading edge
22-28	airfoil streamwise chord length
73-80	card identification, WAFORGJ where J denotes the paricular airfoil, thus WAFORG1 denotes the most inboard airfoil

If a cambered wing has been specified, the next set of wing data cards is the mean camber line cards. There will be NWAFOR values of delta z referenced to the z-ordinate of the airfoil leading edge, each value corresponding to a specified percent chord location on the airfoil. These cards are arranged in the order which begins with the most inboard airfoil and proceeds outboard. Each card may be identified in columns 73-80 as TZORDJ where J denotes the particular airfoil. Note that the z-ordinates are dimensional.

Next are the wing ordinate cards. There will be NWAFOR values of half-thickness specified for each airfoil expressed as percent chord. These cards are arranged in the order which begins with the most inboard airfoil and proceeds outboard. Each card may be identified in columns 73-80 as WAFORDJ where J denotes the particular airfoil.

Fuselage data cards: The first card (or cards) specifies the x values of the fuselage stations of the first segment. There will be NFORX(1) values and the cards may be identified in columns 73-80 by the symbol XFUSJ where J denotes the number of the last fuselage station given on that card.

If the fuselage is circular, the next card (or cards) gives the fuselage cross sectional areas, and may be identified in columns 73-80 by the symbol FUSARDJ where J denotes the number of the last fuselage station given on that card. If the fuselage is of arbitrary shape, NRADX(1) values of the y-ordinates for a half-section are given and identified in columns 73-80 as YJ where J is the station number. Following the y-ordinates are the NRADX(1) values of the corresponding z-ordinates for the half-section identified in columns 73-80 as ZJ where J is the station number. Each station will have a set of y and z, and the convention of ordering the ordinates from bottom to top is observed.

For each fuselage segment a new set of cards as described must be provided. The segment descriptions should be given in order of increasing values of x.

Pod data cards: The first pod (nacelle) data card specifies the location of the origin of the first pod. The card contains the following:

Columns	Contents
1-7	x-ordinate of origin of first pod
8-14	y-ordinate of origin of first pod
15-21	z-ordinate of origin of first pod
73-80	card identification, PODORGJ where J denotes the pod number

The next pod input data card (or cards) contains the x-ordinates, referenced to the pod origin, at which NPODOR values of the pod radii are to be specified. The first x value must be zero and the last x value is the length of the pod. These cards may be identified in columns 73-80 by the symbol XPODJ where J denotes the pod number.

For each additional pod, new PODORG, XPOD, and PODR cards must be provided. Only single pods are described but the program assumes that if the y-ordinate is not zero an exact duplicate is located symmetrically with respect to the xz-plane, a y-ordinate of zero implies a single pod.

Fin data cards: Exactly three data input cards are used to describe a fin (vertical tail). The first fin data card contains the following:

Columns	Contents
1-7	x-ordinate on inboard airfoil leading edge
8-14	y-ordinate of inboard airfoil leading edge
15-21	z-ordinate of inboard airfoil leading edge
22-28	chord length of inboard airfoil
29-35	x-ordinate of outboard airfoil leading edge
36-42	y-ordinate of outboard airfoil leading edge
43-49	z-ordinate of outboard airfoil leading edge
50-56	chord length of outboard airfoil
73-80	card identification, FINORGJ where J denotes the fin number

The second fin input data card contains NFINOR values of x expressed in percent chord at which the fin airfoil ordinates are to be specified. The card may be identified in columns 73-80 as XFINJ where J denotes the fin number.

The third fin input data card contains NFINOR values of the fin airfoil half-thickness expressed in percent chord. Since the fin airfoil must be symmetrical, only the ordinates on the positive y side of the fin chord plane are specified. The card identification FINORDJ may be given in columns 73-80 where J denotes the fin number.

For each fin, new FINORG, XFIN, and FINORD cards must be provided. Only single fins are described but the program assumes that if the y-ordinate is not zero an exact duplicate is located symmetrically with respect to the xz-plane, a y-ordinate of zero implies a single fin.

Canard data cards: If the canard (or horizontal tail) airfoil is symmetrical, exactly three cards are used to describe a canard, and the input is given in the same manner as for a fin. If, however, the canard airfoil is not symmetrical

(indicated by a negative value of NCANOR), a fourth canard input data card will be required to give the lower ordinates. The information presented on the first canard input data card is as follows:

Columns	Contents
1-7	x-ordinate of inboard airfoil leading edge
8-14	y-ordinate of inboard airfoil leading edge
15-21	z-ordinate of inboard airfoil leading edge
22-28	chord length of inboard airfoil
29-35	x-ordinate of outboard airfoil leading edge
36-42	y-ordinate of outboard airfoil leading edge
43-49	z-ordinate of outboard airfoil leading edge
50-56	chord length of outboard airfoil
73-80	card identification, CANORGJ where J denotes the canard number

The second canard input data card contains NCANOR values of x expressed in percent chord at which the canard airfoil ordinates are to be specified. The card may be identified in columns 73-80 as XCANJ where J denotes the canard number.

The third canard input data card contains NCANOR values of the canard airfoil half-thickness expressed in percent chord. This card may be identified in columns 73-80 as CANORDJ where J denotes the canard number. If the canard airfoil is not symmetrical, the lower ordinates are presented on a second CANORD card. The program expects both upper and lower ordinates to be punched as positive values in percent chord.

For another canard, new CANORG, XCAN, and CANORD cards must be provided.

Description of Auxiliary Input Cards

Card 1.1 - Identification.- Card 1.1 contains any desired identifying information in columns 1-80.

Card 1.2 - Boundary condition and control point definition.- Non planar boundary conditions are always applied on a body, however card 1.2 permits the selection of boundary conditions to apply on a wing, fin (vertical tail), or canard (horizontal tail). This card also selects the output print options. This card contains the following:

Columns	Variable	Value	Description
1-3	LINBC	0	Control points on surface of wing, fin (vertical tail), and canard (horizontal tail). This is referred to as the nonplaner boundary condition option.
		1	Control points in plane of wing, fin (vertical tail), and canard (horizontal tail). This is referred to as the planar boundary condition option.
4-6	THICK	0	Do not calculate wing thickness matrix
		1	Calculate wing thickness matrix if LINBC = 1
7-9	PRINT	0	Print out the pressures and the forces and moments
		1	Print out option 0 and the spanwise loads on the wing, fins, and canards
		2	Print out option 1 and the velocity components and source and vortex strengths
		3	Print out option 2 and the steps in the iterative solution
		4	Print out option 3 and the axial and normal velocity matrices

A negative value of print adds the panel geometry print out to the output indicated for options 1-4.

LINBC, THICK, and PRINT are punched as right justified integers. THICK is not used if LINBC = 0.

Card 2.1 - Revised configuration paneling description control integers.- The contents of card 2.1 are punched as right justified integers as follows:

Columns	Variable	Value	Description
1-3	K0	0	No reference lengths
		1	Reference length data to be read
4-6	K1	0	No wing data
		1	Wing data to be read, wing has a sharp leading edge
		3	Wing data to be read, wing has a round leading edge
7-9	K2	0	No body data
		1	Body data follows
10-12	K3		Not used
13-15	K4	0	No fin (vertical tail) data
		1	Fin (vertical tail) data to be read, fin has a sharp leading edge
		3	Fin (vertical tail) data to be read, fin has a round leading edge
16-18	K5	0	No canard (horizontal tail) data
		1	Canard (horizontal tail) data to be read, canard has a sharp leading edge
		3	Canard (horizontal tail) data to be read, canard has a round leading edge
19-21	K6		Not used
22-24	KWAF	0, 2-20	Number of wing sections used to define the inboard and outboard panel edges. If KWAF = 0, the panel edges are defined by NWAF in the geometry input
25-27	KWAFOR	0, 3-30	Number of ordinates used to define the leading and trailing edges of the wing panels. If KWAFOR = 0, the panel edges are defined by NWAFOR in the geometry input

Columns	Variable	Value	Description
28-30	KFUS		The number of fuselage segments. The program sets KFUS = NFUS
31-33	KRADX(1)	0, 3-20	Number of meridian lines used to define panel edges on first body segment. There are three options for defining the panel edges. If KRADX(1) = 0, the meridian lines are defined by NRADX(1) in the geometry input. If KRADX(1) is positive, the meridian lines are calculated at KRADX(1) equally spaced PHIKs. If KRADX(1) is negative, the meridian lines are calculated at specified values of PHIK
34-36	KFORX(1)	0, 2-30	Number of axial stations used to define leading and trailing edges of panels on first body segment. If KFORX(1) = 0, the panel edges are defined by NFORX(1) in the geometry input
37-39	KRADX(2)	0, 3-20	Same as KRADX(1), but for second body segment
40-42	KFORX(2)	0, 2-30	Same as KFORX(1), but for second body segment
43-45	KRADX(3)	0, 3-20	Same as KRADX(1), but for third body segment
46-48	KFORX(3)	0, 2-30	Same as KFORX(1), but for third body segment
49-51	KRADX(4)	0, 3-20	Same as KRADX(1), but for fourth body segment
52-54	KFORX(4)	0, 2-30	Same as KFORX(1), but for fourth body segment

The program is restricted to 600 body singularity panels. For this program there is an additional restriction that the total number of singularity panels in the axial direction on the body (fuselage) cannot exceed 30. The arbitrary body (fuselage) capability of this program is limited to those shapes for which the radius is a single-valued function of PHIK for each cross section of the body.

Card 2.2 - Additional revised configuration paneling description control integers.- The contents of card 2.2 are punched as right justified integers as follows:

Columns	Variable	Value	Description
1-3	KF(1)	0, 2-20	Number of fin sections used to define the inboard and outboard panel edges on the first fin. If KF(1) = 0, the root and tip chords define the panel edges
4-6	KFINOR(1)	0, 3-30	Number of ordinates used to define the leading and trailing edges of the fin panels on the first fin. If KFINOR(1) = 0, the panel edges are defined by NFINOR
7-9	KF(2)	0, 2-20	Same as for KF(1), but for second fin
10-12	KFINOR(2)	0, 3-30	Same as for KFINOR(1), but for second fin
13-15	KF(3)	0, 2-20	Same as for KF(1), but for third fin
16-18	KFINOR(3)	0, 3-30	Same as for KFINOR(1), but for third fin
19-21	KF(4)	0, 2-20	Same as for KF(1), but for fourth fin
22-24	KFINOR(4)	0, 3-30	Same as for KFINOR(1), but for fourth fin
25-27	KF(5)	0, 2-20	Same as for KF(1), but for fifth fin
28-30	KFINOR(5)	0, 3-30	Same as for KFINOR(1), but for fifth fin
31-33	KF(6)	0, 2-20	Same as for KF(1), but for sixth fin
34-36	KFINOR(6)	0, 3-30	Same as for KFINOR(1), but for sixth fin

Columns	Variable	Value	Description
37-39	KCAN(1)	0, 2-20	Number of canard sections used to define the inboard and outboard panel edges on the first canard. If KCAN(1) = 0, the root tip chords define the panel edges. If KCAN(N) negative, no vortex sheets carry through the body and concentrated vortices are shed from the inboard edge of the canard or tail surface
40-42	KCANOR(1)	0, 3-30	Number of ordinates used to define the leading and trailing edges of the first canard. If KCANOR(1)=0, the panel edges are defined by NCANOR
43-45	KCAN(2)	0, 2-20	Same as for KCAN(1), but for second canard
46-48	KCANOR(2)	0, 3-30	Same as for KCANOR(1), but for second canard
49-51	KCAN(3)	0, 2-20	Same as for KCAN(1), but for third canard
52-54	KCANOR(3)	0, 3-30	Same as for KCANOR(1), but for third canard
55-57	KCAN(4)	0, 2-20	Same as for KCAN(1), but for fourth canard
58-60	KCANOR(4)	0, 3-30	Same as for KCANOR(1), but for fourth canard
61-63	KCAN(5)	0, 2-20	Same as for KCAN(1), but for fifth canard
64-66	KCANOR(5)	0, 3-30	Same as for KCANOR(1), but for fifth canard
67-69	KCAN(6)	0, 2-20	Same as for KCAN(1), but for sixth canard
70-72	KCANOR(6)	0, 3-30	Same as for KCANOR(1), but for sixth canard

The program is restricted to a total of 600 singularity panels on the wing-fin-canard combination.

For this program there is an additional restriction that the total number of singularity panels in the spanwise direction on the wing-fin-canard combination cannot exceed 20.

Cards 3, 4, . . . - remaining input data cards.- The remaining input data cards contain a detailed description of the singularity paneling of each component of the configuration. Each card contains up to 10 values, each value punched in a 7-column field with a decimal point and may be identified in columns 73-80. The cards are arranged in the following order: reference lengths, wing data cards, fin (vertical tail) data cards, canard (horizontal tail) data cards, fuselage (body) data cards, and finally Mach number and angle of attack case cards. Note that the present program will not handle a pod and therefore there are no pod panel inputs. However, if the geometry input contains a pod description it will be read and ignored.

Reference length card: This card may be identified as REFL in columns 73-80 and contains the following:

Columns	Variable	Description
1-7	REFA	Wing reference area. If REFA = 0, the reference area is defined by the value of REFA in the geometry input
8-14	REFB	Wing semispan. If REFB = 0, a value of 1.0 is used for the reference semispan
15-21	REFC	Wing reference chord. If REFC = 0, a value of 1.0 is used for the reference chord
22-28	REFD	Body (fuselage) reference diameter. If REFD = 0, a value of 1.0 is used for the reference diameter
29-35	REFL	Body (fuselage) reference length. If REFL = 0, a value of 1.0 is used for the reference length
36-42	REFX	X coordinate of moment center
43-49	REFZ	Z coordinate of moment center

Wing data cards: The first wing data card is the wing leading edge radius card and is required only when K1 = 3. This card contains NWAF values of leading edge radius expressed in percent chord. It may be identified in columns 73-80 as RHOJ where J denotes the number of the last radius given on that card.

Next is the wing panel leading edge card. This card contains KWAFOR values of wing panel leading edge locations expressed in percent chord. This card may be identified in columns 73-80 as XAFKJ where J denotes the last location in percent chord given on that card. Omit if KWAFOR = 0.

The last wing data card gives the wing panel side edge data. This card contains KWAF values of the y ordinate of the panel inboard edges. This card may be identified in columns 73-80 as YKJ where J denotes the last y ordinate on that card. These values are arranged in the order which begins with the most inboard panel edge and proceeds outboard. Omit if KWAF = 0.

Fin (vertical tail) data cards: The first fin data card is the fin leading edge radius card and is required only when K4 = 3. This card contains NF values of leading edge radius expressed in percent chord, one value for each fin. It may be identified in columns 73-80 as RHOFIN.

Next is the fin panel leading edge card for the first fin. This card contains KFINOR(1) values of fin panel leading edge locations expressed in percent chord. This card may be identified in columns 73-80 as XFINKJ where J denotes the fin number. Repeat this card for each fin.

The last fin data card gives the fin panel side edge data for the first fin. This card contains KF(1) values of the z ordinate of the panel inboard edges. This card may be identified in columns 73-80 as ZFINKJ where J denotes the fin number. These values are arranged in the order that begins with the most inboard panel edge and proceeds outboard. Repeat this card for each fin.

Canard (horizontal tail) data cards: The first canard data card is the canard leading edge radius card and is required only when K5 = 3. This card contains NCAN values of leading edge radius expressed in percent chord, one value for each canard. It may be identified in columns 73-80 as RHOCAN.

Next is the canard panel leading edge card for the first canard. This card contains KCANOR(1) values of canard panel leading edge locations expressed in percent chord. This card may be identified in columns 73-80 as XCANKJ where J denotes the canard number. Repeat this card for each canard.

The last canard data card gives the canard panel side edge data for the first canard. This card contains KCAN(1) values of the y ordinate of the panel inboard edges. This card may be identified in columns 73-80 as YCANKJ where J denotes the canard number. These values are arranged in the order that begins with the most inboard panel edge and proceeds outboard. Repeat this card for each canard.

Fuselage (body) data cards: The first body card is the body meridian angle card. This card contains KRADX(1) values of body meridian angle expressed in degrees and may be identified in columns 73-80 as PHIKJ where J denotes the body segment number. The convention is observed that PHIK = 0. at the bottom of the body and PHIK = 180. at the top of the body. Omit unless KRADX(1) is negative. Repeat this card for each fuselage segment.

The second body card is the body axial station card. This card contains KFORX(1) values of the x ordinate of the body axial stations and may be identified in columns 73-80 as XFUSKJ where J denotes the body segment number. Omit if KFORX(1) = 0. Repeat this card for each fuselage segment.

Mach number and angle of attack card: This card may be identified in columns 73-80 as MALPHA and contains the following:

Columns	Variable	Description
1-7	MACH	The subsonic Mach number (including the value MACH = 0.) or the supersonic Mach number at which it is desired to calculate the aerodynamic data
8-14	ALPHA	The angle of attack expressed in degrees at which it is desired to calculate the aerodynamic data

A series of Mach number and angle of attack combinations for the same geometry may be calculated by repeating this card with the desired values.

A value of MACH = -1. on this card signifies the termination of the present case. Geometry cards for a new case can follow such a terminal card.

Program Output Data

All output is processed by a standard 132 characters-per-line printer. The output from each run is always preceded by a complete list of the input data cards. The amount and type of the remaining output depend on the PRINT option selected, the number of panels used, and whether the configuration being analyzed is an isolated wing, an isolated body, or a complete wing-body-tail combination. The program output options are described below:

PRINT = 0 — The program prints the case description, Mach number and angle of attack, followed by a table listing the panel number, control point coordinates (both dimensional and non-dimensional), pressure coefficient, normal force, axial force, and pitching moment. Separate tables are printed for the body and wing panels, noting that any tail, fin or canard panels are included with the wing output. If the planar boundary condition option has been selected, the results for the wing upper surface are given in one table, followed by a separate table giving the results for the wing lower surface. Additional tables giving the total coefficients on the body, the wing and the complete configuration follow the pressure coefficient tables. These include the reference area, reference span and reference chord, the normal force, axial force, pitching moment, lift, and drag coefficients, and the center of pressure of the component.

PRINT = 1 — In addition to the output described for PRINT = 0, the program prints out additional tables giving the normal force, axial force, pitching moment, lift and drag coefficients, and the center of pressure of each column of panels on the wing and tail surfaces. In addition, the indices of the first and last panel in the column are listed, together with the span, chord and origin of the column.

PRINT = 2 — In addition to the output described for PRINT = 1, the program prints out tables listing the panel number, the source or vortex strength of that panel, and the axial velocity u, lateral velocity v, and vertical velocity w at the panel control point. The normal velocity is also calculated for

body panels. Separate tables are printed for the body and wing panels, noting again that any tail, fin, or canard panels are included with the wing output. If the planar boundary condition option has been selected, separate tables are given for the wing upper and lower surfaces.

PRINT = 3 — In addition to the output described for PRINT = 2, the program prints out the iteration number, and the source and vortex strength arrays obtained at each step of the iterative solution procedure.

PRINT = 4 — In addition to the output described for PRINT = 3, the program prints out tables of the axial and normal velocity components which make up the elements of the aerodynamic matrices. The program prints out the matrix row number, and gives the number of elements in that row. A maximum of four matrix partitions will be printed if this option is selected, each of which is identified by number and its influence description prior to printing the velocity component tables.

If a negative value of PRINT is selected, the program prints all the information described above for the positive values, together with the complete panel geometry description of the configuration following the list of input cards. This consists of tables giving the wing panel corner points, control points, inclination angles, areas, and chords. If the configuration has a horizontal tail, fin or canard, additional tables are printed giving the same information as listed above for the wing. Finally, if the configuration includes a body, the body panel corner points, control points, areas, and inclination angles are listed.

The program output is illustrated by the sample case presented in Appendix III.

EXPERIMENTAL VERIFICATION

Several examples of pressure distributions calculated by the program are presented in this section, and compared with experimental data. The examples include isolated bodies, isolated wings, and wing-body combinations in both subsonic and supersonic flow.

Isolated Bodies

Ogive-cylinder body with boattail in subsonic flow.- The theoretical pressure distribution calculated for this body at $M = .40$ and $\alpha = 0$ degrees is presented on Figure 3. The experimental data has been obtained from reference 6, which also contains additional comparisons between the present theory and experiment for this body at $M = .61$ and .83. In this example, the blunt base and sting were replaced by an arbitrarily chosen 12 degree cone aft of the boattail region in an attempt to simulate the flow separation region behind the body. Good agreement between the theory and experiment is achieved over most of the body.

Haack-Adams body with base in supersonic flow.- The theoretical pressure distribution calculated for a Haack-Adams body having $A_{base}/A_{max} = .532$ and $\ell/d_{max} = 10$ is presented on Figure 4, for $M = 2.01$ and $\alpha = 0$ degrees. The experimental data for this body is obtained from reference 7, which also gives the pressure distribution calculated by characteristics theory. The present method agrees closely with the experimental data and the characteristics theory for this body.

Elliptic cone in supersonic flow.- The theoretical pressure distribution on an elliptic cone is compared with experimental data on Figure 5, for $M = 1.89$ and $\alpha = 0$ and 6 degrees. The experimental data was obtained from reference 8. Again, the theory agrees well with experiment except near the leading edge on the lower surface, where the positive pressure is slightly over-estimated.

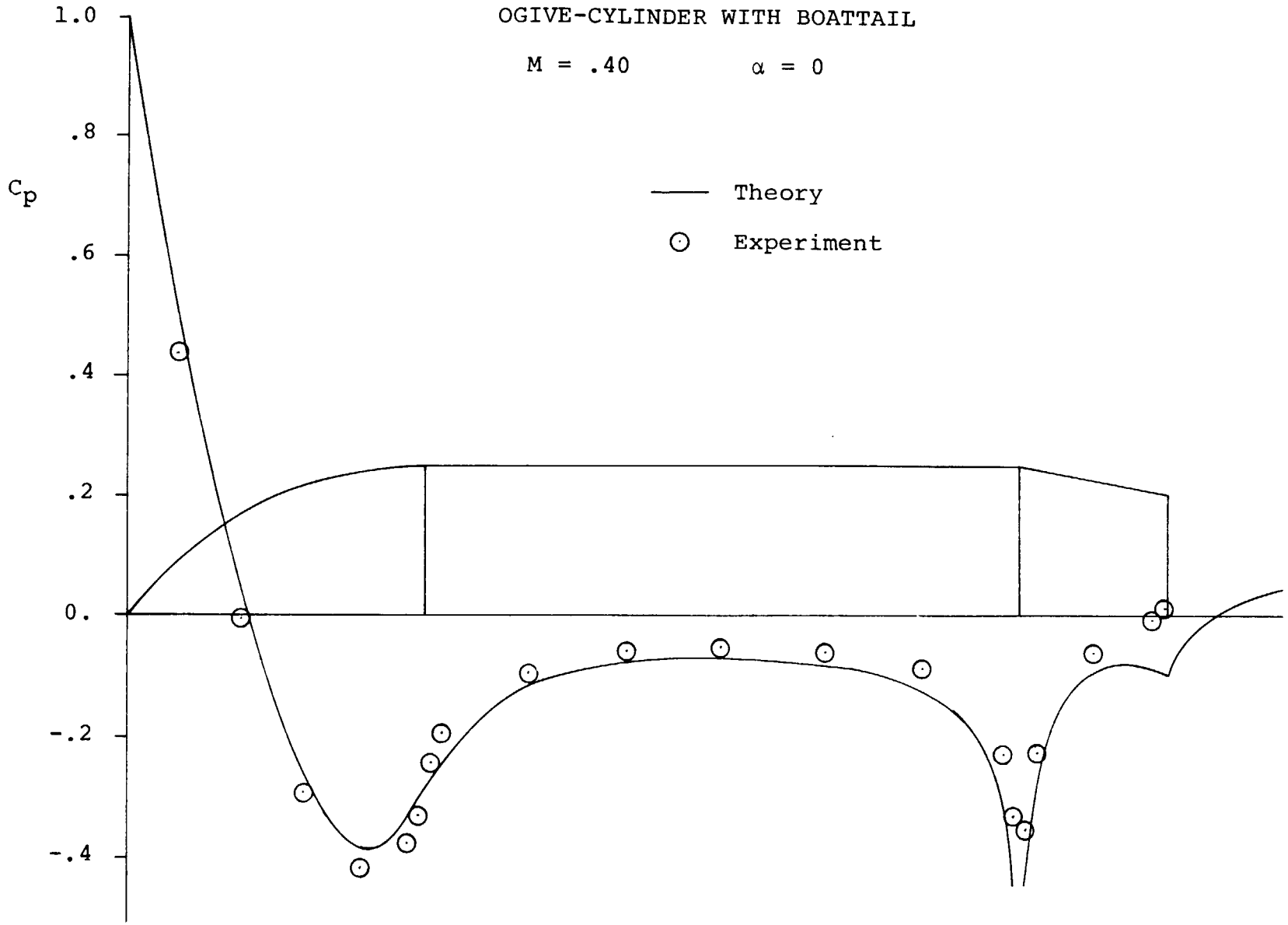

Figure 3 - Subsonic Pressure Distribution on Axisymmetric Body

HAACK-ADAMS BODY

M = 2.01 α = 0

A_{base}/A_{max} = .532 ℓ/d = 10

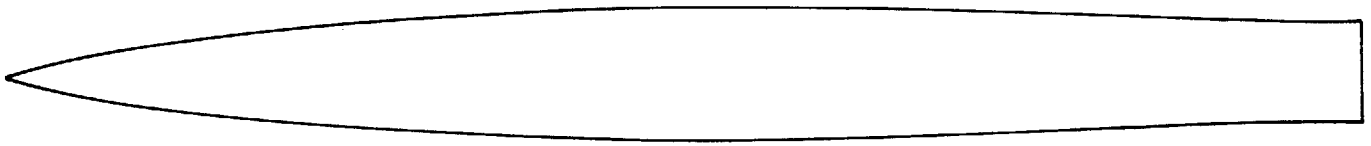

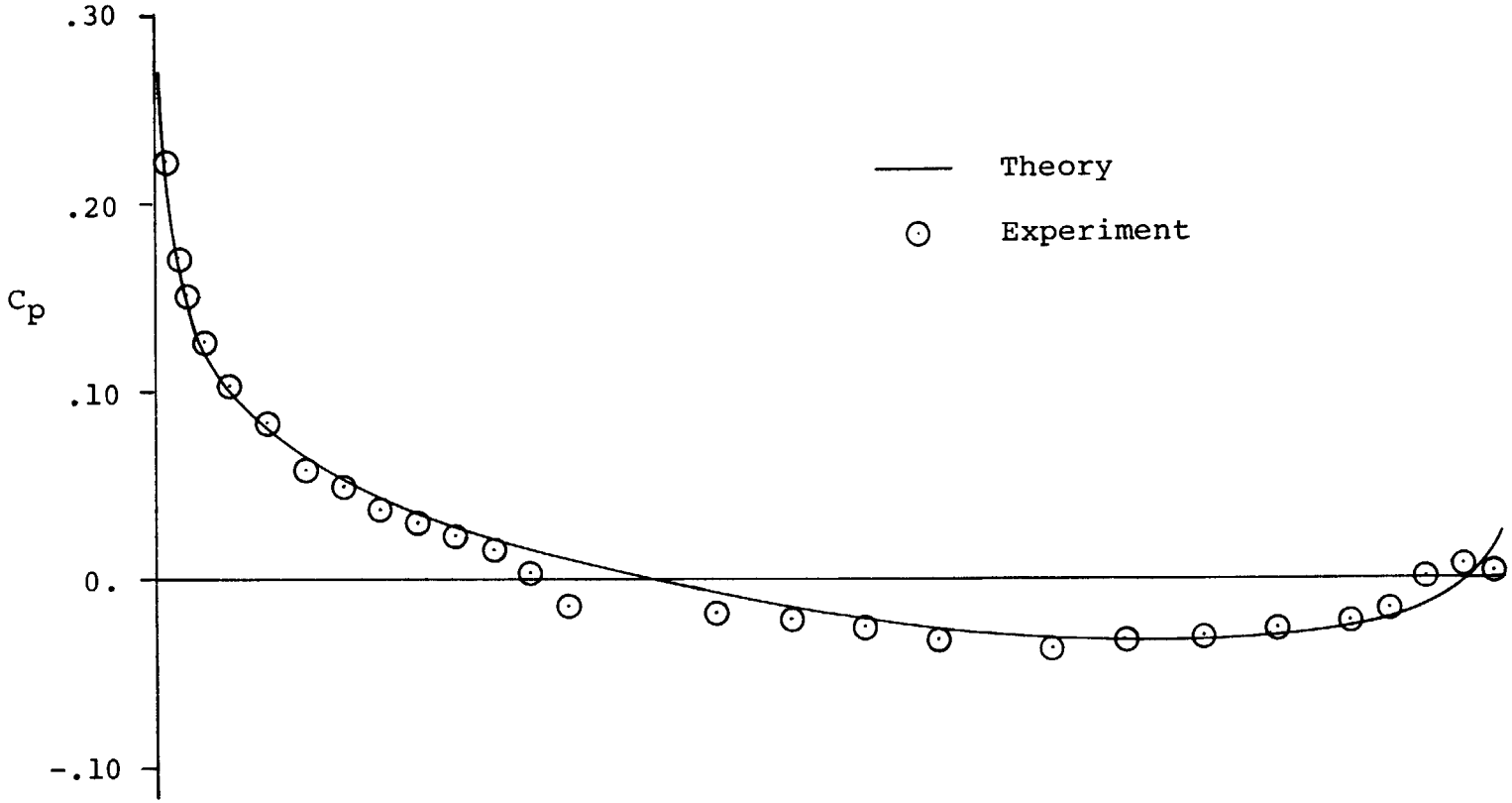

Figure 4 - Supersonic Pressure Distribution on Axisymmetric Body

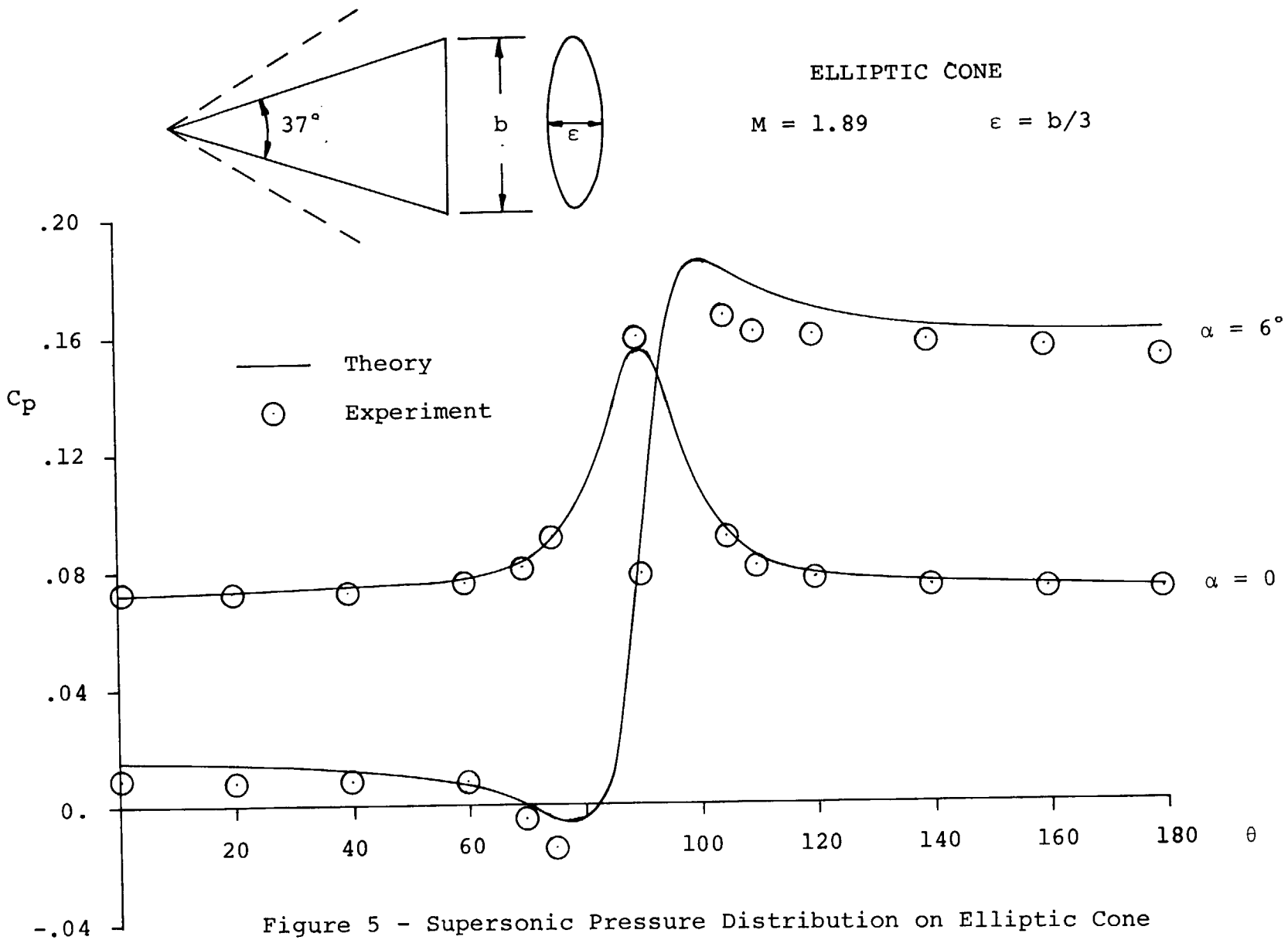

Figure 5 - Supersonic Pressure Distribution on Elliptic Cone

Isolated Wings

Two-dimensional airfoil in subsonic flow.- The pressure distribution on a NACA 64A010 airfoil at M = .167 and α = 8 degrees is compared with the experimental data from reference 9 on Figure 6. In this example, the surface boundary condition option was utilized in the theoretical calculations. The agreement with experiment is excellent on both upper and lower surface of the airfoil, indicating that viscous effects are small. The potential flow solution obtained by the present method also agrees closely with that given by the viscous flow solution presented in reference 10 for this airfoil, except for a small region near the trailing edge. In general, potential flow theory tends to over-estimate the negative pressure peaks in two-dimensional flow.

Figure 7 compares the results of the present program with the exact incompressible pressure distribution around a 10 percent thick Karman-Trefftz airfoil. Here, the program results agree closely with the exact solution, and give considerable confidence in the capability of the present method to reproduce theoretical two-dimensional flows.

Variable sweep wing in subsonic flow.- The pressure distributions calculated on a variable sweep wing having a NACA 64A006 section, 72 degrees inboard sweep, and two outboard wing sweep angles, are compared with experimental data from reference 11 at M = .23 and α = 10.5 degrees on Figure 8. In this example, the boundary conditions are applied in the plane of the wing. The theory agrees reasonably well with experiment at the root and at the mid-span break point. The pressure distribution is less accurate near the wing tip, although the net loading appears to be approximately correct. The agreement between theory and experiment is considered to be acceptable, considering the relatively high angle of attack chosen for this comparison.

Cambered arrow wing in supersonic flow.- The pressure distributions calculated on a cambered and twisted arrow wing having a 3 percent circular arc section and 70 degrees sweepback are compared with experimental data from reference 12 at M = 2.01 and α = 4 degrees on Figure 9. Here, the boundary conditions are applied in the plane of the wing; and the theory can be seen to agree reasonably well with experiment over the entire wing, except in the immediate vicinity of the leading edge.

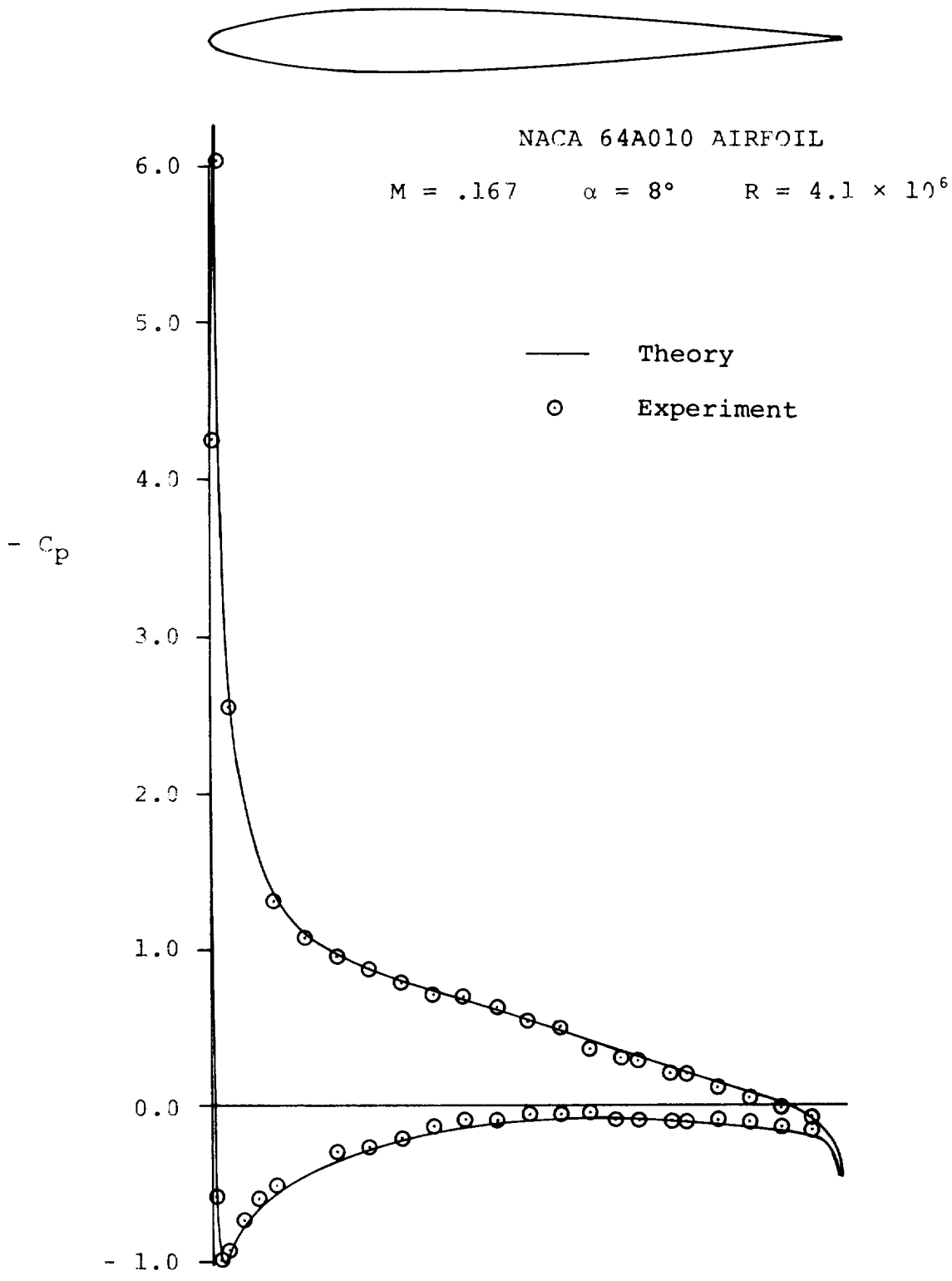

Figure 6 - Pressure Distribution on Two-dimensional Airfoil

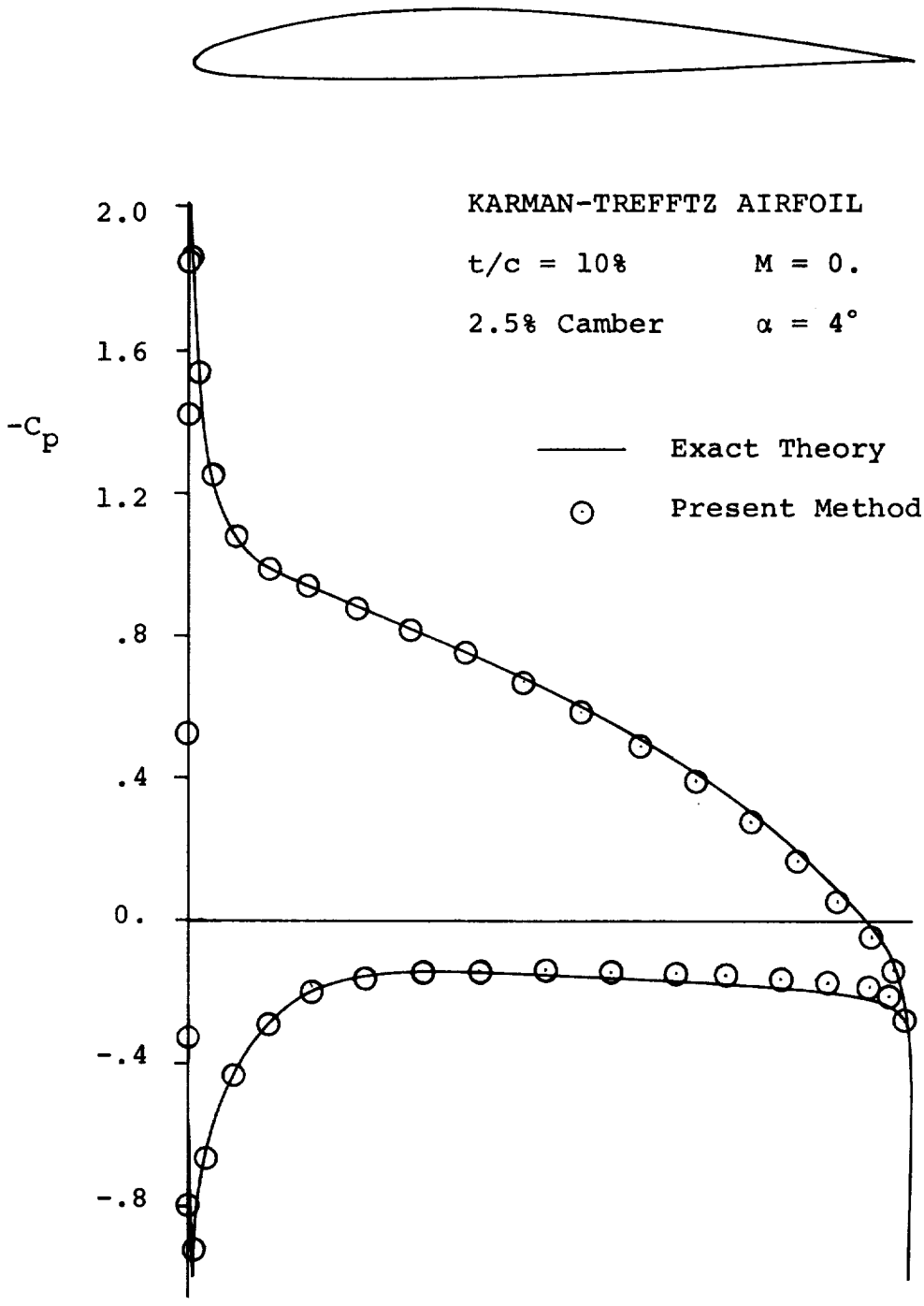

Figure 7 - Incompressible Pressure Distribution on Two-dimensional Airfoil

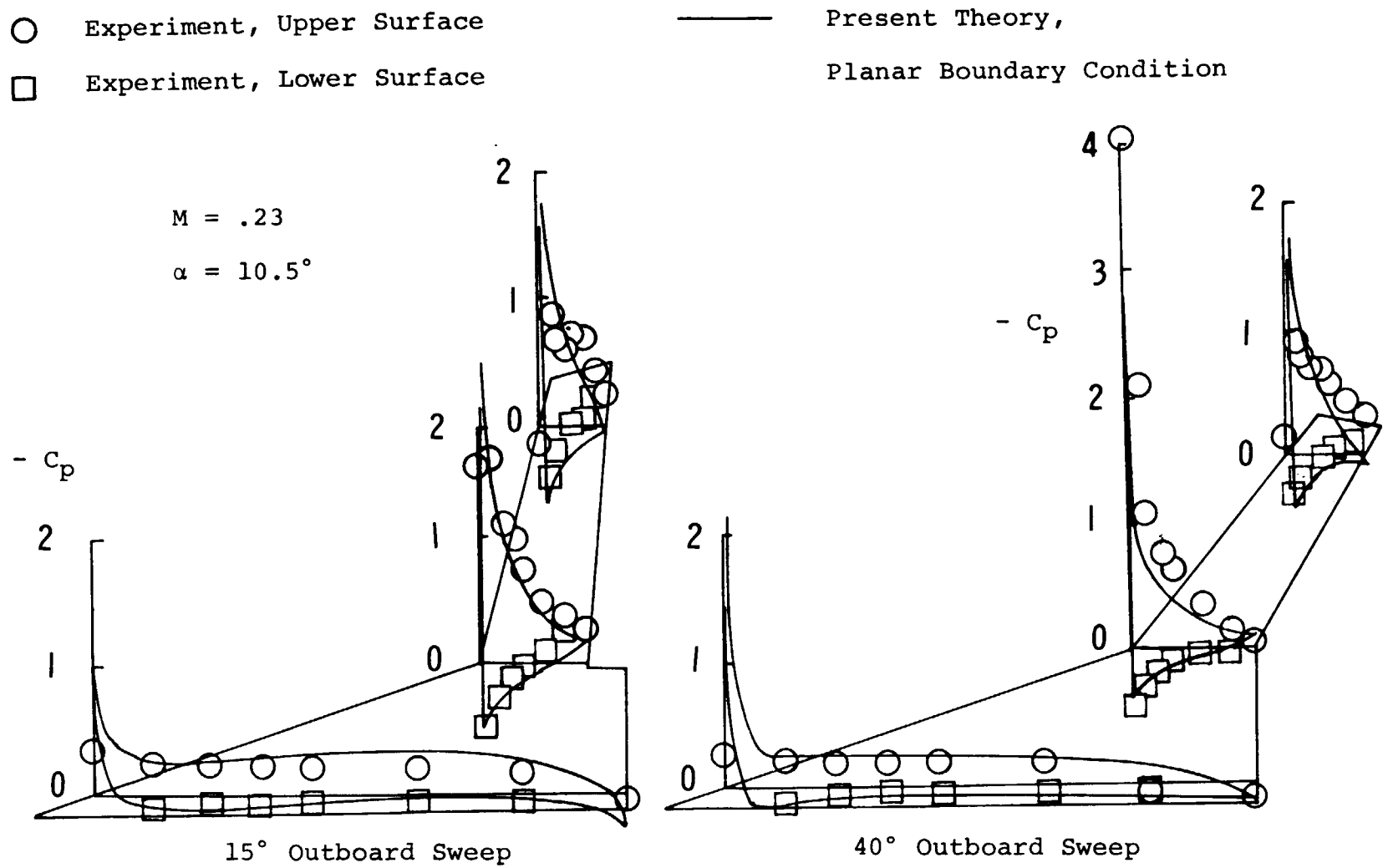

Figure 8 - Subsonic Pressure Distribution on a Variable Sweep Wing with 72 degrees Inboard Sweep and NACA 64A006 Section

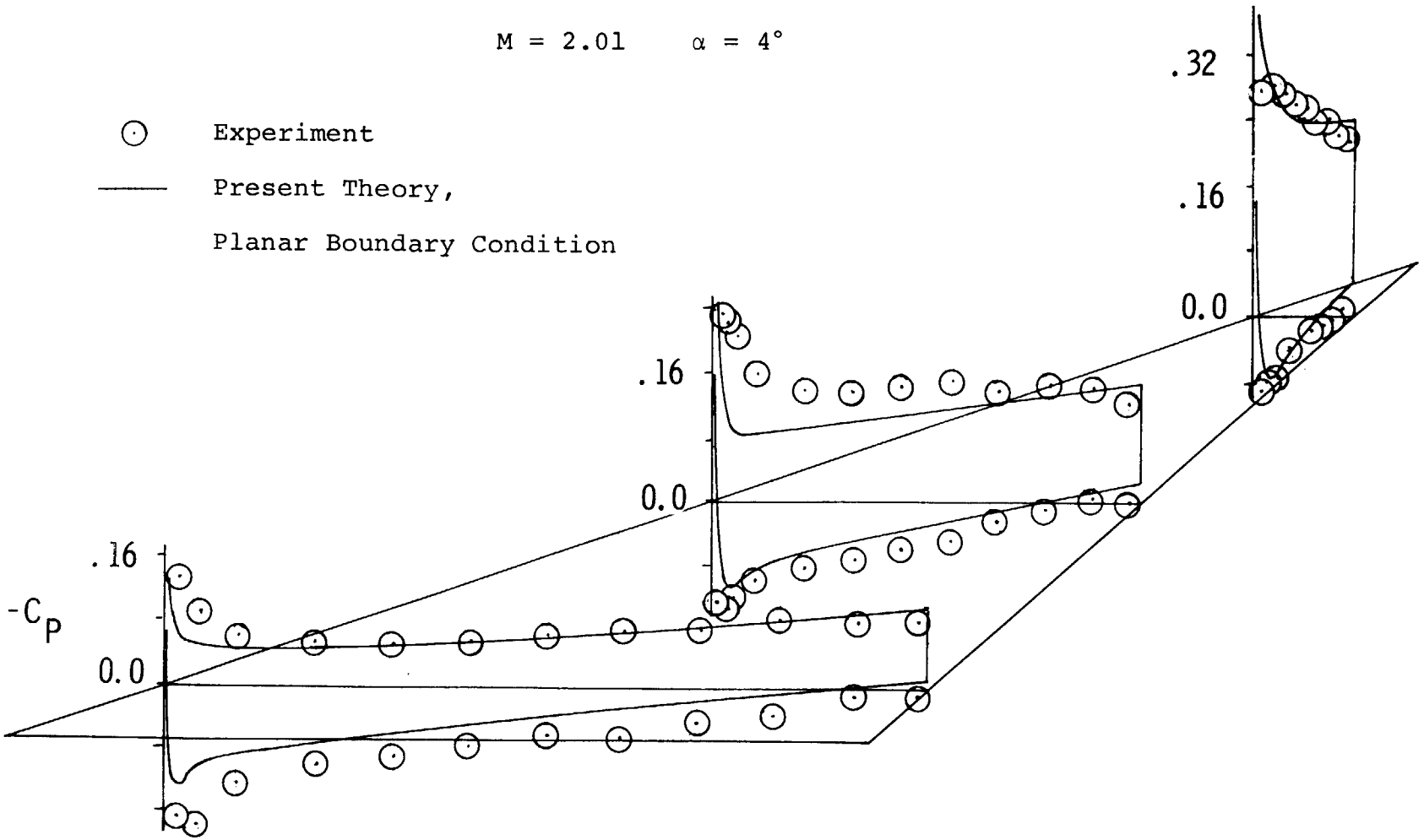

Figure 9 - Supersonic Pressure Distribution on a 70 degree Swept Wing with Camber and Twist and 3% Circular Arc Section

Wing-Body Combinations

Ogive-cylinder body with swept wing in supersonic flow.- The planform of this simple wing-body combination, and the paneling scheme used in the aerodynamic representation are shown on Figure 10. The wing has a NACA 65A004 section, is centrally mounted on the body, and the quarter-chord line is swept back 45 degrees. The ogival nose is 3.5 body diameters in length.

The pressure distribution on the wing is compared with experimental data from reference 13 for M = 2.01 and α = 5 degrees on Figure 11. The theoretical curve was calculated using the planar boundary condition option. The agreement between theory and experiment is reasonably good, except near the wing leading edge. Part of this discrepancy is probably due to shock wave detachment ahead of the round leading edge of the airfoil for this supersonic leading edge wing, allowing a small circulation to develop around the leading edge. The theoretical calculations assume an attached Mach wave along supersonic leading edges, prohibiting the development of any circulatory flow.

The pressure distribution on the upper and lower meridian lines of the body are compared with experimental data on Figure 12. In this example the agreement between theory and experiment is extremely good.

OGIVE CYLINDER BODY WITH CENTRALLY MOUNTED SWEPT WING

NACA 64A005 SECTION

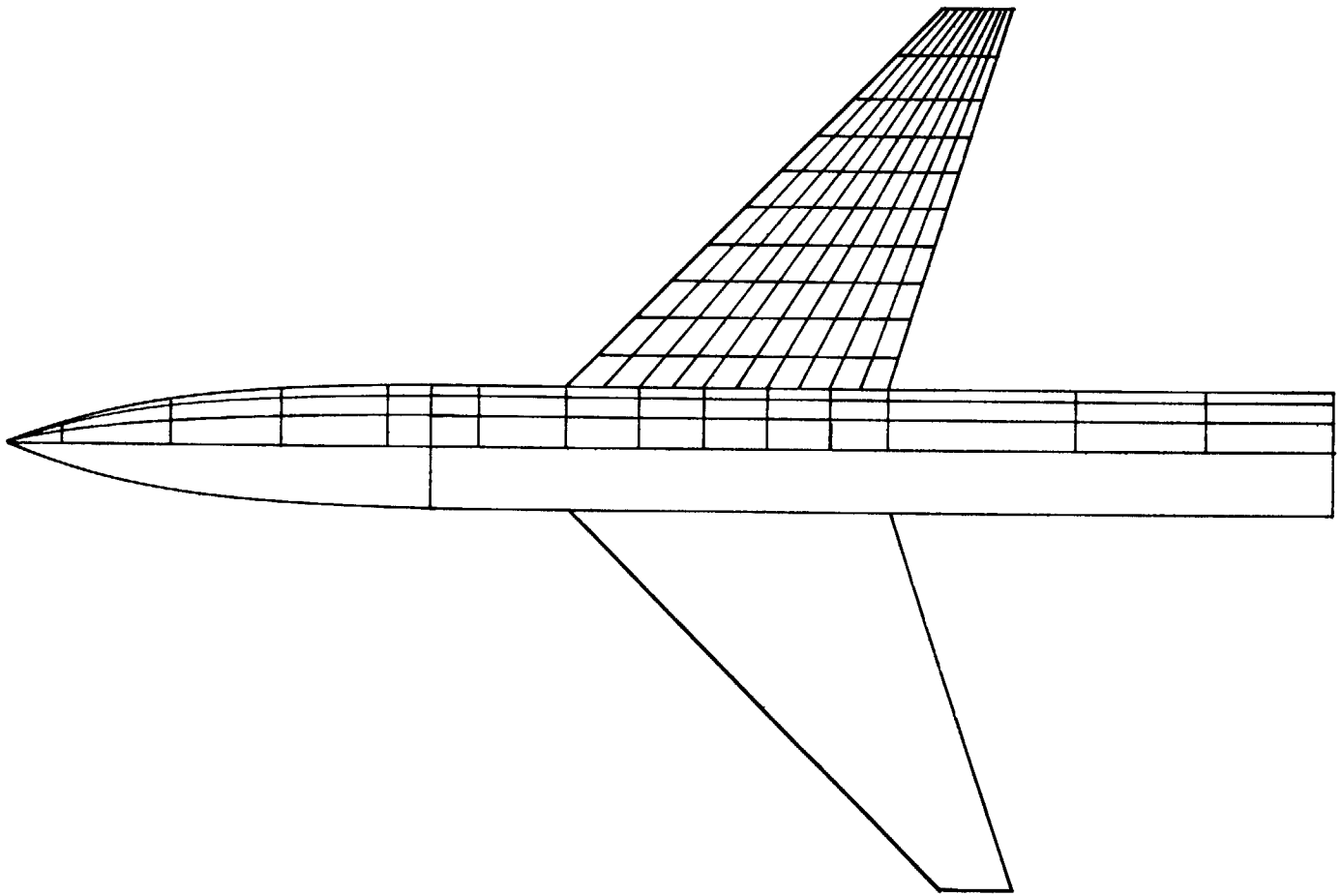

Figure 10 - Aerodynamic Representation of a Simple Wing-Body

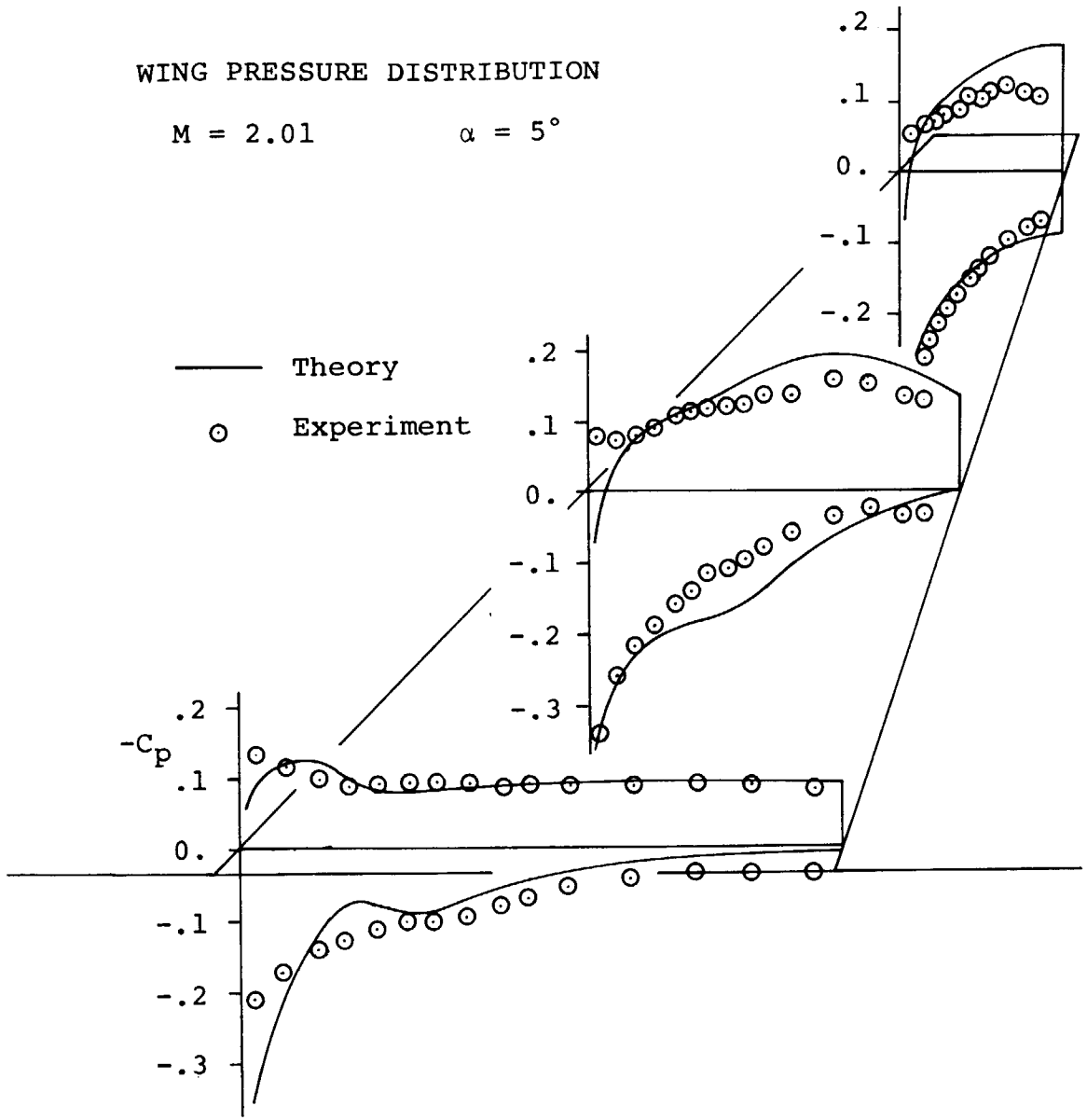

Figure 11 - Supersonic Pressure Distribution on the Wing of a Simple Wing-Body

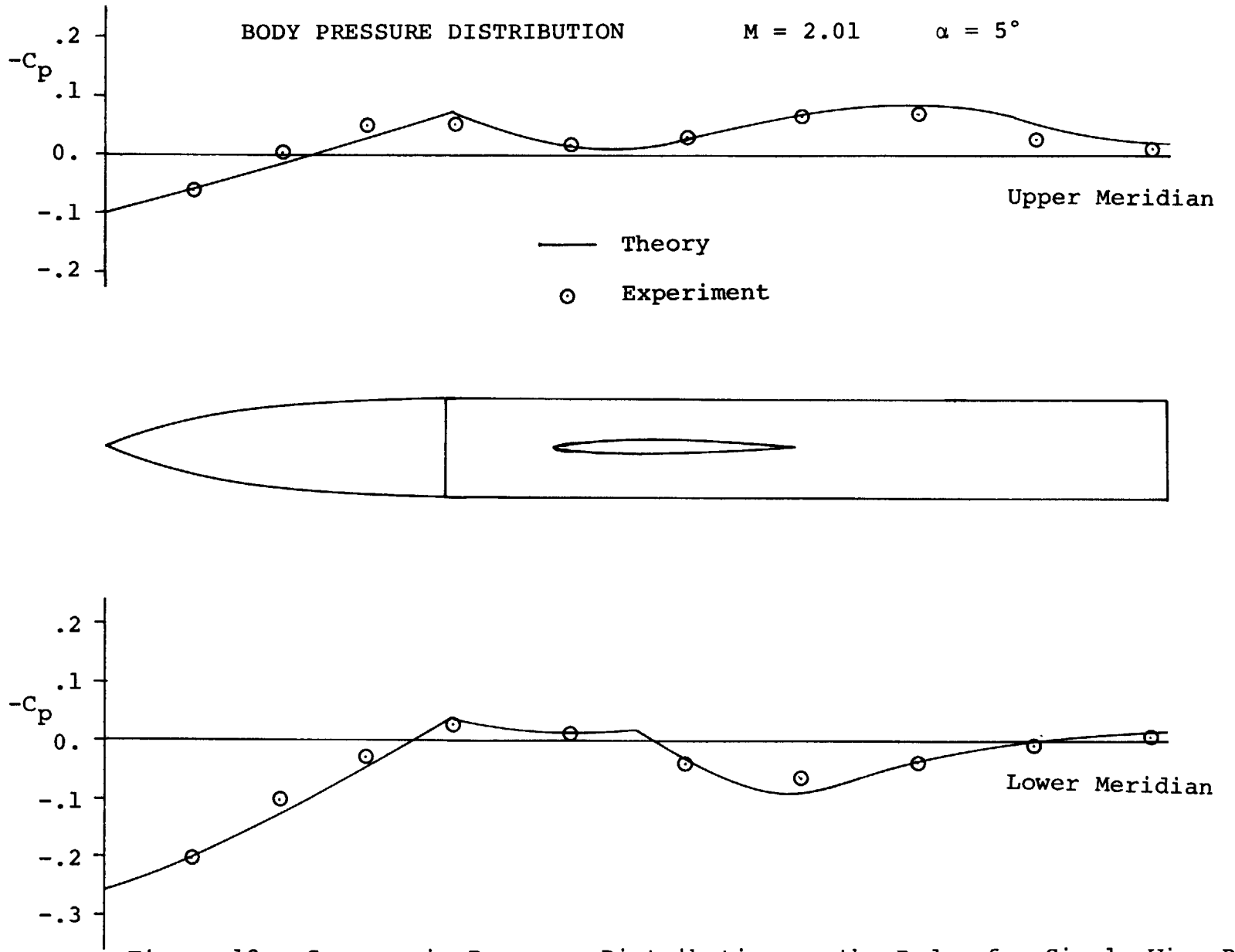

Figure 12 - Supersonic Pressure Distribution on the Body of a Simple Wing-Body

CONCLUSIONS

The aerodynamic analysis method described in this report has been developed to succeed the earlier methods reported in references 1 and 2. Considerable progress has been made in the achievement of this goal, but additional work remains if the full potential of the new method is to be realized. Several promising areas for the future development of this method are described briefly below.

Program refinements.- Increased geometrical capability is required to permit the analysis of engine pods, nacelles, or fairings. In addition, improved programming techniques, including far field approximations to the aerodynamic singularity distributions would be desirable to reduce the time required to calculate the matrix of aerodynamic influence coefficients. Finally, the extension of the force and moment subroutine to include the calculation of additional aerodynamic stability derivatives would be valuable.

Development of the program as a design tool.- The present computer program is restricted to the determination of the pressure distribution, forces and moments on given configurations. The development of the program as a design tool would greatly increase its range of application. For example, the important problem of determining the wing camber and twist distribution which will generate favorable surface pressure distributions in the presence of an arbitrary body, or for minimizing pressure drag and interference effects could be included in this program based on the design procedures described in reference 1.

Development of leading edge vortex model.- The use of linearly varying vortex distributions to represent the circulatory flow around lifting wings permits the Kutta condition to be imposed along leading edges, as well as trailing edges. Using this flow model, the vortex sheet from leading edge panels can be modified to trail downstream from the leading edge or wing tip to simulate a separated flow, and provide a first approximation to the lift distribution on wings at high angles of attack.

Application of the method to the analysis of transonic flows.- The non-linear effects of transonic flow can be approximated by using the local Mach number calculated from the potential flow solution to redefine the regions of influence and the magnitude of the velocity field induced by the aerodynamic singularities. An iterative solution of the boundary condition

equations can then be established, in which the coefficients of the equations depend on the local Mach number distribution of the preceding step. The iterative procedure would be continued until a convergent pressure distribution is obtained.

Analytical Methods, Incorporated
Bellevue, Washington
December 31, 1972

APPENDIX I

Integration Procedures

The velocity component integrals appearing in the text may all be reduced to forms appearing in standard integral tables, and two non-standard integrals given below:

$$J_1 = \int \frac{dv}{(v^2 + e^2)[av^2 + 2bv + c]^{\frac{1}{2}}}$$

$$J_2 = \int \frac{vdv}{(v^2 + e^2)[av^2 + 2bv + c]^{\frac{1}{2}}}$$

The method used to evaluate these integrals is given in reference 1. The results are summarized below:

$$J_1 = \frac{\gamma}{\gamma^4 + b^2e^2}\left[b\,F + \frac{\gamma^2}{e}\,G\right]$$

$$J_2 = \frac{\gamma}{\gamma^4 + b^2e^2}\left[\gamma^2 F - be\,G\right]$$

where γ is a real non-zero root of the equation

$$\gamma^4 - (ae^2 - c)\gamma^2 - b^2e^2 = 0, \quad \delta = be/\gamma$$

and

$$F = \tan^{-1}\frac{\gamma[av^2 + 2bv + c]^{\frac{1}{2}}}{\gamma^2 - bv},$$

$$G = \tanh^{-1}\frac{v\gamma + e\delta}{e[av^2 + 2bv + c]^{\frac{1}{2}}}$$

$$= \sinh^{-1}\frac{v\gamma + e\delta}{[(ae^2 - \gamma^2)v^2 + (c - \delta^2)e^2]^{\frac{1}{2}}}$$

APPENDIX II

Panel Geometry Calculation Procedure

The analytical procedure presented here follows closely the method first developed in reference 14. A quadrilateral surface element is described by four corner points, not necessarily lying in the same plane, as shown in the sketch. Note that the numbering convention of the corner points differs from that used in the preceding text. The quadrilateral element is approximated by a planar panel as follows:

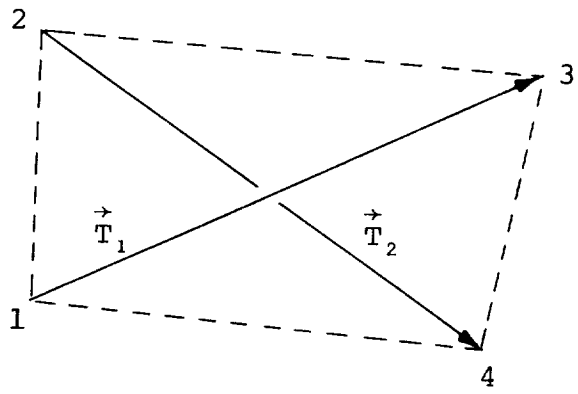

The coordinates in the reference coordinate system are identified by their subscripts. The components of the diagonal vectors $\vec{T}_1$ and $\vec{T}_2$ are

$$T_{1x} = x_3 - x_1 \qquad T_{1y} = y_3 - y_1 \qquad T_{1z} = z_3 - z_1$$

$$T_{2x} = x_4 - x_2 \qquad T_{2y} = y_4 - y_2 \qquad T_{2z} = z_4 - z_2$$

We may now obtain a vector $\vec{N}$ (and its components) by taking the cross product of the diagonal vectors.

$$\vec{N} = \vec{T}_2 \times \vec{T}_1$$

$$N_x = T_{2y}T_{1z} - T_{1y}T_{2z}$$

$$N_y = T_{1x}T_{2z} - T_{2x}T_{1z}$$

$$N_z = T_{2x}T_{1y} - T_{1x}T_{2y}$$

The unit normal vector, $\vec{n}$, to the plane of the element is taken as $\vec{N}$ divided by its own length N (direction cosines of outward unit normal).

$$n_x = \frac{N_x}{N}$$

$$n_y = \frac{N_y}{N}$$

$$n_z = \frac{N_z}{N}$$

where $$N = \left[N_x^2 + N_y^2 + N_z^2 \right]^{\frac{1}{2}}$$

The plane of the element is now completely determined if a point in this plane is specified. This point is taken as the point whose coordinates, $\bar{x}$, $\bar{y}$, $\bar{z}$ are the averages of the coordinates of the four input points.

$$\bar{x} = \frac{1}{4}\left[x_1 + x_2 + x_3 + x_4\right]$$

$$\bar{y} = \frac{1}{4}\left[y_1 + y_2 + y_3 + y_4\right]$$

$$\bar{z} = \frac{1}{4}\left[z_1 + z_2 + z_3 + z_4\right]$$

Now the input points will be projected into the plane of the element along the normal vector. The resulting points are the

corner points of the quadrilateral element. The input points are equidistant from the plane, and this distance is

$$d = \left| n_x(\bar{x} - x_1) + n_y(\bar{y} - y_1) + n_z(\bar{z} - z_1) \right|$$

The coordinates of the corner points in the reference coordinate system are given by

$$x'_k = x_k + (-1)^{k+1} n_x d$$

$$y'_k = y_k + (-1)^{k+1} n_y d \qquad k = 1, 2, 3, 4$$

$$z'_k = z_k + (-1)^{k+1} n_z d$$

Now the element coordinate system must be constructed. This requires the components of three mutually perpendicular unit vectors, one of which points along each of the coordinate axis of the system, and also the coordinates of the origin of the coordinate system. All these quantities must be given in terms of the reference coordinate system. The unit normal vector is taken as one of the unit vectors, so two perpendicular unit vectors in the plane of the element are needed. Denote these unit vectors $\vec{t}_1$ and $\vec{t}_2$. The vector $\vec{t}_1$ is taken as $\vec{T}_1$ divided by its own length T_1, i.e.,

$$t_{1x} = \frac{T_{1x}}{T_1}$$

$$t_{1y} = \frac{T_{1y}}{T_1}$$

$$t_{1z} = \frac{T_{1z}}{T_1}$$

where $$T_1 = \left[T_{1x}^2 + T_{1y}^2 + T_{1z}^2 \right]^{\frac{1}{2}}$$

The vector $\vec{t}_2$ is defined by $\vec{t}_2 = \vec{n} \times \vec{t}_1$, so that its components are

$$t_{2x} = n_y t_{1z} - n_z t_{1y}$$

$$t_{2y} = n_z t_{1x} - n_x t_{1z}$$

$$t_{2z} = n_x t_{1y} - n_y t_{1x}$$

The vector $\vec{t}_1$ is the unit vector parallel to the x or ξ axis of the element coordinate system, while $\vec{t}_2$ is parallel to the y or η axis, and $\vec{n}$ is parallel to the z or ζ axis of this coordinate system.

The corner points are now transformed into the element coordinate system based on the average point as origin. These points have coordinates x'_k, y'_k, z'_k in the reference coordinate system. Their coordinates in the element coordinate system with this origin are denoted by ξ_k, η_k, 0. Because they lie in the plane of the element, they have a zero z or ζ coordinate in the element coordinate system. Also, because the vector $\vec{t}_1$, which defines the x or ξ axis of the element coordinate system, is a multiple of the "diagonal" vector from point 1 to 3, the coordinate η_1 and the coordinate η_3 are equal. In the (ξ,η) coordinate system, the corner points of the element are:

$$\xi_k = t_{1x}(\bar{x} - x'_k) + t_{1y}(\bar{y} - y'_k) + t_{1z}(\bar{z} - z'_k)$$

$$\eta_k = t_{2x}(\bar{x} - x'_k) + t_{2y}(\bar{y} - y'_k) + t_{2z}(\bar{z} - z'_k)$$

These corner points are taken as the corners of a plane quadrilateral as illustrated in the following sketch.

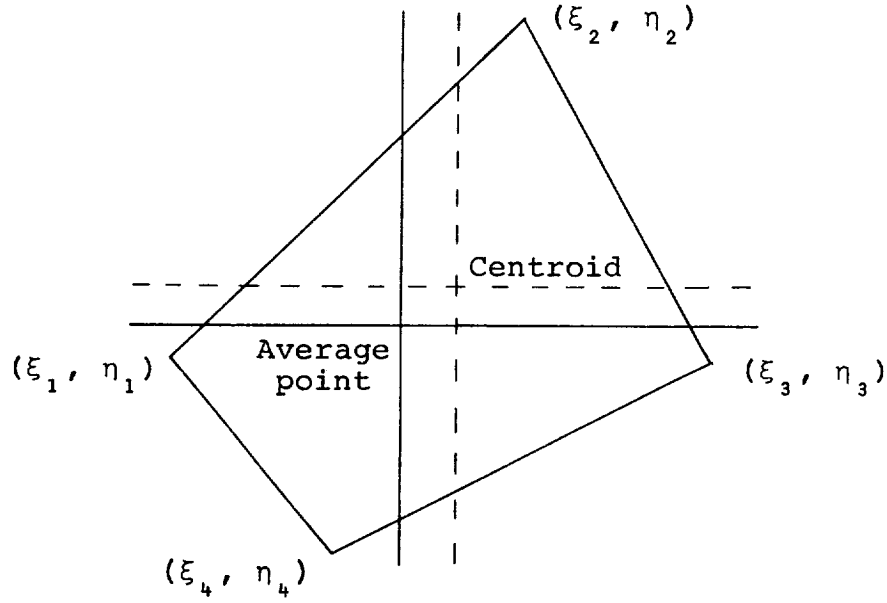

The origin of the element coordinate system is now transferred to the centroid of the area of the quadrilateral. With the average point as origin the coordinates of the centroid in the element coordinate system are:

$$\xi_0 = \frac{1}{3} \frac{1}{\eta_2 - \eta_4} \left[\xi_4 (\eta_1 - \eta_2) + \xi_2 (\eta_4 - \eta_1) \right]$$

$$\eta_0 = - \frac{1}{3} \eta_1$$

These are subtracted from the coordinates of the corner points in the element coordinate system based on the average point as origin to obtain the coordinates of the corner points in the element coordinate system based on the centroid as origin. Accordingly, these latter coordinates are

$$\xi_k = \xi_k - \xi_0 \qquad k = 1, 2, 3, 4$$

$$\eta_k = \eta_k - \eta_0$$

Since the centroid is to be used as the control point of the element, its coordinates in the reference coordinate system are required. These coordinates are

$$x_0 = \bar{x} + t_{1x}\xi_0 + t_{2x}\eta_0$$

$$y_0 = \bar{y} + t_{1y}\xi_0 + t_{2y}\eta_0$$

$$z_0 = \bar{z} + t_{1z}\xi_0 + t_{2z}\eta_0$$

Finally, the area of the quadrilateral is

$$A = \frac{1}{2}(\xi_3 - \xi_1)(\eta_2 - \eta_4)$$

APPENDIX III

SAMPLE CASE

```
UNIFIED SUBSONIC-SUPERSONIC AERODYNAMICS PROGRAM                VERSION A00

                LIST OF INPUT CARDS

00000000011111111112222222222333333333344444444445555555556666666666777777777 8
12345678901234567890123456789012345678901234567890123456789012345678901234567890

      OGIVE CYLINDER BODY WITH 45 DEGREE SWEEP NACA 65A004 MID-WING
  0 -1 -1           -1  2 26  1  5 28
0.      .5      .75     1.25    2.5     5.      7.5     10.     15.     20.       XAF1
25.     30.     35.     40.     45.     50.     55.     60.     65.     70.       XAF2
75.     80.     85.     90.     95.     100.                                      XAF3
13.65   0.      0.      10.                                                       WAFORG1
27.65   12.     0.      2.                                                        WAFORG2
0.      .3075   .373    .4755   .6515   .8745   1.06    1.216   1.463   1.6505    WAFORD1
1.7925  1.8955  1.964   1.9975  1.994   1.9475  1.857   1.728   1.5675  1.3815    WAFORD2
1.174   .949    .715    .480    .2445   .009                                      WAFORD3
0.      .3075   .373    .4755   .6515   .8745   1.06    1.216   1.463   1.6505    WAFORD1
1.7925  1.8955  1.964   1.9975  1.994   1.9475  1.857   1.728   1.5675  1.3815    WAFORD2
1.174   .949    .715    .480    .2445   .009                                      WAFORD3
0.      .5833   1.1667  1.75    2.3333  2.9167  3.5     4.0833  4.6667  5.25      XFUS1
5.8333  6.4167  7.0     7.5833  8.1667  8.75    9.3333  9.9167  10.5    11.0833   XFUS2
11.6667 15.2    18.75   22.3    25.85   29.4    32.95   36.5                      XFUS3
0.      .08605  .32573  .69221  1.16095 1.70920 2.31542 2.96080 3.62713 4.29759  FUSARD1
4.95834 5.59567 6.19717 6.75269 7.25261 7.68955 8.05555 8.34587 8.55610 8.68411  FUSARD2
8.727   8.727   8.727   8.727   8.727   8.727   8.727   8.727                     FUSARD3
      SINGULARITY PANELING FOR SAMPLE CASE
  1  1 -2
  1  3  1              6 11  1  5 16
144.    12.     6.89    3.33    36.5    20.813  0.                               REFL
.204    .204                                                                     RHO2
0.      10.     20.     30.     40.     50.     60.     70.     80.     90.       XAFK10
100.                                                                             XAFK11
1.667   2.97    5.37    7.73    10.1    12.0                                     YK6
0.      1.5     4.5     7.5     10.5    11.667  15.594  17.372  19.150  20.928   XFUSK10
22.7058 24.4835 26.28   29.4    33.     36.5                                     XFUSK16
2.01    0.                                                                       MALPHA
2.01    5.                                                                       MALPHA
-1.                                                                              MALPHA

00000000011111111112222222222333333333344444444445555555556666666666777777777 8
12345678901234567890123456789012345678901234567890123456789012345678901234567890

OGIVE CYLINDER BODY WITH 45 DEGREE SWEEP NACA 65A004 MID-WING
```

WING PANEL CORNER POINT COORDINATES
1 AND 3 INDICATE WING PANEL LEADING-EDGE POINTS, 2 AND 4 INDICATE TRAILING-EDGE POINTS

PANEL	X 1	Y 1	Z 1	X 2	Y 2	Z 2	X 3	Y 3	Z 3	X 4	Y 4	Z 4
1	15.59483	1.66700	0.00000	16.48370	1.66700	0.00000	17.11500	2.97000	0.00000	17.91700	2.97000	0.00000
2	16.48370	1.66700	0.00000	17.37257	1.66700	0.00000	17.91700	2.97000	0.00000	18.71900	2.97000	0.00000
3	17.37257	1.66700	0.00000	18.26143	1.66700	0.00000	18.71900	2.97000	0.00000	19.52100	2.97000	0.00000
4	18.26143	1.66700	0.00000	19.15030	1.66700	0.00000	19.52100	2.97000	0.00000	20.32300	2.97000	0.00000
5	19.15030	1.66700	0.00000	20.03917	1.66700	0.00000	20.32300	2.97000	0.00000	21.12500	2.97000	0.00000
6	20.03917	1.66700	0.00000	20.92803	1.66700	0.00000	21.12500	2.97000	0.00000	21.92700	2.97000	0.00000
7	20.92803	1.66700	0.00000	21.81690	1.66700	0.00000	21.92700	2.97000	0.00000	22.72900	2.97000	0.00000
8	21.81690	1.66700	0.00000	22.70577	1.66700	0.00000	22.72900	2.97000	0.00000	23.53100	2.97000	0.00000
9	22.70577	1.66700	0.00000	23.59463	1.66700	0.00000	23.53100	2.97000	0.00000	24.33300	2.97000	0.00000
10	23.59463	1.66700	0.00000	24.48350	1.66700	0.00000	24.33300	2.97000	0.00000	25.13500	2.97000	0.00000
11	17.11500	2.97000	0.00000	17.91700	2.97000	0.00000	19.91500	5.37000	0.00000	20.55700	5.37000	0.00000
12	17.91700	2.97000	0.00000	18.71900	2.97000	0.00000	20.55700	5.37000	0.00000	21.19900	5.37000	0.00000
13	18.71900	2.97000	0.00000	19.52100	2.97000	0.00000	21.19900	5.37000	0.00000	21.84100	5.37000	0.00000
14	19.52100	2.97000	0.00000	20.32300	2.97000	0.00000	21.84100	5.37000	0.00000	22.48300	5.37000	0.00000
15	20.32300	2.97000	0.00000	21.12500	2.97000	0.00000	22.48300	5.37000	0.00000	23.12500	5.37000	0.00000
16	21.12500	2.97000	0.00000	21.92700	2.97000	0.00000	23.12500	5.37000	0.00000	23.76700	5.37000	0.00000
17	21.92700	2.97000	0.00000	22.72900	2.97000	0.00000	23.76700	5.37000	0.00000	24.40900	5.37000	0.00000
18	22.72900	2.97000	0.00000	23.53100	2.97000	0.00000	24.40900	5.37000	0.00000	25.05100	5.37000	0.00000
19	23.53100	2.97000	0.00000	24.33300	2.97000	0.00000	25.05100	5.37000	0.00000	25.69300	5.37000	0.00000
20	24.33300	2.97000	0.00000	25.13500	2.97000	0.00000	25.69300	5.37000	0.00000	26.33500	5.37000	0.00000
21	19.91500	5.37000	0.00000	20.55700	5.37000	0.00000	22.66833	7.73000	0.00000	23.15300	7.73000	0.00000
22	20.55700	5.37000	0.00000	21.19900	5.37000	0.00000	23.15300	7.73000	0.00000	23.63767	7.73000	0.00000
23	21.19900	5.37000	0.00000	21.84100	5.37000	0.00000	23.63767	7.73000	0.00000	24.12233	7.73000	0.00000
24	21.84100	5.37000	0.00000	22.48300	5.37000	0.00000	24.12233	7.73000	0.00000	24.60700	7.73000	0.00000
25	22.48300	5.37000	0.00000	23.12500	5.37000	0.00000	24.60700	7.73000	0.00000	25.09167	7.73000	0.00000
26	23.12500	5.37000	0.00000	23.76700	5.37000	0.00000	25.09167	7.73000	0.00000	25.57633	7.73000	0.00000
27	23.76700	5.37000	0.00000	24.40900	5.37000	0.00000	25.57633	7.73000	0.00000	26.06100	7.73000	0.00000
28	24.40900	5.37000	0.00000	25.05100	5.37000	0.00000	26.06100	7.73000	0.00000	26.54567	7.73000	0.00000
29	25.05100	5.37000	0.00000	25.69300	5.37000	0.00000	26.54567	7.73000	0.00000	27.03033	7.73000	0.00000
30	25.69300	5.37000	0.00000	26.33500	5.37000	0.00000	27.03033	7.73000	0.00000	27.51500	7.73000	0.00000
31	22.66833	7.73000	0.00000	23.15300	7.73000	0.00000	25.43333	10.10000	0.00000	25.76000	10.10000	0.00000
32	23.15300	7.73000	0.00000	23.63767	7.73000	0.00000	25.76000	10.10000	0.00000	26.08667	10.10000	0.00000
33	23.63767	7.73000	0.00000	24.12233	7.73000	0.00000	26.08667	10.10000	0.00000	26.41333	10.10000	0.00000
34	24.12233	7.73000	0.00000	24.60700	7.73000	0.00000	26.41333	10.10000	0.00000	26.74000	10.10000	0.00000
35	24.60700	7.73000	0.00000	25.09167	7.73000	0.00000	26.74000	10.10000	0.00000	27.06667	10.10000	0.00000
36	25.09167	7.73000	0.00000	25.57633	7.73000	0.00000	27.06667	10.10000	0.00000	27.39333	10.10000	0.00000
37	25.57633	7.73000	0.00000	26.06100	7.73000	0.00000	27.39333	10.10000	0.00000	27.72000	10.10000	0.00000
38	26.06100	7.73000	0.00000	26.54567	7.73000	0.00000	27.72000	10.10000	0.00000	28.04667	10.10000	0.00000
39	26.54567	7.73000	0.00000	27.03033	7.73000	0.00000	28.04667	10.10000	0.00000	28.37333	10.10000	0.00000
40	27.03033	7.73000	0.00000	27.51500	7.73000	0.00000	28.37333	10.10000	0.00000	28.70000	10.10000	0.00000
41	25.43333	10.10000	0.00000	25.76000	10.10000	0.00000	27.65000	12.00000	0.00000	27.85000	12.00000	0.00000
42	25.76000	10.10000	0.00000	26.08667	10.10000	0.00000	27.85000	12.00000	0.00000	28.05000	12.00000	0.00000
43	26.08667	10.10000	0.00000	26.41333	10.10000	0.00000	28.05000	12.00000	0.00000	28.25000	12.00000	0.00000
44	26.41333	10.10000	0.00000	26.74000	10.10000	0.00000	28.25000	12.00000	0.00000	28.45000	12.00000	0.00000
45	26.74000	10.10000	0.00000	27.06667	10.10000	0.00000	28.45000	12.00000	0.00000	28.65000	12.00000	0.00000
46	27.06667	10.10000	0.00000	27.39333	10.10000	0.00000	28.65000	12.00000	0.00000	28.85000	12.00000	0.00000
47	27.39333	10.10000	0.00000	27.72000	10.10000	0.00000	28.85000	12.00000	0.00000	29.05000	12.00000	0.00000
48	27.72000	10.10000	0.00000	28.04667	10.10000	0.00000	29.05000	12.00000	0.00000	29.25000	12.00000	0.00000
49	28.04667	10.10000	0.00000	28.37333	10.10000	0.00000	29.25000	12.00000	0.00000	29.45000	12.00000	0.00000
50	28.37333	10.10000	0.00000	28.70000	10.10000	0.00000	29.45000	12.00000	0.00000	29.65000	12.00000	0.00000

WING PANEL CONTROL POINTS AND INCLINATION ANGLES

POINT	X CP	Y CP	Z CP	THETA	CAMBER SLOPE	THICKNESS SLOPE
1	16.34190	2.30734	0.00000	0.00000	0.00000	.17879
2	17.18808	2.30734	0.00000	0.00000	0.00000	.05696
3	18.03425	2.30734	0.00000	0.00000	0.00000	.03265
4	18.88043	2.30734	0.00000	0.00000	0.00000	.01709
5	19.72661	2.30734	0.00000	0.00000	0.00000	.00315
6	20.57279	2.30734	0.00000	0.00000	0.00000	-.01379
7	21.41896	2.30734	0.00000	0.00000	0.00000	-.02918
8	22.26514	2.30734	0.00000	0.00000	0.00000	-.03946
9	23.11132	2.30734	0.00000	0.00000	0.00000	-.04623
10	23.95749	2.30734	0.00000	0.00000	0.00000	-.04704
11	24.80367	2.30734	0.00000	0.00000	0.00000	-.04710
12	18.46329	4.12568	0.00000	0.00000	0.00000	.17879
13	19.18825	4.12568	0.00000	0.00000	0.00000	.05696
14	19.91320	4.12568	0.00000	0.00000	0.00000	.03265
15	20.63816	4.12568	0.00000	0.00000	0.00000	.01709
16	21.36311	4.12568	0.00000	0.00000	0.00000	.00315
17	22.08807	4.12568	0.00000	0.00000	0.00000	-.01379
18	22.81302	4.12568	0.00000	0.00000	0.00000	-.02918
19	23.53798	4.12568	0.00000	0.00000	0.00000	-.03946
20	24.26293	4.12568	0.00000	0.00000	0.00000	-.04623
21	24.98788	4.12568	0.00000	0.00000	0.00000	-.04704
22	25.71284	4.12568	0.00000	0.00000	0.00000	-.04710
23	21.22759	6.49507	0.00000	0.00000	0.00000	.17879
24	21.79458	6.49507	0.00000	0.00000	0.00000	.05696
25	22.36158	6.49507	0.00000	0.00000	0.00000	.03265
26	22.92857	6.49507	0.00000	0.00000	0.00000	.01709
27	23.49557	6.49507	0.00000	0.00000	0.00000	.00315
28	24.06256	6.49507	0.00000	0.00000	0.00000	-.01379
29	24.62956	6.49507	0.00000	0.00000	0.00000	-.02918
30	25.19655	6.49507	0.00000	0.00000	0.00000	-.03946
31	25.76355	6.49507	0.00000	0.00000	0.00000	-.04623
32	26.33054	6.49507	0.00000	0.00000	0.00000	-.04704
33	26.89754	6.49507	0.00000	0.00000	0.00000	-.04710
34	23.96109	8.83808	0.00000	0.00000	0.00000	.17879
35	24.37188	8.83808	0.00000	0.00000	0.00000	.05696
36	24.78268	8.83808	0.00000	0.00000	0.00000	.03265
37	25.19347	8.83808	0.00000	0.00000	0.00000	.01709
38	25.60427	8.83808	0.00000	0.00000	0.00000	.00315
39	26.01506	8.83808	0.00000	0.00000	0.00000	-.01379
40	26.42586	8.83808	0.00000	0.00000	0.00000	-.02918
41	26.83665	8.83808	0.00000	0.00000	0.00000	-.03946
42	27.24745	8.83808	0.00000	0.00000	0.00000	-.04623
43	27.65824	8.83808	0.00000	0.00000	0.00000	-.04704
44	28.06904	8.83808	0.00000	0.00000	0.00000	-.04710
45	26.45281	10.97384	0.00000	0.00000	0.00000	.17879
46	26.72122	10.97384	0.00000	0.00000	0.00000	.05696
47	26.98963	10.97384	0.00000	0.00000	0.00000	.03265
48	27.25805	10.97384	0.00000	0.00000	0.00000	.01709
49	27.52646	10.97384	0.00000	0.00000	0.00000	.00315
50	27.79487	10.97384	0.00000	0.00000	0.00000	-.01379
51	28.06328	10.97384	0.00000	0.00000	0.00000	-.02918
52	28.33169	10.97384	0.00000	0.00000	0.00000	-.03946
53	28.60010	10.97384	0.00000	0.00000	0.00000	-.04623
54	28.86851	10.97384	0.00000	0.00000	0.00000	-.04704
55	29.13692	10.97384	0.00000	0.00000	0.00000	-.04710

WING PANEL AREAS AND CHORDS

PANEL	AREA	CHORD
1	1.10160	.84618
2	1.10160	.84618
3	1.10160	.84618
4	1.10160	.84618
5	1.10160	.84618
6	1.10160	.84618
7	1.10160	.84618
8	1.10160	.84618
9	1.10160	.84618
10	1.10160	.84618
11	1.73280	.72495
12	1.73280	.72495
13	1.73280	.72495
14	1.73280	.72495
15	1.73280	.72495
16	1.73280	.72495
17	1.73280	.72495
18	1.73280	.72495
19	1.73280	.72495
20	1.73280	.72495
21	1.32947	.56700
22	1.32947	.56700
23	1.32947	.56700
24	1.32947	.56700
25	1.32947	.56700
26	1.32947	.56700
27	1.32947	.56700
28	1.32947	.56700
29	1.32947	.56700
30	1.32947	.56700
31	.96143	.41079
32	.96143	.41079
33	.96143	.41079
34	.96143	.41079
35	.96143	.41079
36	.96143	.41079
37	.96143	.41079
38	.96143	.41079
39	.96143	.41079
40	.96143	.41079
41	.50033	.26841
42	.50033	.26841
43	.50033	.26841
44	.50033	.26841
45	.50033	.26841
46	.50033	.26841
47	.50033	.26841
48	.50033	.26841
49	.50033	.26841
50	.50033	.26841

BODY PANEL CORNER POINT COORDINATES
1 AND 3 INDICATE BODY PANEL LEADING-EDGE POINTS, 2 AND 4 INDICATE TRAILING-EDGE POINTS

PANEL	X 1	Y 1	Z 1	X 2	Y 2	Z 2	X 3	Y 3	Z 3	X 4	Y 4	Z 4
1	0.00000	0.00000	0.00000	1.50000	.00000	-.40622	0.00000	0.00000	0.00000	1.50000	.28724	-.28724
2	0.00000	0.00000	0.00000	1.50000	.28724	-.28724	0.00000	0.00000	0.00000	1.50000	.40622	.00000
3	0.00000	0.00000	0.00000	1.50000	.40622	.00000	0.00000	0.00000	0.00000	1.50000	.28724	.28724
4	0.00000	0.00000	0.00000	1.50000	.28724	.28724	0.00000	0.00000	0.00000	1.50000	-.00000	.40622
5	1.50000	.00000	-.40622	4.50000	.00000	-1.04487	1.50000	.28724	-.28724	4.50000	.73883	-.73883
6	1.50000	.28724	-.28724	4.50000	.73883	-.73883	1.50000	.40622	.00000	4.50000	1.04487	.00000
7	1.50000	.40622	.00000	4.50000	1.04487	.00000	1.50000	.28724	.28724	4.50000	.73883	.73883
8	1.50000	.28724	.28724	4.50000	.73883	.73883	1.50000	-.00000	.40622	4.50000	-.00000	1.04487
9	4.50000	.00000	-1.04487	7.50000	.00000	-1.45730	4.50000	.73883	-.73883	7.50000	1.03047	-1.03047
10	4.50000	.73883	-.73883	7.50000	1.03047	-1.03047	4.50000	1.04487	.00000	7.50000	1.45730	.00000
11	4.50000	1.04487	.00000	7.50000	1.45730	.00000	4.50000	.73883	.73883	7.50000	1.03047	1.03047
12	4.50000	.73883	.73883	7.50000	1.03047	1.03047	4.50000	-.00000	1.04487	7.50000	-.00000	1.45730
13	7.50000	.00000	-1.45730	10.50000	.00000	-1.65030	7.50000	1.03047	-1.03047	10.50000	1.16694	-1.16694
14	7.50000	1.03047	-1.03047	10.50000	1.16694	-1.16694	7.50000	1.45730	.00000	10.50000	1.65030	.00000
15	7.50000	1.45730	.00000	10.50000	1.65030	.00000	7.50000	1.03047	1.03047	10.50000	1.16694	1.16694
16	7.50000	1.03047	1.03047	10.50000	1.16694	1.16694	7.50000	-.00000	1.45730	10.50000	-.00000	1.65030
17	10.50000	.00000	-1.65030	11.66700	.00000	-1.66670	10.50000	1.16694	-1.16694	11.66700	1.17854	-1.17854
18	10.50000	1.16694	-1.16694	11.66700	1.17854	-1.17854	10.50000	1.65030	.00000	11.66700	1.66670	.00000
19	10.50000	1.65030	.00000	11.66700	1.66670	.00000	10.50000	1.16694	1.16694	11.66700	1.17854	1.17854
20	10.50000	1.16694	1.16694	11.66700	1.17854	1.17854	10.50000	-.00000	1.65030	11.66700	-.00000	1.66670
21	11.66700	.00000	-1.66670	15.59480	.00000	-1.66670	11.66700	1.17854	-1.17854	15.59480	1.17854	-1.17854
22	11.66700	1.17854	-1.17854	15.59480	1.17854	-1.17854	11.66700	1.66670	.00000	15.59480	1.66670	.00000
23	11.66700	1.66670	.00000	15.59480	1.66670	.00000	11.66700	1.17854	1.17854	15.59480	1.17854	1.17854
24	11.66700	1.17854	1.17854	15.59480	1.17854	1.17854	11.66700	-.00000	1.66670	15.59480	-.00000	1.66670
25	15.59480	.00000	-1.66670	17.37260	.00000	-1.66670	15.59480	1.17854	-1.17854	17.37260	1.17854	-1.17854
26	15.59480	1.17854	-1.17854	17.37260	1.17854	-1.17854	15.59480	1.66670	.00000	17.37260	1.66670	.00000
27	15.59480	1.66670	.00000	17.37260	1.66670	.00000	15.59480	1.17854	1.17854	17.37260	1.17854	1.17854
28	15.59480	1.17854	1.17854	17.37260	1.17854	1.17854	15.59480	-.00000	1.66670	17.37260	-.00000	1.66670
29	17.37260	.00000	-1.66670	19.15030	.00000	-1.66670	17.37260	1.17854	-1.17854	19.15030	1.17854	-1.17854
30	17.37260	1.17854	-1.17854	19.15030	1.17854	-1.17854	17.37260	1.66670	.00000	19.15030	1.66670	.00000
31	17.37260	1.66670	.00000	19.15030	1.66670	.00000	17.37260	1.17854	1.17854	19.15030	1.17854	1.17854
32	17.37260	1.17854	1.17854	19.15030	1.17854	1.17854	17.37260	-.00000	1.66670	19.15030	-.00000	1.66670
33	19.15030	.00000	-1.66670	20.92800	.00000	-1.66670	19.15030	1.17854	-1.17854	20.92800	1.17854	-1.17854
34	19.15030	1.17854	-1.17854	20.92800	1.17854	-1.17854	19.15030	1.66670	.00000	20.92800	1.66670	.00000
35	19.15030	1.66670	.00000	20.92800	1.66670	.00000	19.15030	1.17854	1.17854	20.92800	1.17854	1.17854
36	19.15030	1.17854	1.17854	20.92800	1.17854	1.17854	19.15030	-.00000	1.66670	20.92800	-.00000	1.66670
37	20.92800	.00000	-1.66670	22.70580	.00000	-1.66670	20.92800	1.17854	-1.17854	22.70580	1.17854	-1.17854
38	20.92800	1.17854	-1.17854	22.70580	1.17854	-1.17854	20.92800	1.66670	.00000	22.70580	1.66670	.00000
39	20.92800	1.66670	.00000	22.70580	1.66670	.00000	20.92800	1.17854	1.17854	22.70580	1.17854	1.17854
40	20.92800	1.17854	1.17854	22.70580	1.17854	1.17854	20.92800	-.00000	1.66670	22.70580	-.00000	1.66670
41	22.70580	.00000	-1.66670	24.48350	.00000	-1.66670	22.70580	1.17854	-1.17854	24.48350	1.17854	-1.17854
42	22.70580	1.17854	-1.17854	24.48350	1.17854	-1.17854	22.70580	1.66670	.00000	24.48350	1.66670	.00000
43	22.70580	1.66670	.00000	24.48350	1.66670	.00000	22.70580	1.17854	1.17854	24.48350	1.17854	1.17854
44	22.70580	1.17854	1.17854	24.48350	1.17854	1.17854	22.70580	-.00000	1.66670	24.48350	-.00000	1.66670
45	24.48350	.00000	-1.66670	26.28000	.00000	-1.66670	24.48350	1.17854	-1.17854	26.28000	1.17854	-1.17854
46	24.48350	1.17854	-1.17854	26.28000	1.17854	-1.17854	24.48350	1.66670	.00000	26.28000	1.66670	.00000
47	24.48350	1.66670	.00000	26.28000	1.66670	.00000	24.48350	1.17854	1.17854	26.28000	1.17854	1.17854
48	24.48350	1.17854	1.17854	26.28000	1.17854	1.17854	24.48350	-.00000	1.66670	26.28000	-.00000	1.66670
49	26.28000	.00000	-1.66670	29.40000	.00000	-1.66670	26.28000	1.17854	-1.17854	29.40000	1.17854	-1.17854
50	26.28000	1.17854	-1.17854	29.40000	1.17854	-1.17854	26.28000	1.66670	.00000	29.40000	1.66670	.00000
51	26.28000	1.66670	.00000	29.40000	1.66670	.00000	26.28000	1.17854	1.17854	29.40000	1.17854	1.17854
52	26.28000	1.17854	1.17854	29.40000	1.17854	1.17854	26.28000	-.00000	1.66670	29.40000	-.00000	1.66670
53	29.40000	.00000	-1.66670	33.00000	.00000	-1.66670	29.40000	1.17854	-1.17854	33.00000	1.17854	-1.17854
54	29.40000	1.17854	-1.17854	33.00000	1.17854	-1.17854	29.40000	1.66670	.00000	33.00000	1.66670	.00000
55	29.40000	1.66670	.00000	33.00000	1.66670	.00000	29.40000	1.17854	1.17854	33.00000	1.17854	1.17854
56	29.40000	1.17854	1.17854	33.00000	1.17854	1.17854	29.40000	-.00000	1.66670	33.00000	-.00000	1.66670
57	33.00000	.00000	-1.66670	36.50000	.00000	-1.66670	33.00000	1.17854	-1.17854	36.50000	1.17854	-1.17854
58	33.00000	1.17854	-1.17854	36.50000	1.17854	-1.17854	33.00000	1.66670	.00000	36.50000	1.66670	.00000
59	33.00000	1.66670	.00000	36.50000	1.66670	.00000	33.00000	1.17854	1.17854	36.50000	1.17854	1.17854
60	33.00000	1.17854	1.17854	36.50000	1.17854	1.17854	33.00000	-.00000	1.66670	36.50000	-.00000	1.66670

BODY PANEL CONTROL POINT COORDINATES

POINT	X CP	Y CP	Z CP
1	1.00000	.09575	-.23116
2	1.00000	.23116	-.09575
3	1.00000	.23116	.09575
4	1.00000	.09575	.23116
5	3.22006	.27308	-.65928
6	3.22006	.65928	-.27308
7	3.22006	.65928	.27308
8	3.22006	.27308	.65928
9	6.08242	.44633	-1.07754
10	6.08242	1.07754	-.44633
11	6.08242	1.07754	.44633
12	6.08242	.44633	1.07754
13	9.03105	.55006	-1.32796
14	9.03105	1.32796	-.55006
15	9.03105	1.32796	.55006
16	9.03105	.55006	1.32796
17	11.08446	.58637	-1.41563
18	11.08446	1.41563	-.58637
19	11.08446	1.41563	.58637
20	11.08446	.58637	1.41563
21	13.63090	.58927	-1.42262
22	13.63090	1.42262	-.58927
23	13.63090	1.42262	.58927
24	13.63090	.58927	1.42262
25	16.48370	.58927	-1.42262
26	16.48370	1.42262	-.58927
27	16.48370	1.42262	.58927
28	16.48370	.58927	1.42262
29	18.26145	.58927	-1.42262
30	18.26145	1.42262	-.58927
31	18.26145	1.42262	.58927
32	18.26145	.58927	1.42262
33	20.03915	.58927	-1.42262
34	20.03915	1.42262	-.58927
35	20.03915	1.42262	.58927
36	20.03915	.58927	1.42262
37	21.81690	.58927	-1.42262
38	21.81690	1.42262	-.58927
39	21.81690	1.42262	.58927
40	21.81690	.58927	1.42262
41	23.59465	.58927	-1.42262
42	23.59465	1.42262	-.58927
43	23.59465	1.42262	.58927
44	23.59465	.58927	1.42262
45	25.38175	.58927	-1.42262
46	25.38175	1.42262	-.58927
47	25.38175	1.42262	.58927
48	25.38175	.58927	1.42262
49	27.84000	.58927	-1.42262
50	27.84000	1.42262	-.58927
51	27.84000	1.42262	.58927
52	27.84000	.58927	1.42262
53	31.20000	.58927	-1.42262
54	31.20000	1.42262	-.58927
55	31.20000	1.42262	.58927
56	31.20000	.58927	1.42262
57	34.75000	.58927	-1.42262
58	34.75000	1.42262	-.58927
59	34.75000	1.42262	.58927
60	34.75000	.58927	1.42262

BODY PANEL AREAS AND INCLINATION ANGLES

PANEL	AREA	DELTA	THETA
1	.24037	.24517	-2.74889
2	.24037	.24517	-1.96350
3	.24037	.24517	-1.17810
4	.24037	.24517	-.39270
5	1.69784	.19420	-2.74889
6	1.69784	.19420	-1.96350
7	1.69784	.19420	-1.17810
8	1.69784	.19420	-.39270
9	2.89570	.12634	-2.74889
10	2.89570	.12634	-1.96350
11	2.89570	.12634	-1.17810
12	2.89570	.12634	-.39270
13	3.57398	.05937	-2.74889
14	3.57398	.05937	-1.96350
15	3.57398	.05937	-1.17810
16	3.57398	.05937	-.39270
17	1.48147	.01298	-2.74889
18	1.48147	.01298	-1.96350
19	1.48147	.01298	-1.17810
20	1.48147	.01298	-.39270
21	5.01045	0.00000	-2.74889
22	5.01045	0.00000	-1.96350
23	5.01045	0.00000	-1.17810
24	5.01045	0.00000	-.39270
25	2.26783	0.00000	-2.74889
26	2.26783	0.00000	-1.96350
27	2.26783	0.00000	-1.17810
28	2.26783	0.00000	-.39270
29	2.26770	0.00000	-2.74889
30	2.26770	0.00000	-1.96350
31	2.26770	0.00000	-1.17810
32	2.26770	0.00000	-.39270
33	2.26770	0.00000	-2.74889
34	2.26770	0.00000	-1.96350
35	2.26770	0.00000	-1.17810
36	2.26770	0.00000	-.39270
37	2.26783	0.00000	-2.74889
38	2.26783	0.00000	-1.96350
39	2.26783	0.00000	-1.17810
40	2.26783	0.00000	-.39270
41	2.26770	0.00000	-2.74889
42	2.26770	0.00000	-1.96350
43	2.26770	0.00000	-1.17810
44	2.26770	0.00000	-.39270
45	2.29168	0.00000	-2.74889
46	2.29168	0.00000	-1.96350
47	2.29168	0.00000	-1.17810
48	2.29168	0.00000	-.39270
49	3.97999	0.00000	-2.74889
50	3.97999	0.00000	-1.96350
51	3.97999	0.00000	-1.17810
52	3.97999	0.00000	-.39270
53	4.59229	0.00000	-2.74889
54	4.59229	0.00000	-1.96350
55	4.59229	0.00000	-1.17810
56	4.59229	0.00000	-.39270
57	4.46473	0.00000	-2.74889
58	4.46473	0.00000	-1.96350
59	4.46473	0.00000	-1.17810
60	4.46473	0.00000	-.39270

PARTITION = 1 TIME = 49.82100
INFLUENCE OF BODY ON BODY

PARTITION = 2 TIME = 61.21900
INFLUENCE OF WING ON BODY

PARTITION = 3 TIME = 72.21100
INFLUENCE OF BODY ON WING

PARTITION = 4 TIME = 82.85100
INFLUENCE OF WING ON WING

TIME = 94.18100

TIME = 95.90300

TIME = 103.35700

VELOCITIES ON BODY, MACH=2.010 ALPHA= 0.000

PANEL NO.	SOURCE STRENGTH	AXIAL VELOCITY	LATERAL VELOCITY	VERTICAL VELOCITY	NORMAL VELOCITY
1	.19642	-.09678	.08648	-.20879	.25020
2	.19642	-.09678	.20879	-.08648	.25020
3	.19642	-.09678	.20879	.08648	.25020
4	.19642	-.09678	.08648	.20879	.25020
5	.17261	-.07016	.06998	-.16896	.19668
6	.17261	-.07016	.16896	-.06998	.19668
7	.17261	-.07016	.16896	.06998	.19668
8	.17261	-.07016	.06998	.16896	.19668
9	.11296	-.03539	.04689	-.11319	.12701
10	.11296	-.03539	.11319	-.04689	.12701
11	.11296	-.03539	.11319	.04689	.12701
12	.11296	-.03539	.04689	.11319	.12701
13	.05198	-.00181	.02270	-.05481	.05944
14	.05198	-.00181	.05481	-.02270	.05944
15	.05198	-.00181	.05481	.02270	.05944
16	.05198	-.00181	.02270	.05481	.05944
17	-.02286	.02050	.00507	-.01224	.01298
18	-.02286	.02050	.01224	-.00507	.01298
19	-.02286	.02050	.01224	.00507	.01298
20	-.02286	.02050	.00507	.01224	.01298
21	-.00277	.01807	.00000	.00000	-.00000
22	-.00277	.01807	.00000	.00000	-.00000
23	-.00277	.01807	-.00000	.00000	-.00000
24	-.00277	.01807	-.00000	.00000	-.00000
25	.02891	.00714	.00000	.00000	-.00000
26	.02891	.00714	-.00000	-.00000	.00000
27	.02891	.00714	.00000	-.00000	-.00000
28	.02891	.00714	-.00000	.00000	-.00000
29	-.00208	.00751	-.00000	-.00000	-.00000
30	.02371	-.00814	-.00807	-.01949	-.00000
31	.02371	-.00814	-.00807	.01949	-.00000
32	-.00208	.00751	.00000	-.00000	.00000
33	-.02323	.00037	-.01946	-.00806	.00000
34	.01089	.00055	-.00635	-.01534	-.00000
35	.01089	.00055	-.00635	.01534	-.00000
36	-.02323	.00037	-.01946	.00806	.00000
37	-.04014	-.00101	-.01001	-.00415	.00000
38	-.01999	.01434	.00025	.00060	.00000
39	-.01999	.01434	.00025	-.00060	.00000
40	-.04014	-.00101	-.01001	.00415	.00000
41	.00854	-.00006	.00244	.00101	-.00000
42	-.00627	.01918	.00711	.01716	.00000
43	-.00627	.01918	.00711	-.01716	.00000
44	.00854	-.00006	.00244	-.00101	.00000
45	.03622	.00587	.01490	.00617	-.00000
46	-.01324	.01811	.01223	.02952	.00000
47	-.01324	.01811	.01223	-.02952	.00000
48	.03622	.00587	.01490	-.00617	-.00000
49	.01694	.01450	.02036	.00843	-.00000
50	-.06066	.00777	.00965	.02329	.00000
51	-.06066	.00777	.00965	-.02329	.00000
52	.01694	.01450	.02036	-.00843	-.00000
53	.03094	.01317	.02397	.00993	.00000
54	-.05393	.01141	.01118	.02698	.00000
55	-.05393	.01141	.01118	-.02698	.00000
56	.03094	.01317	.02397	-.00993	.00000
57	.01268	.00842	.02074	.00859	.00000
58	-.07801	.00925	.01240	.02993	.00000
59	-.07801	.00925	.01240	-.02993	.00000
60	.01268	.00842	.02074	-.00859	.00000

OGIVE CYLINDER BODY WITH 45 DEGREE SWEEP NACA 65A004 MID-WING
SINGULARITY PANELING FOR SAMPLE CASE

INTEGRATION OF THE PRESSURE DISTRIBUTION

ON THE BODY

MACH= 2.0100
ALPHA= 0.0000

POINT	X	Y	Z	X/C	2Y/B	Z/C	CP	CN	CT	CM	POINT
1	1.00000	.09575	-.23116	.02740	.02875	-.06942	.15199	.03274	.00887	.64669	1
2	1.00000	.23116	-.09575	.02740	.06942	-.02875	.15199	.01356	.00887	.26787	2
3	1.00000	.23116	.09575	.02740	.06942	.02875	.15199	-.01356	.00887	-.26787	3
4	1.00000	.09575	.23116	.02740	.02875	.06942	.15199	-.03274	.00887	-.64669	4
5	3.22006	.27308	-.65928	.08822	.08201	-.19798	.11288	.17374	.03699	3.03221	5
6	3.22006	.65928	-.27308	.08822	.19798	-.08201	.11288	.07197	.03699	1.25598	6
7	3.22006	.65928	.27308	.08822	.19798	.08201	.11288	-.07197	.03699	-1.25598	7
8	3.22006	.27308	.65928	.08822	.08201	.19798	.11288	-.17374	.03699	-3.03222	8
9	6.08242	.44633	-1.07754	.16664	.13403	-.32359	.05759	.15283	.02101	2.22865	9
10	6.08242	1.07754	-.44633	.16664	.32359	-.13403	.05759	.06330	.02101	.92314	10
11	6.08242	1.07754	.44633	.16664	.32359	.13403	.05759	-.06330	.02101	-.92314	11
12	6.08242	.44633	1.07754	.16664	.13403	.32359	.05759	-.15283	.02101	-2.22865	12
13	9.03105	.55006	-1.32796	.24743	.16518	-.39879	.00010	.00034	.00002	.00392	13
14	9.03105	1.32796	-.55006	.24743	.39879	-.16518	.00010	.00014	.00002	.00163	14
15	9.03105	1.32796	.55006	.24743	.39879	.16518	.00010	-.00014	.00002	-.00163	15
16	9.03105	.55006	1.32796	.24743	.16518	.39879	.00010	-.00034	.00002	-.00392	16
17	11.08446	.58637	-1.41563	.30368	.17609	-.42511	-.03988	-.05458	-.00077	-.52986	17
18	11.08446	1.41563	-.58637	.30368	.42511	-.17609	-.03988	-.02261	-.00077	-.21948	18
19	11.08446	1.41563	.58637	.30368	.42511	.17609	-.03988	.02261	-.00077	.21948	19
20	11.08446	.58637	1.41563	.30368	.17609	.42511	-.03988	.05458	-.00077	.52986	20
21	13.63090	.58927	-1.42262	.37345	.17696	-.42721	-.03515	-.16270	0.00000	-1.16854	21
22	13.63090	1.42262	-.58927	.37345	.42721	-.17696	-.03515	-.06739	0.00000	-.48402	22
23	13.63090	1.42262	.58927	.37345	.42721	.17696	-.03515	.06739	0.00000	.48402	23
24	13.63090	.58927	1.42262	.37345	.17696	.42721	-.03515	.16270	0.00000	1.16854	24
25	16.48370	.58927	-1.42262	.45161	.17696	-.42721	-.01413	-.02960	0.00000	-.12817	25
26	16.48370	1.42262	-.58927	.45161	.42721	-.17696	-.01413	-.01226	0.00000	-.05309	26
27	16.48370	1.42262	.58927	.45161	.42721	.17696	-.01413	.01226	0.00000	.05309	27
28	16.48370	.58927	1.42262	.45161	.17696	.42721	-.01413	.02960	0.00000	.12817	28
29	18.26145	.58927	-1.42262	.50031	.17696	-.42721	-.01486	-.03112	0.00000	-.07942	29
30	18.26145	1.42262	-.58927	.50031	.42721	-.17696	.01602	.01390	0.00000	.03547	30
31	18.26145	1.42262	.58927	.50031	.42721	.17696	.01602	-.01390	0.00000	-.03547	31
32	18.26145	.58927	1.42262	.50031	.17696	.42721	-.01486	.03112	0.00000	.07942	32
33	20.03915	.58927	-1.42262	.54902	.17696	-.42721	-.00118	-.00248	0.00000	-.00192	33
34	20.03915	1.42262	-.58927	.54902	.42721	-.17696	-.00137	-.00119	0.00000	-.00092	34
35	20.03915	1.42262	.58927	.54902	.42721	.17696	-.00137	.00119	0.00000	.00092	35
36	20.03915	.58927	1.42262	.54902	.17696	.42721	-.00118	.00248	0.00000	.00192	36
37	21.81690	.58927	-1.42262	.59772	.17696	-.42721	.00191	.00400	0.00000	-.00401	37
38	21.81690	1.42262	-.58927	.59772	.42721	-.17696	-.02805	-.02434	0.00000	.02443	38
39	21.81690	1.42262	.58927	.59772	.42721	.17696	-.02805	.02434	0.00000	-.02443	39
40	21.81690	.58927	1.42262	.59772	.17696	.42721	.00191	-.00400	0.00000	.00401	40
41	23.59465	.58927	-1.42262	.64643	.17696	-.42721	.00010	.00022	0.00000	-.00061	41
42	23.59465	1.42262	-.58927	.64643	.42721	-.17696	-.03756	-.03259	0.00000	.09066	42
43	23.59465	1.42262	.58927	.64643	.42721	.17696	-.03756	.03259	0.00000	-.09066	43
44	23.59465	.58927	1.42262	.64643	.17696	.42721	.00010	-.00022	0.00000	.00061	44
45	25.38175	.58927	-1.42262	.69539	.17696	-.42721	-.01188	-.02515	0.00000	.11491	45
46	25.38175	1.42262	-.58927	.69539	.42721	-.17696	-.03616	-.03171	0.00000	.14490	46
47	25.38175	1.42262	.58927	.69539	.42721	.17696	-.03616	.03171	0.00000	-.14490	47
48	25.38175	.58927	1.42262	.69539	.17696	.42721	-.01188	.02515	0.00000	-.11491	48
49	27.84000	.58927	-1.42262	.76274	.17696	-.42721	-.02881	-.10593	0.00000	.74438	49
50	27.84000	1.42262	-.58927	.76274	.42721	-.17696	-.01596	-.02431	0.00000	.17085	50
51	27.84000	1.42262	.58927	.76274	.42721	.17696	-.01596	.02431	0.00000	-.17085	51
52	27.84000	.58927	1.42262	.76274	.17696	.42721	-.02881	.10593	0.00000	-.74438	52
53	31.20000	.58927	-1.42262	.85479	.17696	-.42721	-.02645	-.11222	0.00000	1.16565	53
54	31.20000	1.42262	-.58927	.85479	.42721	-.17696	-.02323	-.04083	0.00000	.42408	54
55	31.20000	1.42262	.58927	.85479	.42721	.17696	-.02323	.04083	0.00000	-.42408	55
56	31.20000	.58927	1.42262	.85479	.17696	.42721	-.02645	.11222	0.00000	-1.16565	56
57	34.75000	.58927	-1.42262	.95205	.17696	-.42721	-.01712	-.07061	0.00000	.98404	57
58	34.75000	1.42262	-.58927	.95205	.42721	-.17696	-.01924	-.03288	0.00000	.45826	58
59	34.75000	1.42262	.58927	.95205	.42721	.17696	-.01924	.03288	0.00000	-.45826	59
60	34.75000	.58927	1.42262	.95205	.17696	.42721	-.01712	.07061	0.00000	-.98404	60

TOTAL COEFFICIENTS

ON THE BODY

REFA= 144.0000 REFD= 3.3300 REFL= 36.5000

REFX= 20.8130 REFZ= 0.0000

CN= .0000
CT= .0037
CM= -.0000
CL= .0000
CD= .0037
XCP= -1.5870

VELOCITIES ON WING UPPER SURFACE, MACH=2.010 ALPHA= 0.000

PANEL NO.	VORTEX STRENGTH	AXIAL VELOCITY	LATERAL VELOCITY	VERTICAL VELOCITY
1	-.00000	-.12191	.14872	.17879
2	-.00000	.02325	-.06309	.05696
3	.00000	.00695	-.03468	.03265
4	.00000	.00518	-.02358	.01709
5	.00000	.00868	-.01760	.00315
6	-.00000	.01821	-.02061	-.01379
7	-.00000	.02206	-.01522	-.02918
8	.00000	.02414	-.00917	-.03946
9	.00000	.02864	-.01025	-.04623
10	.00000	.02582	-.00434	-.04704
11	-.00000	.02247	.00144	-.04710
12	.00000	-.12687	.15178	.17879
13	-.00000	-.03264	.04060	.05696
14	-.00000	-.00618	.00164	.03265
15	-.00000	.02367	-.05002	.01709
16	-.00000	.01651	-.03580	.00315
17	.00000	.02284	-.04163	-.01379
18	.00000	.02992	-.04226	-.02918
19	-.00000	.03571	-.04406	-.03946
20	-.00000	.03733	-.04194	-.04623
21	-.00000	.03439	-.03595	-.04704
22	-.00000	.03269	-.03250	-.04710
23	-.00000	-.12591	.14680	.17879
24	-.00000	-.03502	.04206	.05696
25	.00000	-.01856	.02123	.03265
26	-.00000	-.00934	.00966	.01709
27	-.00000	.00056	-.00363	.00315
28	-.00000	.02291	-.03670	-.01379
29	-.00000	.04714	-.07500	-.02918
30	-.00000	.04349	-.06282	-.03946
31	-.00000	.04270	-.05353	-.04623
32	-.00000	.04277	-.05200	-.04704
33	-.00000	.04111	-.04856	-.04710
34	-.00000	-.12906	.15068	.17879
35	.00000	-.03764	.04531	.05696
36	-.00000	-.01850	.01967	.03265
37	-.00000	-.00791	.00540	.01709
38	-.00000	-.00023	-.00397	.00315
39	-.00000	.01061	-.01688	-.01379
40	.00000	.01939	-.02695	-.02918
41	-.00000	.02434	-.03331	-.03946
42	-.00000	.02815	-.03980	-.04623
43	-.00000	.02809	-.04334	-.04704
44	.00000	.03065	-.04243	-.04710
45	-.00000	-.14159	.17134	.17879
46	-.00000	-.04752	.06159	.05696
47	.00000	-.01946	.02050	.03265
48	.00000	-.01057	.00896	.01709
49	-.00000	-.00287	-.00036	.00315
50	.00000	.00763	-.01249	-.01379
51	.00000	.01648	-.02250	-.02918
52	-.00000	.02364	-.03263	-.03946
53	-.00000	.02826	-.04052	-.04623
54	-.00000	.02754	-.04298	-.04704
55	-.00000	.02755	-.04707	-.04710

OGIVE CYLINDER BODY WITH 45 DEGREE SWEEP NACA 65A004 MID-WING
SINGULARITY PANELING FOR SAMPLE CASE

INTEGRATION OF THE PRESSURE DISTRIBUTION

ON THE WING UPPER SURFACE

MACH= 2.0100
ALPHA= 0.0000

POINT	X	Y	Z	X/C	2Y/B	Z/C	CP	CN	CT	CM	POINT
1	16.76499	2.30734	0.00000	.05000	.19228	0.00000	.07831	-.08627	.01017	-.34921	1
2	17.61117	2.30734	0.00000	.15000	.19228	0.00000	-.03365	.03707	-.00166	.11869	2
3	18.45734	2.30734	0.00000	.25000	.19228	0.00000	-.01353	.01490	-.00037	.03511	3
4	19.30352	2.30734	0.00000	.35000	.19228	0.00000	-.01427	.01572	-.00016	.02373	4
5	20.14970	2.30734	0.00000	.45000	.19228	0.00000	-.02670	.02941	.00016	.01951	5
6	20.99587	2.30734	0.00000	.55000	.19228	0.00000	-.03980	.04384	.00094	-.00802	6
7	21.84205	2.30734	0.00000	.65000	.19228	0.00000	-.04580	.05046	.00173	-.05192	7
8	22.68823	2.30734	0.00000	.75000	.19228	0.00000	-.05237	.05769	.00247	-.10819	8
9	23.53441	2.30734	0.00000	.85000	.19228	0.00000	-.05418	.05969	.00278	-.16243	9
10	24.38058	2.30734	0.00000	.95000	.19228	0.00000	-.04851	.05343	.00252	-.19063	10
11	18.82577	4.12568	0.00000	.05000	.34381	0.00000	.14091	-.24418	.02878	-.48523	11
12	19.55072	4.12568	0.00000	.15000	.34381	0.00000	.03717	-.06441	.00289	-.08131	12
13	20.27568	4.12568	0.00000	.25000	.34381	0.00000	-.01839	.03187	-.00079	.01712	13
14	21.00063	4.12568	0.00000	.35000	.34381	0.00000	-.04077	.07065	-.00071	-.01326	14
15	21.72559	4.12568	0.00000	.45000	.34381	0.00000	-.03961	.06864	.00037	-.06264	15
16	22.45054	4.12568	0.00000	.55000	.34381	0.00000	-.05263	.09119	.00196	-.14933	16
17	23.17550	4.12568	0.00000	.65000	.34381	0.00000	-.06497	.11258	.00386	-.26596	17
18	23.90045	4.12568	0.00000	.75000	.34381	0.00000	-.07210	.12494	.00535	-.38575	18
19	24.62541	4.12568	0.00000	.85000	.34381	0.00000	-.07093	.12292	.00573	-.46861	19
20	25.35036	4.12568	0.00000	.95000	.34381	0.00000	-.06657	.11534	.00543	-.52336	20
21	21.51108	6.49507	0.00000	.05000	.54126	0.00000	.14331	-.19052	.02246	.13300	21
22	22.07808	6.49507	0.00000	.15000	.54126	0.00000	.05227	-.06950	.00311	.08792	22
23	22.64507	6.49507	0.00000	.25000	.54126	0.00000	.02754	-.03662	.00091	.06708	23
24	23.21207	6.49507	0.00000	.35000	.54126	0.00000	.00870	-.01157	.00012	.02776	24
25	23.77906	6.49507	0.00000	.45000	.54126	0.00000	-.02337	.03107	.00017	-.09215	25
26	24.34606	6.49507	0.00000	.55000	.54126	0.00000	-.06915	.09194	.00198	-.32482	26
27	24.91305	6.49507	0.00000	.65000	.54126	0.00000	-.08921	.11860	.00407	-.48628	27
28	25.48005	6.49507	0.00000	.75000	.54126	0.00000	-.08484	.11279	.00483	-.52638	28
29	26.04704	6.49507	0.00000	.85000	.54126	0.00000	-.08398	.11164	.00521	-.58435	29
30	26.61404	6.49507	0.00000	.95000	.54126	0.00000	-.08242	.10958	.00516	-.63568	30
31	24.16649	8.83808	0.00000	.05000	.73651	0.00000	.14910	-.14335	.01690	.48071	31
32	24.57728	8.83808	0.00000	.15000	.73651	0.00000	.05497	-.05285	.00237	.19893	32
33	24.98808	8.83808	0.00000	.25000	.73651	0.00000	.02608	-.02507	.00062	.10468	33
34	25.39887	8.83808	0.00000	.35000	.73651	0.00000	.00806	-.00775	.00008	.03552	34
35	25.80967	8.83808	0.00000	.45000	.73651	0.00000	-.01044	.01004	.00005	-.05018	35
36	26.22046	8.83808	0.00000	.55000	.73651	0.00000	-.03020	.02904	.00062	-.15701	36
37	26.63126	8.83808	0.00000	.65000	.73651	0.00000	-.04417	.04247	.00146	-.24711	37
38	27.04205	8.83808	0.00000	.75000	.73651	0.00000	-.05322	.05117	.00219	-.31873	38
39	27.45285	8.83808	0.00000	.85000	.73651	0.00000	-.05728	.05507	.00257	-.36568	39
40	27.86364	8.83808	0.00000	.95000	.73651	0.00000	-.05967	.05737	.00270	-.40449	40
41	26.58702	10.97384	0.00000	.05000	.91449	0.00000	.16990	-.08500	.01002	.49082	41
42	26.85543	10.97384	0.00000	.15000	.91449	0.00000	.06594	-.03299	.00148	.19936	42
43	27.12384	10.97384	0.00000	.25000	.91449	0.00000	.02978	-.01490	.00037	.09402	43
44	27.39225	10.97384	0.00000	.35000	.91449	0.00000	.01342	-.00672	.00007	.04419	44
45	27.66066	10.97384	0.00000	.45000	.91449	0.00000	-.00483	.00242	.00001	-.01656	45
46	27.92907	10.97384	0.00000	.55000	.91449	0.00000	-.02441	.01221	.00026	-.08692	46
47	28.19748	10.97384	0.00000	.65000	.91449	0.00000	-.04067	.02035	.00070	-.15026	47
48	28.46589	10.97384	0.00000	.75000	.91449	0.00000	-.05268	.02636	.00113	-.20172	48
49	28.73430	10.97384	0.00000	.85000	.91449	0.00000	-.05689	.02847	.00133	-.22549	49
50	29.00271	10.97384	0.00000	.95000	.91449	0.00000	-.05653	.02828	.00133	-.23164	50

VELOCITIES ON WING LOWER SURFACE, MACH=2.010 ALPHA= 0.000

PANEL NO.	VORTEX STRENGTH	AXIAL VELOCITY	LATERAL VELOCITY	VERTICAL VELOCITY
1	-.00000	-.12191	.14872	-.17879
2	-.00000	.02325	-.06309	-.05696
3	.00000	.00695	-.03468	-.03265
4	.00000	.00518	-.02358	-.01709
5	.00000	.00868	-.01760	-.00315
6	-.00000	.01821	-.02061	.01379
7	-.00000	.02206	-.01522	.02918
8	.00000	.02414	-.00917	.03946
9	.00000	.02864	-.01025	.04623
10	.00000	.02582	-.00434	.04704
11	-.00000	.02247	.00144	.04710
12	.00000	-.12687	.15178	-.17879
13	-.00000	-.03264	.04060	-.05696
14	-.00000	-.00618	.00164	-.03265
15	-.00000	.02367	-.05002	-.01709
16	-.00000	.01651	-.03580	-.00315
17	.00000	.02284	-.04163	.01379
18	.00000	.02992	-.04226	.02918
19	-.00000	.03571	-.04406	.03946
20	-.00000	.03733	-.04194	.04623
21	-.00000	.03439	-.03595	.04704
22	-.00000	.03269	-.03250	.04710
23	-.00000	-.12591	.14680	-.17879
24	-.00000	-.03502	.04206	-.05696
25	.00000	-.01856	.02123	-.03265
26	-.00000	-.00934	.00966	-.01709
27	-.00000	.00056	-.00363	-.00315
28	-.00000	.02291	-.03670	.01379
29	-.00000	.04714	-.07500	.02918
30	-.00000	.04349	-.06282	.03946
31	-.00000	.04270	-.05353	.04623
32	-.00000	.04277	-.05200	.04704
33	-.00000	.04111	-.04856	.04710
34	-.00000	-.12906	.15068	-.17879
35	.00000	-.03764	.04531	-.05696
36	-.00000	-.01850	.01967	-.03265
37	-.00000	-.00791	.00540	-.01709
38	-.00000	-.00023	-.00397	-.00315
39	-.00000	.01061	-.01688	.01379
40	.00000	.01939	-.02695	.02918
41	-.00000	.02434	-.03331	.03946
42	-.00000	.02815	-.03980	.04623
43	-.00000	.02809	-.04334	.04704
44	.00000	.03065	-.04243	.04710
45	-.00000	-.14159	.17134	-.17879
46	-.00000	-.04752	.06159	-.05696
47	.00000	-.01946	.02050	-.03265
48	.00000	-.01057	.00896	-.01709
49	-.00000	-.00287	-.00036	-.00315
50	.00000	.00763	-.01249	.01379
51	.00000	.01648	-.02250	.02918
52	-.00000	.02364	-.03263	.03946
53	-.00000	.02826	-.04052	.04623
54	-.00000	.02754	-.04298	.04704
55	-.00000	.02755	-.04707	.04710

OGIVE CYLINDER BODY WITH 45 DEGREE SWEEP NACA 65A004 MID-WING
SINGULARITY PANELING FOR SAMPLE CASE

INTEGRATION OF THE PRESSURE DISTRIBUTION

ON THE WING LOWER SURFACE

MACH= 2.0100
ALPHA= 0.0000

POINT	X	Y	Z	X/C	2Y/B	Z/C	CP	CN	CT	CM	POINT
1	16.76499	2.30734	0.00000	.05000	.19228	0.00000	.07831	.08627	.01017	.34921	1
2	17.61117	2.30734	0.00000	.15000	.19228	0.00000	-.03365	-.03707	-.00166	-.11869	2
3	18.45734	2.30734	0.00000	.25000	.19228	0.00000	-.01353	-.01490	-.00037	-.03511	3
4	19.30352	2.30734	0.00000	.35000	.19228	0.00000	-.01427	-.01572	-.00016	-.02373	4
5	20.14970	2.30734	0.00000	.45000	.19228	0.00000	-.02670	-.02941	.00016	-.01951	5
6	20.99587	2.30734	0.00000	.55000	.19228	0.00000	-.03980	-.04384	.00094	.00802	6
7	21.84205	2.30734	0.00000	.65000	.19228	0.00000	-.04580	-.05046	.00173	.05192	7
8	22.68823	2.30734	0.00000	.75000	.19228	0.00000	-.05237	-.05769	.00247	.10819	8
9	23.53441	2.30734	0.00000	.85000	.19228	0.00000	-.05418	-.05969	.00278	.16243	9
10	24.38058	2.30734	0.00000	.95000	.19228	0.00000	-.04851	-.05343	.00252	.19063	10
11	18.82577	4.12568	0.00000	.05000	.34381	0.00000	.14091	.24418	.02878	.48523	11
12	19.55072	4.12568	0.00000	.15000	.34381	0.00000	.03717	.06441	.00289	.08131	12
13	20.27568	4.12568	0.00000	.25000	.34381	0.00000	-.01839	-.03187	-.00079	-.01712	13
14	21.00063	4.12568	0.00000	.35000	.34381	0.00000	-.04077	-.07065	-.00071	.01326	14
15	21.72559	4.12568	0.00000	.45000	.34381	0.00000	-.03961	-.06864	.00037	.06264	15
16	22.45054	4.12568	0.00000	.55000	.34381	0.00000	-.05263	-.09119	.00196	.14933	16
17	23.17550	4.12568	0.00000	.65000	.34381	0.00000	-.06497	-.11258	.00386	.26596	17
18	23.90045	4.12568	0.00000	.75000	.34381	0.00000	-.07210	-.12494	.00535	.38575	18
19	24.62541	4.12568	0.00000	.85000	.34381	0.00000	-.07093	-.12292	.00573	.46861	19
20	25.35036	4.12568	0.00000	.95000	.34381	0.00000	-.06657	-.11534	.00543	.52336	20
21	21.51108	6.49507	0.00000	.05000	.54126	0.00000	.14331	.19052	.02246	-.13300	21
22	22.07808	6.49507	0.00000	.15000	.54126	0.00000	.05227	.06950	.00311	-.08792	22
23	22.64507	6.49507	0.00000	.25000	.54126	0.00000	.02754	.03662	.00091	-.06708	23
24	23.21207	6.49507	0.00000	.35000	.54126	0.00000	.00870	.01157	.00012	-.02776	24
25	23.77906	6.49507	0.00000	.45000	.54126	0.00000	-.02337	-.03107	.00017	.09215	25
26	24.34606	6.49507	0.00000	.55000	.54126	0.00000	-.06915	-.09194	.00198	.32482	26
27	24.91305	6.49507	0.00000	.65000	.54126	0.00000	-.08921	-.11860	.00407	.48628	27
28	25.48005	6.49507	0.00000	.75000	.54126	0.00000	-.08484	-.11279	.00483	.52638	28
29	26.04704	6.49507	0.00000	.85000	.54126	0.00000	-.08398	-.11164	.00521	.58435	29
30	26.61404	6.49507	0.00000	.95000	.54126	0.00000	-.08242	-.10956	.00516	.63568	30
31	24.16649	8.83808	0.00000	.05000	.73651	0.00000	.14910	.14335	.01690	-.48071	31
32	24.57728	8.83808	0.00000	.15000	.73651	0.00000	.05497	.05285	.00237	-.19893	32
33	24.98808	8.83808	0.00000	.25000	.73651	0.00000	.02608	.02507	.00062	-.10468	33
34	25.39887	8.83808	0.00000	.35000	.73651	0.00000	.00806	.00775	.00008	-.03552	34
35	25.80967	8.83808	0.00000	.45000	.73651	0.00000	-.01044	-.01004	.00005	.05018	35
36	26.22046	8.83808	0.00000	.55000	.73651	0.00000	-.03020	-.02904	.00062	.15701	36
37	26.63126	8.83808	0.00000	.65000	.73651	0.00000	-.04417	-.04247	.00146	.24711	37
38	27.04205	8.83808	0.00000	.75000	.73651	0.00000	-.05322	-.05117	.00219	.31873	38
39	27.45285	8.83808	0.00000	.85000	.73651	0.00000	-.05728	-.05507	.00257	.36568	39
40	27.86364	8.83808	0.00000	.95000	.73651	0.00000	-.05967	-.05737	.00270	.40449	40
41	26.58702	10.97384	0.00000	.05000	.91449	0.00000	.16990	.08500	.01002	-.49082	41
42	26.85543	10.97384	0.00000	.15000	.91449	0.00000	.06594	.03299	.00148	-.19936	42
43	27.12384	10.97384	0.00000	.25000	.91449	0.00000	.02978	.01490	.00037	-.09402	43
44	27.39225	10.97384	0.00000	.35000	.91449	0.00000	.01342	.00672	.00007	-.04419	44
45	27.66066	10.97384	0.00000	.45000	.91449	0.00000	-.00483	-.00242	.00001	.01656	45
46	27.92907	10.97384	0.00000	.55000	.91449	0.00000	-.02441	-.01221	.00026	.08692	46
47	28.19748	10.97384	0.00000	.65000	.91449	0.00000	-.04067	-.02035	.00070	.15026	47
48	28.46589	10.97384	0.00000	.75000	.91449	0.00000	-.05268	-.02636	.00113	.20172	48
49	28.73430	10.97384	0.00000	.85000	.91449	0.00000	-.05689	-.02847	.00133	.22549	49
50	29.00271	10.97384	0.00000	.95000	.91449	0.00000	-.05653	-.02828	.00133	.23164	50

TOTAL COEFFICIENTS
ON THE WING

REFA=	144.0000	REFB=	12.0000	REFC=	6.8900
REFX=	20.8130	REFZ=	0.0000		

CN=	-.0000
CT=	.0046
CM=	.0000
CL=	-.0000
CD=	.0046
XCP=	-.105e

TOTAL COEFFICIENTS
ON THE COMPLETE CONFIGURATION

REFA=	144.0000	REFB=	12.0000	REFC=	6.8900
REFX=	20.8130	REFZ=	0.0000		

CN=	.0000
CT=	.0083
CM=	-.0000
CL=	.0000
CD=	.0083
XCP=	-3.571C

SECTION COEFFICIENTS

ON THE WING

DELY= 1.3030 REFL= 6.8900 XLE= 16.3419

CN= -.0000
CT= .0034
CM= -.0000
CL= -.0000
CD= .0034
XCP= .3338

DELY= 2.4000 REFL= 6.8900 XLE= 18.4633

CN= -.0000
CT= .0061
CM= .0000
CL= -.0000
CD= .0061
XCP= -.1551

DELY= 2.3600 REFL= 6.8900 XLE= 21.2276

CN= -.0000
CT= .0072
CM= .0000
CL= -.0000
CD= .0072
XCP= -.4477

SECTION COEFFICIENTS

ON THE WING

DELY= 2.3700 REFL= 6.8900 XLE= 23.9611

CN= -.0000
CT= .0061
CM= .0000
CL= -.0000
CD= .0061
XCP= -.6329

DELY= 1.9000 REFL= 6.8900 XLE= 26.4528

CN= .0000
CT= .0065
CM= .0000
CL= .0000
CD= .0065
XCP= 3.0337

CPSTAG = 2.45650 CPCRIT = 1.13092 CPVAC = -.35360

TIME = 122.42900

TIME = 124.14500

TIME = 131.60300

VELOCITIES ON BODY, MACH=2.010 ALPHA= 5.000

PANEL NO.	SOURCE STRENGTH	AXIAL VELOCITY	LATERAL VELOCITY	VERTICAL VELOCITY	NORMAL VELOCITY
1	.29821	-.12592	.12742	-.27006	.32977
2	.23814	-.10863	.24926	-.06568	.28260
3	.15320	-.08418	.16672	.10663	.21590
4	.09313	-.06689	.04488	.14592	.16873
5	.29647	-.09585	.11639	-.23061	.27645
6	.22353	-.08065	.21498	-.03868	.22928
7	.12038	-.05914	.12165	.10076	.16258
8	.04744	-.04393	.02305	.10602	.11541
9	.25703	-.05884	.09712	-.17579	.20705
10	.17238	-.04502	.16318	-.00891	.15988
11	.05267	-.02549	.06234	.08451	.09318
12	-.03198	-.01167	-.00371	.04973	.04601
13	.22872	-.01979	.07956	-.11702	.13973
14	.12507	-.00925	.11155	.02886	.09256
15	-.02150	.00564	-.00234	.07409	.02586
16	-.12515	.01618	-.03433	-.00781	-.02131
17	.16034	.00840	.06631	-.07381	.09346
18	.05307	.01544	.07345	.05586	.04629
19	-.09862	.02540	-.04907	.06596	-.02042
20	-.20589	.03245	-.05621	-.04942	-.06759
21	.19295	.01318	.06479	-.06032	.08052
22	.07831	.01601	.06479	.06925	.03335
23	-.08383	.02000	-.06479	.06925	-.03335
24	-.19848	.02282	-.06479	-.06032	-.08052
25	.23512	.00731	.06566	-.05996	.08052
26	.11426	.00720	.06566	.07137	.03335
27	-.05666	.00703	-.06566	.07137	-.03335
28	-.17752	.00692	-.06566	-.05996	-.08052
29	-.15629	.00058	-.00204	-.08800	.08052
30	-.07665	-.03603	.00504	-.07486	.03330
31	.12388	.01975	-.02128	-.03592	-.03340
32	.15214	.01440	.00204	-.08800	-.08052
33	.00748	-.03345	-.02645	-.09813	.08054
34	.00491	-.03148	-.02400	-.14499	.03331
35	.01679	.03255	.01123	-.11439	-.03340
36	-.05376	.03414	-.01240	-.08200	-.08050
37	.05941	-.04515	-.01938	-.09522	.08056
38	-.00215	-.00961	-.00666	-.10331	.03338
39	-.03768	.03816	.00723	-.10454	-.03333
40	-.13940	.04306	-.00056	-.08689	-.08049
41	-.10269	-.01962	.03603	-.07224	.08053
42	-.09683	-.01116	.01946	-.04030	.03340
43	.08433	.04942	-.00515	-.07459	-.03330
44	.11970	.01950	-.03113	-.07425	-.08051
45	.09772	-.03097	.01107	-.08255	.08050
46	-.03546	-.03552	-.01010	-.11170	.03342
47	.00907	.07167	.03465	-.17065	-.03329
48	-.02556	.04271	.01866	-.09491	-.08054
49	.04061	-.02359	.04121	-.07005	.08049
50	-.06008	-.00391	.03051	-.01369	.03343
51	-.06077	.01942	-.01112	-.06012	-.03328
52	-.00687	.05255	-.00061	-.08694	-.08055
53	.16144	-.00624	.06860	-.05875	.08053
54	-.03317	-.00266	.04641	.02451	.03349
55	-.07429	.02541	-.02383	-.02926	-.03321
56	-.09979	.03250	-.02073	-.07855	-.08051
57	.16721	.00258	.06929	-.05847	.08053
58	-.01301	.01136	.06502	.06939	.03351
59	-.14241	.00707	-.03996	.00974	-.03319
60	-.14195	.01420	-.02790	-.07559	-.08051

OGIVE CYLINDER BODY WITH 45 DEGREE SWEEP NACA 65A004 MID-WING
SINGULARITY PANELING FOR SAMPLE CASE

INTEGRATION OF THE PRESSURE DISTRIBUTION

ON THE BODY

MACH= 2.0100
ALPHA= 5.0000

POINT	X	Y	Z	X/C	2Y/B	Z/C	CP	CN	CT	CM	POINT
1	1.00000	.09575	-.23116	.02740	.02875	-.06942	.23352	.05031	.01362	.99362	1
2	1.00000	.23116	-.09575	.02740	.06942	-.02875	.17365	.01550	.01013	.30604	2
3	1.00000	.23116	.09575	.02740	.06942	.02875	.11402	-.01017	.00665	-.20096	3
4	1.00000	.09575	.23116	.02740	.02875	.06942	.08674	-.01869	.00506	-.36905	4
5	3.22006	.27308	-.65928	.08822	.08201	-.19798	.18116	.27883	.05936	4.86624	5
6	3.22006	.65928	-.27308	.08822	.19798	-.08201	.12674	.08080	.04153	1.41019	6
7	3.22006	.65928	.27308	.08822	.19798	.08201	.07717	-.04920	.02529	-.85865	7
8	3.22006	.27308	.65928	.08822	.08201	.19798	.05850	-.09004	.01917	-1.57145	8
9	6.08242	.44633	-1.07754	.16664	.13403	-.32359	.11548	.30647	.04213	4.46908	9
10	6.08242	1.07754	-.44633	.16664	.32359	-.13403	.06657	.07318	.02429	1.06719	10
11	6.08242	1.07754	.44633	.16664	.32359	.13403	.02498	-.02746	.00911	-.40042	11
12	6.08242	.44633	1.07754	.16664	.13403	.32359	.01211	-.03215	.00442	-.46878	12
13	9.03105	.55006	-1.32796	.24743	.16518	-.39879	.04100	.13514	.00869	1.58062	13
14	9.03105	1.32796	-.55006	.24743	.39879	-.16518	.00005	.00006	.00001	.00073	14
15	9.03105	1.32796	.55006	.24743	.39879	.16518	-.02880	.03933	-.00611	.45998	15
16	9.03105	.55006	1.32796	.24743	.16518	.39879	-.03132	.10324	-.00664	1.20759	16
17	11.08446	.58637	-1.41563	.30368	.17609	-.42511	-.01359	-.01860	-.00026	-.18057	17
18	11.08446	1.41563	-.58637	.30368	.42511	-.17609	-.04685	-.02656	-.00090	-.25787	18
19	11.08446	1.41563	.58637	.30368	.42511	.17609	-.06477	.03672	-.00125	.35647	19
20	11.08446	.58637	1.41563	.30368	.17609	.42511	-.05882	.08050	-.00113	.78153	20
21	13.63090	.58927	-1.42262	.37345	.17696	-.42721	-.02320	-.10738	0.00000	-.77118	21
22	13.63090	1.42262	-.58927	.37345	.42721	-.17696	-.05041	-.09667	0.00000	-.69426	22
23	13.63090	1.42262	.58927	.37345	.42721	.17696	-.05761	.11046	0.00000	.79336	23
24	13.63090	.58927	1.42262	.37345	.17696	.42721	-.04146	.19190	0.00000	1.37824	24
25	16.48370	.58927	-1.42262	.45161	.17696	-.42721	-.01193	-.02500	0.00000	-.10824	25
26	16.48370	1.42262	-.58927	.45161	.42721	-.17696	-.03493	-.03031	0.00000	-.13124	26
27	16.48370	1.42262	.58927	.45161	.42721	.17696	-.03462	.03005	0.00000	.13009	27
28	16.48370	.58927	1.42262	.45161	.17696	.42721	-.01116	.02338	0.00000	.10121	28
29	18.26145	.58927	-1.42262	.50031	.17696	-.42721	.00649	.01359	0.00000	.03468	29
30	18.26145	1.42262	-.58927	.50031	.42721	-.17696	.08422	.07309	0.00000	.18649	30
31	18.26145	1.42262	.58927	.50031	.42721	.17696	-.03398	.02949	0.00000	.07524	31
32	18.26145	.58927	1.42262	.50031	.17696	.42721	-.02084	.04367	0.00000	.11142	32
33	20.03915	.58927	-1.42262	.54902	.17696	-.42721	.07774	.16288	0.00000	.12604	33
34	20.03915	1.42262	-.58927	.54902	.42721	-.17696	.06984	.06061	0.00000	.04690	34
35	20.03915	1.42262	.58927	.54902	.42721	.17696	-.05572	.04836	0.00000	.03742	35
36	20.03915	.58927	1.42262	.54902	.17696	.42721	-.05800	.12152	0.00000	.09404	36
37	21.81690	.58927	-1.42262	.59772	.17696	-.42721	.10455	.21906	0.00000	-.21991	37
38	21.81690	1.42262	-.58927	.59772	.42721	-.17696	.02705	.02348	0.00000	-.02357	38
39	21.81690	1.42262	.58927	.59772	.42721	.17696	-.06541	.05676	0.00000	-.05698	39
40	21.81690	.58927	1.42262	.59772	.17696	.42721	-.07379	.15461	0.00000	-.15522	40
41	23.59465	.58927	-1.42262	.64643	.17696	-.42721	.04685	.09816	0.00000	-.27305	41
42	23.59465	1.42262	-.58927	.64643	.42721	-.17696	.02789	.02420	0.00000	-.06733	42
43	23.59465	1.42262	.58927	.64643	.42721	.17696	-.08500	.07377	0.00000	-.20520	43
44	23.59465	.58927	1.42262	.64643	.17696	.42721	-.03171	.06643	0.00000	-.18478	44
45	25.38175	.58927	-1.42262	.69539	.17696	-.42721	.07302	.15461	0.00000	-.70637	45
46	25.38175	1.42262	-.58927	.69539	.42721	-.17696	.08247	.07233	0.00000	-.33046	46
47	25.38175	1.42262	.58927	.69539	.42721	.17696	-.12755	.11186	0.00000	-.51105	47
48	25.38175	.58927	1.42262	.69539	.17696	.42721	-.07352	.15565	0.00000	-.71114	48
49	27.84000	.58927	-1.42262	.76274	.17696	-.42721	.05484	.20165	0.00000	-1.41697	49
50	27.84000	1.42262	-.58927	.76274	.42721	-.17696	.00912	.01390	0.00000	-.09766	50
51	27.84000	1.42262	.58927	.76274	.42721	.17696	-.03128	.04764	0.00000	-.33476	51
52	27.84000	.58927	1.42262	.76274	.17696	.42721	-.09019	.33164	0.00000	-2.33045	52
53	31.20000	.58927	-1.42262	.85479	.17696	-.42721	.01468	.06230	0.00000	-.64709	53
54	31.20000	1.42262	-.58927	.85479	.42721	-.17696	-.00172	-.00303	0.00000	.03142	54
55	31.20000	1.42262	.58927	.85479	.42721	.17696	-.04535	.07970	0.00000	-.82789	55
56	31.20000	.58927	1.42262	.85479	.17696	.42721	-.05531	.23467	0.00000	-2.43756	56
57	34.75000	.58927	-1.42262	.95205	.17696	-.42721	-.00317	-.01308	0.00000	.18229	57
58	34.75000	1.42262	-.58927	.95205	.42721	-.17696	-.04199	-.07174	0.00000	.99979	58
59	34.75000	1.42262	.58927	.95205	.42721	.17696	-.01723	.02943	0.00000	-.41022	59
60	34.75000	.58927	1.42262	.95205	.17696	.42721	-.02134	.08802	0.00000	-1.22679	60

TOTAL COEFFICIENTS

ON THE BODY

REFA= 144.0000 REFD= 3.3300 REFL= 36.5000

REFX= 20.8130 REFZ= 0.0000

CN= .0526
CT= .0035
CM= .0053
CL= .0521
CD= .0081
XCP= .1021

VELOCITIES ON WING UPPER SURFACE, MACH=2.010 ALPHA= 5.000

PANEL NO.	VORTEX STRENGTH	AXIAL VELOCITY	LATERAL VELOCITY	VERTICAL VELOCITY
1	.22406	-.00993	.01805	.09163
2	.20022	.12328	-.18020	-.03020
3	.16902	.09144	-.13524	-.05450
4	.12030	.06533	-.09981	-.07007
5	.07135	.04435	-.07099	-.08401
6	.03408	.03523	-.05783	-.10095
7	.03636	.04023	-.05336	-.11633
8	.06207	.05516	-.05672	-.12661
9	.07180	.06449	-.06097	-.13338
10	.08669	.06911	-.05953	-.13419
11	.11014	.07749	-.06001	-.13426
12	.16587	-.04398	.05506	.09163
13	.16609	.05036	-.05625	-.03020
14	.17415	.08086	-.09951	-.05450
15	.16984	.10855	-.14900	-.07007
16	.15922	.09612	-.12989	-.08401
17	.13547	.09057	-.12543	-.10095
18	.10343	.08163	-.11324	-.11633
19	.06977	.07059	-.10269	-.12661
20	.05319	.06391	-.09504	-.13338
21	.04661	.05768	-.08707	-.13419
22	.04233	.05383	-.08245	-.13426
23	.14925	-.05133	.05979	.09163
24	.14901	.03945	-.04483	-.03020
25	.15071	.05676	-.06657	-.05450
26	.15332	.06729	-.07945	-.07007
27	.15678	.07891	-.09435	-.08401
28	.16070	.10322	-.12910	-.10095
29	.16040	.12730	-.16727	-.11633
30	.15640	.12167	-.15367	-.12661
31	.14848	.11695	-.14177	-.13338
32	.13225	.10889	-.13537	-.13419
33	.11211	.09716	-.12656	-.13426
34	.14331	-.05743	.06712	.09163
35	.14342	.03404	-.03833	-.03020
36	.14370	.05333	-.06412	-.05450
37	.14424	.06417	-.07864	-.07007
38	.14474	.07211	-.08825	-.08401
39	.14546	.08331	-.10147	-.10095
40	.14666	.09269	-.11202	-.11633
41	.14815	.09839	-.11893	-.12661
42	.14990	.10307	-.12600	-.13338
43	.15198	.10406	-.13016	-.13419
44	.15398	.10761	-.12978	-.13426
45	.14022	-.07147	.08951	.09163
46	.14038	.02268	-.02033	-.03020
47	.14054	.05080	-.06147	-.05450
48	.14085	.05984	-.07314	-.07007
49	.14119	.06769	-.08261	-.08401
50	.14151	.07836	-.09488	-.10095
51	.14182	.08737	-.10503	-.11633
52	.14215	.09469	-.11528	-.12661
53	.14254	.09951	-.12328	-.13338
54	.14289	.09895	-.12584	-.13419
55	.14325	.09913	-.13002	-.13426

OGIVE CYLINDER BODY WITH 45 DEGREE SWEEP NACA 65A004 MID-WING
SINGULARITY PANELING FOR SAMPLE CASE

INTEGRATION OF THE PRESSURE DISTRIBUTION

ON THE WING UPPER SURFACE

MACH= 2.0100
ALPHA= 5.0000

POINT	X	Y	Z	X/C	2Y/B	Z/C	CP	CN	CT	CM	POINT
1	16.76499	2.30734	0.00000	.05000	.19228	0.00000	-.10958	.12071	-.01423	.48864	1
2	17.61117	2.30734	0.00000	.15000	.19228	0.00000	-.18922	.20844	-.00934	.66740	2
3	18.45734	2.30734	0.00000	.25000	.19228	0.00000	-.14170	.15610	-.00388	.36772	3
4	19.30352	2.30734	0.00000	.35000	.19228	0.00000	-.09971	.10984	-.00111	.16580	4
5	20.14970	2.30734	0.00000	.45000	.19228	0.00000	-.07159	.07887	.00042	.05231	5
6	20.99587	2.30734	0.00000	.55000	.19228	0.00000	-.06742	.07427	.00160	-.01358	6
7	21.84205	2.30734	0.00000	.65000	.19228	0.00000	-.08517	.09383	.00322	-.09655	7
8	22.68823	2.30734	0.00000	.75000	.19228	0.00000	-.10645	.11727	.00502	-.21991	8
9	23.53441	2.30734	0.00000	.85000	.19228	0.00000	-.11814	.13014	.00607	-.35417	9
10	24.38058	2.30734	0.00000	.95000	.19228	0.00000	-.12830	.14133	.00665	-.50421	10
11	18.82577	4.12568	0.00000	.05000	.34381	0.00000	-.01494	.02588	-.00305	.05143	11
12	19.55072	4.12568	0.00000	.15000	.34381	0.00000	-.11757	.20373	-.00913	.25717	12
13	20.27568	4.12568	0.00000	.25000	.34381	0.00000	-.16626	.28810	-.00716	.15480	13
14	21.00063	4.12568	0.00000	.35000	.34381	0.00000	-.17911	.31036	-.00314	-.05823	14
15	21.72559	4.12568	0.00000	.45000	.34381	0.00000	-.16501	.28593	.00152	-.26094	15
16	22.45054	4.12568	0.00000	.55000	.34381	0.00000	-.15367	.26627	.00572	-.43603	16
17	23.17550	4.12568	0.00000	.65000	.34381	0.00000	-.13760	.23844	.00818	-.56330	17
18	23.90045	4.12568	0.00000	.75000	.34381	0.00000	-.12315	.21339	.00914	-.65883	18
19	24.62541	4.12568	0.00000	.85000	.34381	0.00000	-.11204	.19414	.00905	-.74012	19
20	25.35036	4.12568	0.00000	.95000	.34381	0.00000	-.10303	.17853	.00840	-.81004	20
21	21.51108	6.49507	0.00000	.05000	.54126	0.00000	.00257	-.00342	.00040	.00239	21
22	22.07808	6.49507	0.00000	.15000	.54126	0.00000	-.08677	.11535	-.00517	-.14593	22
23	22.64507	6.49507	0.00000	.25000	.54126	0.00000	-.11058	.14701	-.00366	-.26934	23
24	23.21207	6.49507	0.00000	.35000	.54126	0.00000	-.12933	.17194	-.00174	-.41251	24
25	23.77906	6.49507	0.00000	.45000	.54126	0.00000	-.15894	.21131	.00112	-.62676	25
26	24.34606	6.49507	0.00000	.55000	.54126	0.00000	-.19700	.26191	.00563	-.92533	26
27	24.91305	6.49507	0.00000	.65000	.54126	0.00000	-.21101	.28052	.00963	-1.15017	27
28	25.48005	6.49507	0.00000	.75000	.54126	0.00000	-.20309	.27001	.01157	-1.26013	28
29	26.04704	6.49507	0.00000	.85000	.54126	0.00000	-.19389	.25777	.01202	-1.34916	29
30	26.61404	6.49507	0.00000	.95000	.54126	0.00000	-.17989	.23916	.01126	-1.38737	30
31	24.16649	8.83808	0.00000	.05000	.73651	0.00000	.01376	-.01323	.00156	.04436	31
32	24.57728	8.83808	0.00000	.15000	.73651	0.00000	-.07874	.07570	-.00339	-.28496	32
33	24.98808	8.83808	0.00000	.25000	.73651	0.00000	-.10507	.10102	-.00251	-.42175	33
34	25.39887	8.83808	0.00000	.35000	.73651	0.00000	-.12121	.11654	-.00118	-.53442	34
35	25.80967	8.83808	0.00000	.45000	.73651	0.00000	-.13736	.13206	.00070	-.65988	35
36	26.22046	8.83808	0.00000	.55000	.73651	0.00000	-.15448	.14852	.00319	-.80313	36
37	26.63126	8.83808	0.00000	.65000	.73651	0.00000	-.16686	.16043	.00551	-.93341	37
38	27.04205	8.83808	0.00000	.75000	.73651	0.00000	-.17540	.16863	.00722	-1.05041	38
39	27.45285	8.83808	0.00000	.85000	.73651	0.00000	-.18025	.17330	.00808	-1.15065	39
40	27.86364	8.83808	0.00000	.95000	.73651	0.00000	-.18353	.17646	.00831	-1.24413	40
41	26.58702	10.97384	0.00000	.05000	.91449	0.00000	.03823	-.01913	.00225	.11044	41
42	26.85543	10.97384	0.00000	.15000	.91449	0.00000	-.06559	.03282	-.00147	-.19831	42
43	27.12384	10.97384	0.00000	.25000	.91449	0.00000	-.09898	.04952	-.00123	-.31252	43
44	27.39225	10.97384	0.00000	.35000	.91449	0.00000	-.11357	.05682	-.00057	-.37386	44
45	27.66066	10.97384	0.00000	.45000	.91449	0.00000	-.12942	.06475	.00034	-.44341	45
46	27.92907	10.97384	0.00000	.55000	.91449	0.00000	-.14607	.07308	.00157	-.52006	46
47	28.19748	10.97384	0.00000	.65000	.91449	0.00000	-.15978	.07994	.00274	-.59032	47
48	28.46589	10.97384	0.00000	.75000	.91449	0.00000	-.17000	.08505	.00364	-.65091	48
49	28.73430	10.97384	0.00000	.85000	.91449	0.00000	-.17392	.08702	.00406	-.68928	49
50	29.00271	10.97384	0.00000	.95000	.91449	0.00000	-.17421	.08716	.00410	-.71385	50

VELOCITIES ON WING LOWER SURFACE, MACH=2.010 ALPHA= 5.000

PANEL NO.	VORTEX STRENGTH	AXIAL VELOCITY	LATERAL VELOCITY	VERTICAL VELOCITY
1	.22408	-.23401	.27948	-.26595
2	.20022	-.07694	.05418	-.14412
3	.16902	-.07758	.06587	-.11981
4	.12030	-.05497	.05258	-.10424
5	.07135	-.02700	.03570	-.09031
6	.03408	.00115	.01657	-.07336
7	.03636	.00387	.02286	-.05798
8	.06207	-.00691	.03836	-.04770
9	.07180	-.00731	.04059	-.04093
10	.08669	-.01757	.05097	-.04012
11	.11014	-.03265	.06299	-.04006
12	.16587	-.20984	.24857	-.26595
13	.16609	-.11573	.13752	-.14412
14	.17415	-.09329	.10285	-.11981
15	.16984	-.06128	.04905	-.10424
16	.15922	-.06311	.05825	-.09031
17	.13547	-.04490	.04213	-.07336
18	.10343	-.02179	.02868	-.05798
19	.06977	.00082	.01455	-.04770
20	.05319	.01072	.01115	-.04093
21	.04661	.01107	.01517	-.04012
22	.04233	.01151	.01750	-.04006
23	.14925	-.20058	.23392	-.26595
24	.14901	-.10955	.12903	-.14412
25	.15071	-.09395	.10910	-.11981
26	.15332	-.08603	.09883	-.10424
27	.15678	-.07786	.08716	-.09031
28	.16070	-.05748	.05580	-.07336
29	.16040	-.03310	.01739	-.05798
30	.15640	-.03473	.02806	-.04770
31	.14848	-.03154	.03468	-.04093
32	.13225	-.02336	.03135	-.04012
33	.11211	-.01495	.02941	-.04006
34	.14331	-.20075	.23432	-.26595
35	.14342	-.10938	.12899	-.14412
36	.14370	-.09038	.10350	-.11981
37	.14424	-.08007	.08952	-.10424
38	.14474	-.07263	.08038	-.09031
39	.14546	-.06215	.06778	-.07336
40	.14666	-.05397	.05819	-.05798
41	.14815	-.04976	.05237	-.04770
42	.14990	-.04683	.04647	-.04093
43	.15198	-.04792	.04356	-.04012
44	.15398	-.04636	.04500	-.04006
45	.14022	-.21168	.25309	-.26595
46	.14038	-.11769	.14344	-.14412
47	.14054	-.08974	.10248	-.11981
48	.14085	-.08102	.09111	-.10424
49	.14119	-.07349	.08196	-.09031
50	.14151	-.06315	.06996	-.07336
51	.14182	-.05445	.06007	-.05798
52	.14215	-.04746	.05006	-.04770
53	.14254	-.04303	.04231	-.04093
54	.14289	-.04393	.03996	-.04012
55	.14325	-.04412	.03598	-.04006

OGIVE CYLINDER BODY WITH 45 DEGREE SWEEP NACA 65A004 MID-WING
SINGULARITY PANELING FOR SAMPLE CASE

INTEGRATION OF THE PRESSURE DISTRIBUTION

ON THE WING LOWER SURFACE

MACH= 2.0100
ALPHA= 5.0000

POINT	X	Y	Z	X/C	2Y/B	Z/C	CP	CN	CT	CM	POINT
1	16.76499	2.30734	0.00000	.05000	.19228	0.00000	.29517	.32516	.03833	1.31626	1
2	17.61117	2.30734	0.00000	.15000	.19228	0.00000	.17381	.19147	.00858	.61305	2
3	18.45734	2.30734	0.00000	.25000	.19228	0.00000	.14959	.16478	.00410	.38817	3
4	19.30352	2.30734	0.00000	.35000	.19228	0.00000	.09354	.10304	.00104	.15554	4
5	20.14970	2.30734	0.00000	.45000	.19228	0.00000	.03394	.03738	-.00020	.02480	5
6	20.99587	2.30734	0.00000	.55000	.19228	0.00000	.00168	.00185	-.00004	-.00034	6
7	21.84205	2.30734	0.00000	.65000	.19228	0.00000	.00857	.00944	-.00032	-.00971	7
8	22.68823	2.30734	0.00000	.75000	.19228	0.00000	.01865	.02054	-.00088	-.03852	8
9	23.53441	2.30734	0.00000	.85000	.19228	0.00000	.02880	.03172	-.00148	-.08633	9
10	24.38058	2.30734	0.00000	.95000	.19228	0.00000	.05438	.05990	-.00282	-.21371	10
11	18.82577	4.12568	0.00000	.05000	.34381	0.00000	.31460	.34513	.06426	1.08331	11
12	19.55072	4.12568	0.00000	.15000	.34381	0.00000	.22655	.24857	.01759	.49553	12
13	20.27568	4.12568	0.00000	.25000	.34381	0.00000	.17245	.29882	.00743	.16056	13
14	21.00063	4.12568	0.00000	.35000	.34381	0.00000	.14107	.24443	.00247	-.04587	14
15	21.72559	4.12568	0.00000	.45000	.34381	0.00000	.12247	.21221	-.00113	-.19366	15
16	22.45054	4.12568	0.00000	.55000	.34381	0.00000	.07674	.13297	-.00286	-.21774	16
17	23.17550	4.12568	0.00000	.65000	.34381	0.00000	.02777	.04812	-.00165	-.11367	17
18	23.90045	4.12568	0.00000	.75000	.34381	0.00000	-.00584	-.01011	.00043	.03122	18
19	24.62541	4.12568	0.00000	.85000	.34381	0.00000	-.01631	-.02825	.00132	.10772	19
20	25.35036	4.12568	0.00000	.95000	.34381	0.00000	-.01720	-.02980	.00140	.13520	20
21	21.51108	6.49507	0.00000	.05000	.54126	0.00000	.30197	.40146	.04732	-.28025	21
22	22.07808	6.49507	0.00000	.15000	.54126	0.00000	.22019	.29274	.01312	-.37033	22
23	22.64507	6.49507	0.00000	.25000	.54126	0.00000	.19751	.26258	.00653	-.48107	23
24	23.21207	6.49507	0.00000	.35000	.54126	0.00000	.18127	.24099	.00244	-.57815	24
25	23.77906	6.49507	0.00000	.45000	.54126	0.00000	.15125	.20109	-.00107	-.59643	25
26	24.34606	6.49507	0.00000	.55000	.54126	0.00000	.10311	.13708	-.00295	-.48431	26
27	24.91305	6.49507	0.00000	.65000	.54126	0.00000	.07770	.10330	-.00354	-.42354	27
28	25.48005	6.49507	0.00000	.75000	.54126	0.00000	.07472	.09934	-.00426	-.46362	28
29	26.04704	6.49507	0.00000	.85000	.54126	0.00000	.06182	.08219	-.00383	-.43018	29
30	26.61404	6.49507	0.00000	.95000	.54126	0.00000	.04414	.05868	-.00276	-.34040	30
31	24.16049	8.83808	0.00000	.05000	.73651	0.00000	.30182	.29018	.03420	-.97310	31
32	24.57728	8.83808	0.00000	.15000	.73651	0.00000	.21633	.20799	.00932	-.78293	32
33	24.98808	8.83808	0.00000	.25000	.73651	0.00000	.18771	.18047	.00449	-.75347	33
34	25.39887	8.83808	0.00000	.35000	.73651	0.00000	.16950	.16296	.00165	-.74733	34
35	25.80967	8.83808	0.00000	.45000	.73651	0.00000	.15022	.14442	-.00077	-.72164	35
36	26.22046	8.83808	0.00000	.55000	.73651	0.00000	.12952	.12452	-.00268	-.67336	36
37	26.63126	8.83808	0.00000	.65000	.73651	0.00000	.11537	.11092	-.00381	-.64536	37
38	27.04205	8.83808	0.00000	.75000	.73651	0.00000	.10711	.10298	-.00441	-.64146	38
39	27.45285	8.83808	0.00000	.85000	.73651	0.00000	.10512	.10106	-.00471	-.67103	39
40	27.86364	8.83808	0.00000	.95000	.73651	0.00000	.10462	.10059	-.00473	-.70920	40
41	26.38702	10.97384	0.00000	.05000	.91449	0.00000	.31643	.15832	.01866	-.91414	41
42	26.85543	10.97384	0.00000	.15000	.91449	0.00000	.22349	.11182	.00501	-.67565	42
43	27.32384	10.97384	0.00000	.25000	.91449	0.00000	.18804	.09408	.00234	-.59373	43
44	27.79225	10.97384	0.00000	.35000	.91449	0.00000	.17134	.08573	.00087	-.56403	44
45	27.66066	10.97384	0.00000	.45000	.91449	0.00000	.15208	.07609	-.00041	-.52104	45
46	27.92907	10.97384	0.00000	.55000	.91449	0.00000	.13093	.06551	-.00141	-.46617	46
47	28.19748	10.97384	0.00000	.65000	.91449	0.00000	.11329	.05668	-.00195	-.41859	47
48	28.46589	10.97384	0.00000	.75000	.91449	0.00000	.10052	.05029	-.00215	-.38490	48
49	28.73430	10.97384	0.00000	.85000	.91449	0.00000	.09666	.04836	-.00226	-.38310	49
50	29.00271	10.97384	0.00000	.95000	.91449	0.00000	.09814	.04910	-.00231	-.40212	50

TOTAL COEFFICIENTS

ON THE WING

REFA=	144.0000	REFB=	12.0000	REFC=	6.8900
REFX=	20.8130	REFZ=	0.0000		

CN=	.1969
CT=	.0046
CM=	-.0705
CL=	.1957
CD=	.0217
XCP=	-.3600

TOTAL COEFFICIENTS

ON THE COMPLETE CONFIGURATION

REFA=	144.0000	REFB=	12.0000	REFC=	6.8900
REFX=	20.8130	REFZ=	0.0000		

CN=	.2495
CT=	.0081
CM=	-.0651
CL=	.2479
CD=	.0298
XCP=	-.2628

SECTION COEFFICIENTS

ON THE WING

DELY= 1.3030 REFL= 6.8900 XLE= 16.3419

CN= .1974
CT= .0037
CM= .0356
CL= .1963
CD= .0209
XCP= .1812

DELY= 2.4000 REFL= 6.8900 XLE= 18.4633

CN= .2305
CT= .0063
CM= -.0135
CL= .2291
CD= .0263
XCP= -.0590

DELY= 2.3600 REFL= 6.8900 XLE= 21.2276

CN= .2863
CT= .0069
CM= -.1299
CL= .2846
CD= .0318
XCP= -.4563

SECTION COEFFICIENTS

ON THE WING

DELY= 2.3700 REFL= 6.8900 XLE= 23.9611

CN= .2841
CT= .0058
CM= -.2140
CL= .2825
CD= .0305
XCP= -.7577

DELY= 1.9000 REFL= 6.8900 XLE= 26.4528

CN= .2732
CT= .0062
CM= -.2762
CL= .2716
CD= .0300
XCP= -1.0171

CPSTAG = 2.45650 CPCRIT = 1.13092 CPVAC = -.35360

TIME = 150.55900

REFERENCES

1. Woodward, F. A., Tinoco, E. N., and Larsen, J. W.; Analysis and Design of Supersonic Wing-Body Combinations, Including Flow Properties in the Near Field. NASA CR-73106, August, 1967.

2. Woodward, F. A.; Analysis and Design of Wing-Body Combinations, at Subsonic and Supersonic Speeds. Journal of Aircraft, Vol. 5, No. 6, Nov.- Dec., 1968.

3. Craidon, C. B.; Description of a Digital Computer Program for Airplane Configuration Plots. NASA TM X-2074, September, 1970.

4. Gothert, B.; Plane and Three-Dimensional Flow at High Subsonic Speeds. NACA TM 1105, 1946.

5. Labrujere, T. E., Loeve, W., and Slooff, J. W.; An Approximate Method for the Calculation of Pressure Distribution on Wing-Body Combinations at Subcritical Speeds. AGARD Conference Proceedings No. 71, September, 1970.

6. Fox, C. H. Jr.; Experimental Surface Pressure Distributions for a Family of Axisymmetric Bodies at Subsonic Speeds. NASA TM X-2439, December, 1971.

7. Harris, R. V. Jr., and Landrum, E. J.; Drag Characteristics of a Series of Low-Drag Bodies of Revolution at Mach Numbers from 0.6 to 4.0. NASA TN D-3163, December, 1965.

8. Maslen, S. H.; Pressure Distribution on Thin Conical Body of Elliptic Cross Section at Mach Number 1.89. NACA RM E8K05, January, 1949.

9. Peterson, R. F.; The Boundary-Layer and Stalling Characteristics of the NACA 64A010 Airfoil Section. NACA TN 2235, 1950.

10. Stevens, W. A., Goradia, S. H., and Braden, J. A.; Mathematical Model for Two-Dimensional Multi-Component Airfoils in Viscous Flow. NASA CR-1843, July, 1971.

11. Lamar, J. E., and McKinney, L. W.; Low Speed Static Wind Tunnel Investigation of a Half-Span Fuselage and Variable Sweep Pressure Wing Model. NASA TN D-6215, August, 1971.

12. Carlson, H. W.; Pressure Distributions at Mach Number 2.05 on a Series of Highly Swept Arrow Wings Employing Various Degrees of Twist and Camber. NASA TN D-1264, May, 1962.

13. Gapcynski, J. P., and Landrum, E. J.; Tabulated Data from a Pressure Distribution Investigation at Mach Number 2.01 of a 45 degree Sweptback-Wing Airplane Model at Combined Angles of Attack and Sideslip. NASA MEMO 10-15-58L, November, 1958.

14. Hess, J. L., and Smith, A. M. O.; Calculation of Nonlifting Potential Flow about Arbitrary Three-Dimensional Bodies. Douglas Aircraft Company Report, No. ES 40622, March, 1962.

*U.S. GOVERNMENT PRINTING OFFICE: 1973-739-027/31